OPTIMIZATION STUDIES FOR PHYSICS PROBLEMS IN INDIAN PHWRs

By

SURENDRA MISHRA

Nuclear Power Corporation of India Limited, Mumbai

A thesis submitted to the Board of Studies in Physical Sciences In partial fulfillment of requirements For the Degree of

DOCTOR OF PHILOSOPHY

of

HOMI BHABHA NATIONAL INSTITUTE

April, 2012

Homi Bhabha National Institute

Recommendations of the Viva Voce Board

As members of the Viva Voce Board, we certify that we have read the dissertation prepared by **SURENDRA MISHRA** entitled "**OPTIMIZATION STUDIES FOR PHYSICS PROBLEMS IN INDIAN PHWRs**" and recommend that it may be accepted as fulfilling the dissertation requirement for the Degree of Doctor of Philosophy.

---**Date:** 16-7-2012

Chairman – Prof. **P. K. Vijayan** (RED, BARC)

---**Date:** 16-7-2012

Guide / Convener – Prof. **B. N. Jagatap** (AMPD, BARC)

---**Date:** 16-7-2012

Technology Adviser – Dr. **R. S. Modak** (ThPD, BARC)

---**Date:** 16-7-2012

Member 1 – Prof. **P. D. Krishnani** (RPDD, BARC)

---**Date:** 16-7-2012

Member 2 – Prof. **S. B. Degweker** (ThPD, BARC)

Final approval and acceptance of this dissertation is contingent upon the candidate's submission of the final copies of the dissertation to HBNI.

I hereby certify that I have read this dissertation prepared under my direction and recommend that it may be accepted as fulfilling the dissertation requirement.

Date: 16-7-2012

Place: Anushaktinagar, Mumbai

STATEMENT BY AUTHOR

This dissertation has been submitted in partial fulfillment of requirements for an advanced degree at Homi Bhabha National Institute (HBNI) and is deposited in the Library to be made available to borrowers under rules of the HBNI.

Brief quotations from this dissertation are allowable without special permission, provided that accurate acknowledgement of source is made. Requests for permission for extended quotation or reproduction of this manuscript in whole or in part may be granted by the Competent Authority of HBNI when in his or her judgment the proposed use of the material is in the interests of scholarship. In all other instances, however, permission must be obtained from the author.

SURENDRA MISHRA

DECLARATION

I, hereby declare that the investigation presented in the thesis has been carried out by me. The work is original and has not been submitted earlier as a whole or in part for a degree / diploma at this or any other Institution / University.

SURENDRA MISHRA

ACKNOWLEDGEMENTS

I would like to take this opportunity to thank everyone who shared their moments with me in various walks of life.

I wish to express sincere gratitude to my present Ph. D. guide Prof. B. N. Jagatap (AMPD, BARC) and earlier guide Prof. S. Ganesan (RPDD, BARC) for their energetic encouragement and support during the course of this work.

I would like to express my deepest gratitude and thanks to my technology advisor Dr. R. S. Modak (ThPD, BARC) for being such a great source of information and motivation. It is his invaluable advices and support that guided me to successfully complete this thesis. I am also grateful to Shri Kislay Bhatt for his support on parallel computing.

I wish to thank Prof. P. K. Vijayan (RED), Prof. P. D. Krishnani (RPDD), Prof. S. B. Degwekar (ThPD), Dr. V. Jagannathan (RPDD), Prof. Vinod Kumar (ThPD) and Dr. H. P. Gupta (ThPD) from BARC for useful advice. I would like to thank Shri A. N. Kumar and Smt Sherly Ray from NPCIL for precious discussions during my research work.

Finally, I wish to express my gratefulness to the authorities of Nuclear Power Corporation of Indian Limited, Mumbai and Bhabha Atomic Research Centre, Mumbai for providing a very conducive atmosphere for carrying out this research.

CONTENTS

SYNOPSIS

OPTIMIZATION STUDIES FOR PHYSICS PROBLEMS IN INDIAN PHWRs

The thesis presents an account of original contribution of the author towards the optimization studies for some physics problems in Indian Pressurised Heavy Water Reactors (PHWRs).

The concept of Nuclear Reactors has its origin in the discovery of nuclear fission in 1939. In a nuclear fission, a neutron is absorbed in a heavy nucleus such as U^{235} and two or more fragments are produced. This reaction has two interesting features. First is that a significant amount of energy (about 200 MeV) is produced which is in the form of kinetic energy of fission fragments. Secondly, a few (on the average 2 to 3) neutrons are also produced. These facts immediately suggested the possibility of utilizing the emergent neutrons to cause further fissions in other heavy nuclei and thus to have a self-sustained steady fission chain reaction. Such a system, called a nuclear reactor, could then act as a steady source of energy. Since the first reactor built by Fermi in 1942, the field has continuously evolved leading to the very many complex nuclear reactors of today.

There have been various ways in which reactors are classified. The research reactors operate at low powers, the primary aim being research, isotope production etc. Power Reactors, on the contrary, are designed to act as a source of energy. On the basis of neutron energy, two major types are Thermal and Fast reactors. The Thermal Reactors use a moderator material such as Light Water, Heavy Water or Graphite. Neutrons are slowed down by the moderator to make use of the high value of fission cross-section at low neutron energy. Light Water Reactors (LWR) need enrichment of Uranium to about 3 to 5 percent. They come in two major categories: Pressurised Water Reactors (PWR) and Boiling Water Reactors (BWR). LWRs form a dominant source of Nuclear Energy in the world.

Another popular type of Thermal reactors, which is a subject of the present thesis, is the Pressurised Heavy Water Reactor (PHWR). These reactor designs originated in Canada and are often referred to as CANDU (CANada Deuterium Uranium) Reactor. The use of heavy water moderator is the key to the PHWR system, enabling them to use Natural uranium (NU) as fuel. The PHWR can be operated without expensive uranium enrichment facilities. The relatively lower temperature and high density moderator leads to sufficiently thermalised neutrons and hence a better fuel utilization. There are

fifteen small sized 220 MWe PHWRs and two medium sized 540 MWe PHWRs operating in India. The more advanced 700 MWe PHWR is in design stage and would start operation in near future [1]. The PHWRs constitute the first stage of the "Three-stage Indian Nuclear Power Programme". These reactors can produce the Plutonium needed in the Second stage for the construction of Fast Breeder Reactors. The Third stage involves utilisation of Thorium to further multiply the power generation capability.

The subject of optimization has permeated the field of nuclear reactors at all stages. Indeed, the choice of most suitable nuclear energy programme depending on the needs and resources of a country is an optimization problem. The design of any specific reactor type would also involve optimization while designing details of fuel lattice, fuel assemblies, full core parameters, thermal hydraulics, shielding, control system and fuel management. In the present thesis, a small subset of these optimization problems, relevant to Indian PHWRs has been studied.

In general, there are two factors which are crucial to optimization problems in Nuclear Power industry: Safety and Economy. For safety, the power distribution in a reactor should be such that the heat is removed safely. Moreover, in case of emergency, it should be always possible to shut down the reactor safely. From the economy point of view, it is always desirable to draw maximum power from the reactor and core parameters (like bulk power, zone power etc.) used in reactor regulation are estimated accurately. Moreover, it is desirable to maximise fuel utilization. Often, all these requirements conflict with each other and what is needed is Optimization.

Specific problems studied in the thesis

The problems studied can be broadly classified in to three types A, B and C.

A. Loading Pattern Optimization

A good part of the studies in the present thesis are concerned with optimization of initial fuel loading in PHWRs, which is a part of the overall Fuel Management over full life time of a reactor. The optimization of initial fuel loading has to be such that maximum economy is achieved without violating any safety constraints. In particular, for economy, it is desirable to operate the reactor at full power right from beginning. This is not possible if the full core is loaded with Natural Uranium (NU) because power peaking would be high. After the reactor has operated for an year or so, power is flattened throughout the life of reactor by having two or three burn-up zones which enables full power operation. In a fresh core, however, the burn-up zones would not be there leading to relatively higher peaking. Hence, it is necessary to load few Thorium or Depleted Uranium (DU) bundles at selected locations in the core. Out

of the total 3672 bundle locations in 220 MWe PHWR, a few tens of locations have to be identified for Thorium/DU bundles. DU bundle contains about 0.3wt% to 0.6wt% U^{235}, which is lower as compared to NU (0.7115wt%). Choice of location of Thorium/DU should be such that full power can be drawn, K-effective is large as far as possible and safety constraints related to thermal hydraulic and control are satisfied. This is a very large constrained combinatorial optimization problem. The number of possible arrangements is so huge (say 10^{50}) that it is impossible to try them all. This problem is addressed in the present thesis by the use of evolutionary algorithms. Optimization methods based on the well-known Genetic Algorithm (GA) and a very recent algorithm called Estimation of Distribution Algorithm (EDA) were tried. The EDA was found to work better than GA in the sense it gives better results with lesser computational effort. Hence, further studies like determining fresh core loading pattern for 220 MWe and 700 MWe PHWR with DU bundles were carried out using EDA.

There are several variations of the above problem that are needed in practice:

1) The required amount of flattening in flux can be achieved by loading either Thorium or DU bundles. The number of DU bundles to be loaded is usually larger (say a few hundreds) as compared to Thorium bundles.
2) It may be desirable to load DU bundles in such a way that they are removed at the first refueling of that channel.
3) For convenience in loading, it may be desirable to load DU bundles in only specific axial locations, say 7^{th} location out of the 12 locations.
4) In case of the large sized 700 MWe PHWR, many new considerations arise. For instance, one has to satisfy two stuck rod criterion instead of the one stuck rod criterion in the 220 MWe PHWR. The 700 MWe core has more symmetry properties providing an opportunity to reduce problem size.

All the above variations of fresh PHWR loading have been analysed in the present thesis.

B. TPMS Optimization

A completely different optimization problem concerned with the Thermal Power Monitoring System (TPMS) in the 700 MWe PHWR is considered. These reactors are equipped with 44 instrumented channels out of the total 392 channels. The instrumented channels are used to estimate reactor bulk power and zone powers. Choosing the 44 channels from amongst 392 channels so as to maximize the power prediction accuracy is a combinatorial optimization problem. There are several constraints to be followed. From the similarity of this problem with the fresh core loading pattern

generation problem discussed in Section A, slightly modified EDA is applied. A more accurate TPMS design was obtained.

C. FMS Optimization

An on-line Flux Mapping System (FMS) is used in 700 MWe PHWRs. There are 102 in-core neutron detectors. The purpose of FMS is to generate a detailed flux map at all points in reactor using the 102 detector readings. It is usually based on use of higher K-modes and certain shape functions as basis functions. There is scope for optimization in terms of choice basis functions and computational method. This optimization problem is completely different in nature from the extremely large sized problems in sections A and B. It is solved by judicious trial and error techniques.

Layout of the thesis

The overall work is presented in nine chapters as follows:

Chapter 1 presents a brief introduction to the topic. The Pressurized Heavy Water Reactors (PHWRs) operating in India and their evolution is described. An outline of the research work presented in the thesis is also given.

Chapter 2 describes the design detail of Indian PHWRs. The 220 MWe PHWR consists of 306 horizontal fuel channels containing coolant and fuel bundles whereas, 540 and 700 MWe PHWR consist of 392 fuel channels. For the purpose of reactor regulation in 220 MWe PHWR, there are 4 Adjuster Rods (ARs), 2 Regulating Rods (RRs) and 2 Shim Rods (2SRs). The prime difference between 220 MWe and 540/700 MWe PHWRs is the neutronic coupling. The 540 MWe reactor, being large sized, is loosely coupled and hence is prone to spatial oscillations during its operation. For the purpose of reactor regulation, the core is logically divided into 14 zones. The zone powers also need to be monitored along with the total reactor power. There are 14 Zone Control Compartments (ZCC), 17 Adjuster Rods (ARs) symmetrically grouped into eight banks and 4 Control Rods (CRs). The zone powers are measured using zone control detectors (i.e. SPNDs). The zone powers measured by these small sized SPNDs need to be corrected by zone powers estimated by some other more accurate means like Thermal Power Measurement System (TPMS) or Flux Mapping System (FMS). The physics optimization problems related to PHWRs are described.

Chapter 3 describes the steady-state neutronic core simulation method for PHWR. The purpose is to find power distribution and effective multiplication factor (K_{eff}) for any given configuration of the

reactor core. The solution of optimization problem requires repeated use of this capability. Neutron transport equation is described by considering the rates at which neutrons of different energies moving in different directions enter and leave a small phase space element [3]. The equation consists of nuclear cross-sections (i.e. absorption, scattering and fission) and neutron flux distribution. The cross sections are the quantities which define the particle interaction probabilities and it is measured in barns (10^{-24} cm^2). The cross sections of each material are highly dependent on the energy of the incident neutron [2]. At reasonably low energies of incident neutrons, cross sections are quite smooth in energy. However, as the energy increase, the cross sections are dominated by resonance peaks that result from unstable state of compound nucleus formed by the collision. In the off-resonance region, the variation in cross section shows $1/E^{1/2}$ or 1/v dependence. The relative geometric arrangement of fuel bundles, pressure tubes, coolant materials, calandria tubes, moderating material follows regular patterns inside the core. These patterns are referred to as lattices. Homogenous lattice cross-sections are obtained by solving neutron transport equation using the 69-energy group nuclear cross section data library in WIMSD conventions. For this purpose 2-D code 'CLUB' [9] that is based on collision probability method is used. The incremental cross-sections corresponding to various reactivity devices present in the core are obtained by solving 3-D neutron transport code 'BOXER' [10]. Full reactor core simulation is carried out by solving neutron diffusion equation applied to the full core. Diffusion theory is sufficiently accurate [4] to provide a quantitative understanding of many physics features of nuclear reactors and is, in fact, the workhorse computational method of nuclear reactor physics. A computer code 'DOLP' has been developed for full core simulation. It solves neutron diffusion equation by finite difference method. The finite differenced multi-group neutron diffusion equation can be written [5] as

$$M\phi = \frac{1}{K}F\phi$$

The matrix M represents absorption, leakage and group to group transfer. The matrix F represents fission neutron generation. There are many eigen solutions corresponding to different values of K. The K values are real and positive. The largest one is called effective multiplication factor (K_{eff}). It corresponds to fundamental mode. This mode is found by power iterations (or outer iterations). Inner iterations are used to solve within group source problem. The outer iterations can be accelerated using Chebyshev method [7]. There exists another quite efficient approach based on Orthomin(1) algorithm [8] to solve the eigenvalue problem $M\phi = \lambda F\phi$. The residual vector $r = M\phi - \lambda F\phi$ is determined. The function $f(\phi) = (r, r)$ is minimized in Orthomin(1) algorithm. All the three options are provided in

DOLP. A comparison of CPU time is made between power iteration, Chebyshev method and Orthomin(1) algorithm.

Chapter 4 outlines the basic ideas in optimization methods. Objective function, decision variables and constraints are three main components of an optimization problem. A typical optimization problem can be stated as follows:

To find $x=\begin{bmatrix} x_1 \\ x_2 \\ \vdots \\ x_n \end{bmatrix}$, which minimizes or maximizes $f(x)$;

Subject to the constraints

$$g_i(x) \leq 0; \;\; i = 1,2,3 \ldots m$$

$$h_j(x) = 0; \;\; j = 1,2,3 \ldots p$$

where x is an n-dimensional vector called design variable, $f(x)$ is called the objective function, and $g_i(x)$ and $h_j(x)$ are known as inequality and equality constraints respectively. This type of problem is called constrained optimization problem. Optimization problems can be classified based on the type of constraints, nature of design variables, nature of the equations involved and type & number of objective functions. As per the classification suitable solution method is applied to solve the optimization problem. The classical optimization techniques are useful in finding the optimum solution or unconstrained maxima or minima of continuous and differentiable functions. These methods assume that the function is differentiable twice with respect to the design variables and that the derivatives are continuous. For problems with equality constraints the Lagrange multiplier method can be used. Graphical optimization and method of steepest descent can also be used to solve the problem.

Most of the real world optimization problems involve complexities like discrete, continuous or mixed variables, multiple conflicting objectives, non-linearity, discontinuity etc. The search space may be so large that the global optimum can not be found in reasonable time. The classical methods may not be efficient to solve such problems. Various stochastic methods like hill climbing [26], simulated annealing [13] or evolutionary algorithm [12, 15, 18, 25] can be used in such situations. Some methods start with a single guess solution and improve it gradually. Evolutionary Algorithm (EA) is a population based search procedure that incorporates random (stochastic) variation and selection. It is developed to arrive

at near-optimum solutions to a large scale optimization problem. The problem having very large number of decision variables and non-linear objective functions are often solved by EAs. The first evolutionary-based optimization technique was the genetic algorithm (GA). GA was developed based on the Darwinian principle of the survival of the fittest and the natural process of evolution through reproduction. It involves selection of better individuals and cross-over to produce new individuals. The present thesis makes use of another algorithm called Estimation of Distribution Algorithm (EDA). EDA involves selection of better individuals, estimating probability distribution function and sampling to produce new individuals. There exist other variants such as Particle Swarm Optimization (PSO) and Ant Colony Optimization (ACO).

Chapter 5 describes the optimization of Thorium/DU loading in fresh core of 220 MWe PHWRs. A suitable fresh core loading pattern to extract full power from the reactor core is required for a new reactor as well as for a reactor which has undergone EMCCR (EnMass Coolant Channel Replacement). Few Thorium or Depleted Uranium (DU) bundles and rest Natural Uranium (NU) bundles are used in the fresh core to obtain required amount of flattening in the flux. The problem of choosing locations of Thorium/DU bundles in the initial core to achieve nearly full power is considered. This is a fairly complex combinatorial problem with many conflicting requirements. One has to obtain more than 95% full power, maximum possible reactivity, permitted bundle and channel powers and sufficient shutdown system worth. Two evolutionary algorithms Genetic Algorithm and Estimation of Distribution Algorithm [24] are used. In our approach, it is necessary to perform a very large number (~10^5) of neutron diffusion calculations. This has been possible due to the use of parallel super computer system ANUPAM at BARC and CRL at Pune. The two models using X-symmetry (half core) and X&Z-symmetry (one-fourth core) are elaborated. The random correction approach and penalty approach were applied [29] to the cheaper XZ-model. It was observed that the random correction approach applied on XZ-model is more economic. Several patterns have been generated that contain a range (from 12 to 44) of Thorium bundles and rest NU bundles. A loading pattern consisting of 92 DU (0.3wt% U235) and remaining NU fuel bundles generated using the algorithm has been loaded on December 2010 at KAPS#1, Kakrapar, Gujarat after EMCCR (EnMass Coolant Channel Replacement).

Chapter 6 describes the optimization of DU loading in fresh core 700 MWe PHWRs. Estimation of Distribution Algorithm is used to find optimum DU loading. The core lay-out, control devices and safety parameters of 700 MWe PHWR differ widely from those of 220 MWe. A requirement imposed in the present study was that the DU bundles should lie only at certain axial location to make loading

operation easy. Four types of optimization studies (case A, case B, case C and case D) are carried out in which DU bundles are placed at only one axial location and that is 7^{th}, 8^{th}, 9^{th} or 10^{th} location respectively. The optimum fresh core configuration was obtained [30] in each of the 4 cases. It was found that three cases satisfy all the safety constraints and give 100 % FP. Later on, burn-up of the optimum configurations was simulated for about 115 FPD during which no refueling is needed. On the basis of behavior of maximum CPPF in this period and better operating margin for regional over power (ROP) system, optimum configuration of DU in case A (i.e. axially at 7^{th} location) is found to be most suitable. Finally, to satisfy the stuck rod criterion, additional DU bundles were loaded at axial ends. It may be mentioned that the stuck rod criterion cannot be introduced in the form of penalty function because the maximum worth rods can vary with the various DU configurations tried by the EDA algorithm.

Chapter 7 describes optimization of the design of Thermal Power Monitoring System (TPMS) for the forthcoming 700 MWe PHWR. The problem of choosing 44 fuel channels for instrumentation (out of 392 fuel channels) which can predict reactor bulk power and zone powers (on per unit basis) accurately is a combinatorial constraint optimization problem. The problem has been solved using Estimation of Distribution Algorithm and the constraints were handled in a different way. The individuals are generated (during initial and subsequent generations) in such a way that the constraints are satisfied. 44 fuel channels are selected for instrumentation. The selected fuel channels are satisfying all the imposed constraints. The error by TPMS in estimating reactor bulk power and zone powers are determined for reactor core having various reactivity device configurations to ensure that the movement of reactivity devices does not affect the TPMS results. The per unit basis bulk power estimated by instrumented channels lies between 0.995 and 1.005. Thus error in bulk power is less than ±0.5%. The %error in estimating reactor zone power lies between -2% and 2%.

Chapter 8 describes the optimization of the Flux Mapping method in Online Flux Mapping System (FMS) for 700 MWe PHWR. The choice of computational method for FMS is a sensitive issue since it is expected to be versatile, accurate and fast. Three computational methods namely Flux Synthesis (FS) method [33, 34], Internal Boundary Condition (IBC) method [41] and Combined Least Square (CLSQ) method [40, 42] were numerically tested to carry out flux mapping for some representative cases that can occur frequently in a 700 MWe PHWR. The FS method needs very little computation but has poor accuracy. The main reason for the inaccuracy is that the precise knowledge of prevailing snap-shot configuration such as burn-up distribution, AR positions and ZCCs water levels is

not used in the calculations. The IBC method also has errors comparable with FS method. On the other hand, the CLSQ method, which is based on sound principles, gives good accuracy in the proposed application but needs too much computational effort. In particular, the CGNR (Conjugate Gradient Normal Residual) [43] calculations need maximum effort. In view of this, a new hybrid method called modified FS (MFS) method [44] based on combination of FS and CLSQ methods was tried. It is found to give good accuracy without too much computational effort. It makes use of precise knowledge of prevailing state for fundamental K-mode calculation. In addition, it makes use of pre-computed higher K-modes of reference state for minimizing error at detector locations; a procedure which requires solving only a few tens of linear equations. The most difficult CGNR calculations are avoided altogether. The MFS method was further studied for cases with detector failures. It seems better to avoid faulty detectors in the calculation. It may be possible to identify faulty detectors by comparison of detector fluxes with flux predicted by standard mesh K-calculation for the snap-shot configuration.

Chapter 9 summarizes overall work and discusses possible extensions of the work.

LIST OF PUBLICATIONS

A. PUBLICATION IN REFEREED JOURNALS

1) **Surendra Mishra**, R. S. Modak and S. Ganesan; "Optimization of Thorium loading in fresh core of Indian PHWR by evolutionary algorithms". Annals of Nuclear Energy 36 (2009), 948-955.

2) **Surendra Mishra**, R. S. Modak and S. Ganesan; "Optimization of depleted uranium bundle loading in fresh core of Indian PHWR by evolutionary algorithm". Annals of Nuclear Energy 37 (2010) 208-217.

3) **Surendra Mishra**, R. S. Modak and S. Ganesan; "Optimization of depleted uranium loading in fresh core of large sized Indian PHWR by evolutionary algorithm". Annals of Nuclear Energy 38 (2011) 905-909.

4) **Surendra Mishra**, R. S. Modak and S. Ganesan; "Selection of Fuel Channels for Thermal Power Measurement in 700 MWe Indian PHWR by evolutionary algorithm". *Nuclear Engineering and Design 247 (2012), 116-122.*

5) **Surendra Mishra**, R. S. Modak and S. Ganesan; "Computational Schemes for On-line Flux Mapping System in a large sized Pressurized Heavy Water Reactor". *Nuclear Science and Engineering 170 (2012), 280-289.*

B. POSTERS IN CONFERENCES

1) **Surendra Mishra**, R. S. Modak, S. Ray, A.N. Kumar and S. Ganesan; "On the Optimization of Thorium Bundle Distribution in the initial core loading for a PHWR". International Conference on Peaceful Uses of Atomic Energy-2009, Sep.29-Oct. 1, 2009, New Delhi, India.

LIST OF FIGURES

LIST OF TABLES

LIST OF ACRONYMS

Acronym	Meaning
PHWR	Pressurized Heavy Water Reactor
NU	Natural Uranium
DU	Depleted Uranium (U^{235} fissile content is about 0.3 to 0.6 wt%)
TPMS	Thermal Power Measurement System
ICMS	Instrumented Channel Monitoring System
FMS	Flux Mapping System
GA	Genetic Algorithm
EDA	Estimation of Distribution Algorithm
LWR	Light Water Reactor
BSS	Bundle Shift Scheme
SPND	Self Powered Neutron Detector
ZCD	Zone Control Detector
IC	Instrumented Channel
FP	Full Power
MBP	Maximum Bundle Power
MCP	Maximum Channel Power
MCOT	Maximum Channel Outlet Temperature
PSS	Primary Shutdown System
SSS	Secondary Shutdown System
EMCCR	En-Mass Coolant Channel Replacement
CPPF	Channel Power Peaking Factor
ZCC	Zone Control Compartment
FSM	Flux Synthesis Method
IBCM	Internal Boundary Condition Method
CLSQM	Combined Least Square Method
MFSM	Modified Flux Synthesis Method

CHAPTER 1

INTRODUCTION

In this chapter a brief description of nuclear reactors and Indian nuclear power programme is given. The role of optimization is this context is also described.

The discovery of nuclear fission in 1939 can be regarded as the origin of the concept of nuclear reactors. In fission a neutron interacts with heavy nuclei such as U^{235} to break it into two or more fragments. Hahn and Strassman showed that fission not only released a lot of energy but that it also released additional neutrons which could cause fission in other uranium nuclei and hence it can lead to self-sustaining chain reaction. Bohr soon proposed that fission was much more likely to occur in the U^{235} isotope than in U^{238} and that fission would occur more effectively with slow-moving neutrons than with fast neutrons. Fermi designed the first reactor in 1942. After that a series of power and research reactors were designed and operated successfully. Presently, about 16-17% of total world electricity requirement comes from nuclear power. Nuclear reactors can be classified based on the kinetic energy of the neutrons causing most of the fissions in the reactor. If the reactor contains a considerable proportion of moderator, the high energy of the fission neutrons will be rapidly decreased to the thermal value (around 0.025 ev) and such reactors are called thermal reactors. The light nuclei elements like light water, heavy water and graphite are used for moderation purpose. In the fast reactor no moderator is present and nearly all the neutrons causing fission have high energy (average values lie between 1 ev to 2 Mev). Fast reactor needs at least 20% enriched fissile material as a fuel. Thermal reactor which uses light water needs enrichment of U^{235} to about 2 to 5 percent. The majority of the worldwide operating nuclear power plants are light water reactors; i.e. either pressurized water reactors (PWRs) or boiling water reactors (BWRs).

Another popular type is the Pressurized Heavy Water Reactor (PHWRs) [1]. There are more than 44 PHWRs operating in the world. PHWR uses Natural Uranium (NU) as fuel and heavy water as coolant and moderator. The use of heavy water moderator is the key to the PHWR system. Since heavy

water has much lower neutron absorption cross-section [2], it is possible to use NU as fuel. The PHWR can be operated without expensive uranium enrichment facilities. The relatively lower temperature and high density moderator results into sufficiently thermalized neutrons and hence a better fuel utilization [2, 3, 4, 5, 6, 7]. There are some drawbacks associated with PHWR also. PHWR needs a costlier heavy water in tons. The lower fissile content in NU necessitates the continuous online fueling requirement. The increased rate of refueling results higher volumes of spent fuel.

The Indian PHWR programme consists of 220 MWe, 540 MWe and 700 MWe units [1]. They constitute the first stage of the "Three-stage Indian Nuclear Power Programme". These reactors can produce the Plutonium needed in the Second stage for the construction of Fast Breeder Reactors. The Third stage involves utilisation of Thorium to further multiply the power generation capability. The earliest PHWR units (RAPS-1 and RAPS-2) of India are of Canadian design (based on Douglas point). MAPS-1&2 design was evolved from RAPS-1&2, with modifications carried out to suit the coastal site requirement. With experience of design and operation of earlier units and indigenous R&D efforts, major modifications were introduced in NAPS-1&2. These units are the basis of standardized Indian PHWRs. The important features introduced in these units include: two diverse and fast acting shutdown systems, double containment of reactor building, water filled Calandria vault etc. The design of KAPS-1&2 was similar to that of NAPS units. The design of subsequent units i.e. KGS-1, KGS-2, RAPS-3, RAPS-4, RAPS-5, RAPS-6, KGS-3 and KGS-4 is of standard 220 MWe Indian PHWR design. TAPS-3 and TAPS-4 are medium size Indian PHWRs designed for 540 MWe electricity. The thermal power of standard 220 MWe PHWR is 756 MWth whereas, it is 129% more (i.e. 1730 MWth) for 540 MWe PHWR. Thermal power increases by 50% if one increases the total number of fuel channels from 306 to 392 and total number of fuel bundles in each channel (effective region) of the core from 10.1 to 12.0. For the rest 79% increase in thermal power, the fuel bundle design has been changed. In 220 MWe PHWRs 19 pin bundles are used whereas, in 540 MWe PHWR 37 pin bundles are used. With the 37 pin bundle about 98% more power can be extracted as compared to 19 pin bundle because of its lesser diameter. It is obvious that as 540 MWe PHWR is concerned, there is still about 19% margin on bundle power that can be utilized to increase the total reactor power. The successful operation of 220 and 540 MWe PHWRs forms the basis of designing higher capacity like 700 MWe PHWR. In the same core configuration as that of 540 MWe, the reactor total power has been increased by utilizing the margin available in bundle power. In the total 25% increase in reactor power, 18% is by using margin available

on bundle power and 7% is by more flattening. Extraction of additional heat is achieved by allowing boiling of coolant near the channel exit.

In the field of nuclear reactors, optimization problems are faced at various stages. A country has to make optimum choice of reactor types based on its resources. Optimization is needed in the detailed design of a particular type of reactor. This can involve design of fuel lattices, heat transfer system, power maneuvering, control system and so on. The objective can be of various types. The aim could be to save natural uranium, or maximize power production by Thorium, or reduce doubling period in a fast reactor, or employ proliferation resistant schemes. **The optimization schemes studied in this thesis are concerned with the design and operation of PHWRs.**

Fuel Management is a very important activity for continuous operation of PHWRs. It has a bearing on the two factors which are crucial to the Nuclear Power industry namely Safety and Economy. From the economy point of view, it is always desirable to draw maximum power from the reactor. For safety, the power distribution in a reactor should be such that the heat is safely removed. **The optimization of fresh core loading is addressed in this thesis.**

The reactors are equipped with regulation and protection systems so that they can be operated safely. The regulating system prevents any deviation from normal operation but if the deviation remains uncontrolled, the unwanted operational occurrences are eliminated by protection system (also called shutdown system). **Optimization of design of Thermal Power Measurement System (TPMS) and algorithm for flux map generation in On-line Flux Mapping System (OFMS), which are part of regulating system, is considered in this thesis.**

The solution of above optimization problems needs neutronic simulation of the full PHWR core and knowledge of the power distribution inside the reactor. In the chapter 2, a detailed description of Indian PHWR is given and the optimization problems studied in thesis are described in more detail. Chapter 3 gives the computational method [8, 9, 10, 11] employed for the neutronic simulation of PHWRs. Chapter 4 describes the optimization techniques in perspective. It may be mentioned that the problems having very large number of decision variables are often solved by Evolutionary Algorithms (EAs) [12]. EAs and Simulated Annealing are well known optimization methods [13, 14, 15, 16, 17] that have been used to solve various type of problems in science and engineering. The Simulated Annealing, Genetic Algorithm, Particle Swarm Optimization and Ant Colony Optimization have been extensively used to solve light water reactor fuel management and control design problems [13, 18, 19, 20, 21, 22].

In case of PHWR, however, the problem of generating fresh core loading pattern in PHWR has been often solved simply by manual trials and experience. The aim is to get sufficient power flattening by adding some Depleted Uranium or Thorium bundles so as to draw full power without violating safety features. The number of possible configurations is generally very large and manual trials may not yield solution close to optimum. The first significant improvement was made two decades ago by Balakrishnan and Kakodkar [23]. They used a gradient-based method. In the present thesis evolutionary algorithms are used for the first time for optimization of PHWR initial fuel loading. Two types of EAs namely Genetic Algorithm (GA) and Estimation of Distribution Algorithm (EDA) were tried. Chapter 5 describes the initial fuel loading problem in a 220 MWe PHWR. The EDA was found to be more efficient than GA. Chapter 6 is concerned with the use of estimation of distribution algorithm to solve initial core loading problem in 700 MWe PHWR. For the problem of finding optimum choice of instrumented channels for the design of Thermal Power Monitoring System, only EDA was tried and was found to work well as described in chapter 7. Chapter 8 describes the problem of optimization of computational scheme for flux mapping in which the decision variables are not too many and it is solved by explicitly trying the possible choices. Chapter 9 gives conclusion and scope for future work.

CHAPTER 2

OPTIMIZATION PROBLEMS IN PHWRs

In this chapter the design and operation of the Indian PHWR is described in some detail. Later on the specific optimization problems in Indian PHWRs studied in this thesis are described.

2.1. General Description of Indian PHWR

The Pressurized Heavy Water Reactor (PHWR) belongs to two categories: PHWR with moderator dump as a shutdown system and PHWR having shutoff rods and liquid poison addition for shutdown. The 220 MWe PHWR at RAPS and MAPS (RAPS#2, MAPS#1 and MAPS#2) have moderator dump as shut down system. The reactor is made critical by raising the moderator level in the reactor core. The standard 220 MWe PHWR (NAPS#1, NAPS#2, KAPS#1, KAPS#2, KGS#1, KGS#2, KGS#3, KGS#4, RAPS#3, RAPS#4, RAPS#5 and RAPS#6) uses two independent shutdown systems: 14 mechanical shutoff rods known as Primary Shutdown System (PSS) and 12 liquid poison tubes known as Secondary Shutdown System (SSS). The 540 MWe PHWRs at TAPS (TAPS#3 and TAPS#4) are also equipped with two independent shut down systems: 28 mechanical shutoff rods (SRs) and 6 horizontal tubes to mix the neutron poison in the moderator.

The PHWR is a horizontal tube type reactor (as shown in Fig.2.1) fuelled with Natural Uranium (NU) with heavy water as both coolant and moderator. The coolant is physically separated from the moderator by being contained inside the pressure tube where it is maintained at high temperature and pressure. The moderator heavy water is at a relatively low temperature and is unpressurized. The reactor core consists of 306 in 220 MWe and 392 in 540 MWe pressure tubes arranged along a square lattice pitch (22.86 cm in 220 MWe and 28.6 cm in 540 MWe). The fuel pins and the coolant are contained within these pressure tubes. The direction of coolant flow in adjacent channels is in opposite directions. The direction of the bundle movement (fuelling direction) is the same as that of the coolant flow, so that alternate channels are fuelled in opposite directions. In 220 MWe PHWRs, there are 12 fuel bundles along a fuel channel but only 10 remain in the active portion of the core. In 540 MWe PHWRs, there are

13 fuel bundles along a fuel channel but only 12 remain in the active portion of the core. Each bundle in 220 MWe PHWR is a 19-rod cluster of 49.5 cm length. Similarly each bundle in 540 MWe PHWR is a 37-pin cluster of 49.5 cm length.

The total reactor power is measured using Instrumented Channel power Measurement System (ICMS) in 220 MWe PHWRs. In ICMS 18 fuel channels are instrumented which measure inlet temperature, outlet temperature and flow and they are used to estimate total reactor power. For the purpose of reactor regulation in 220 MWe PHWR, there are 4 Adjuster Rods (ARs), 2 Regulating Rods (RRs) and 2 Shim Rods (2SRs). The prime difference between 220 MWe and 540 MWe PHWRs is the neutronic coupling. The 540 MWe reactor, being large sized, is loosely coupled and hence is prone to spatial flux/power oscillations during its operation. Hence, for reactor regulation, the core is logically divided into 14 zones. The zone powers also need to be monitored along with the total reactor power. There are 14 Zone Control Compartments (ZCC), 17 Adjuster Rods (ARs) symmetrically grouped into eight banks and 4 Control Rods (CRs). The zone powers are measured using zone control detectors (i.e. SPNDs). The zone powers measured by these small sized SPNDs can be corrected by ICMS zone powers or zone powers estimated by Flux Mapping System (FMS). For the measurement of reactor total power and zone powers, 44 fuel channels are instrumented to measure temperatures and flow. In FMS, there are 102 vanadium SPNDs. They are well distributed inside the reactor core. With the help of these vanadium detector readings detailed flux distribution in side core is obtained by flux mapping algorithm. The study related with ICMS and FMS is presented in the thesis.

The 700 MWe PHWR is in design stage and it has similar core dimensions of 540 MWe PHWRs [1]. In the same core configuration as that of 540 MWe, the reactor total power has been increased by utilizing the margin available in the fuel linear heat rating (LHR). The time average bundle power is 640 kW (LHR=40kW/M) and 790 kW (LHR=50kW/M) in 540 and 700 MWe PHWR respectively. In the total 25% increased in reactor power, 18% is by jacking up the flux/power profile (maximum time average channel power 5.5 MW in 540 MWe and 6.5 MW in 700 MWe) and 7% is by more flattening. Extraction of additional heat is achieved by allowing boiling of coolant near the channel exit. The regional over power trip (ROP) system is an additional feature in 700 MWe, whose function is to trip the reactor prior to the coolant dry out or fuel centre line melting in any region of the core. The ICMS like system is known as Thermal Power Monitoring System (TPMS) in 700 MWe. The PHT (Primary Heat Transfer) system in 220MWe reactor core is in single loop but to reduce the effect of voiding in coolant

two radial half PHT loops are used in 540 MWe PHWR. The reactivity gain due to voiding in coolant has been further reduced in 700 MWe by using interleaved PHT system.

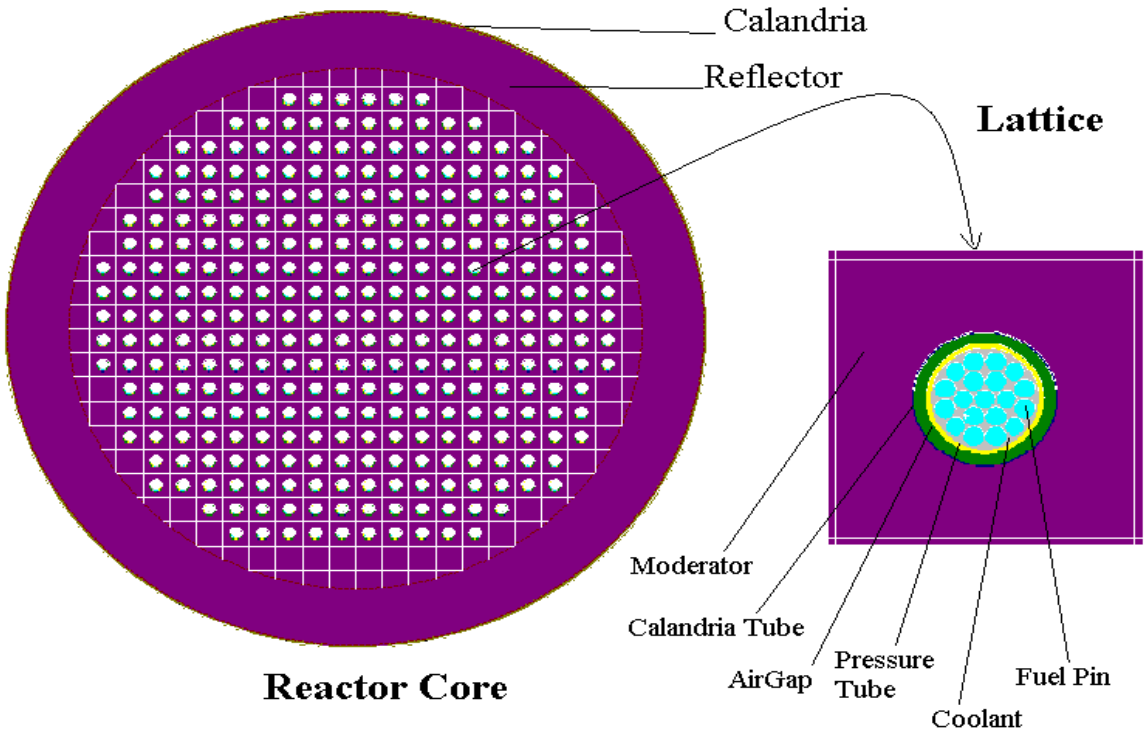

Figure 2.1: Typical PHWR core and its lattice

2.2. Fuel Management

At the outset, it should be mentioned that there exist two distinct types of fuelling:

1) Batch fuelling
2) Continuous on-power fuelling.

The LWRs mostly use the Batch Fuelling. Owing to the use of slightly enriched Uranium, these reactors have substantial excess reactivity at the beginning of life. It can operate without any additional fuel for about a year or so [2]. At the end of such a period, the reactor is shut down and a pre-decided fraction (say 1/3) of the fuel is replaced by fresh fuel. The U-235 content in fresh fuel in about 2 to 5% whereas it less than 1% in the discharged fuel bundles. This procedure is repeated periodically throughout the life of the reactor. One has to arrive at the best possible distribution of the old and new fuel which gives the design power and also satisfies all the safety requirements. This activity is referred to as 'Generation of Loading Pattern'. This is essentially a constrained combinatorial optimization

problem. The number of possible configurations is usually so huge that it is impossible to analyze each one of them.

The fuel management in PHWR is completely different than that in LWR. It employs the continuous on-power fuelling.

2.2.1. Three operating regimes of PHWR operation

The Pressurised Heavy Water Reactors (PHWR) use Natural Uranium (NU) fuel and have very little excess reactivity. They need continuous on-power fuelling. The fuelling procedure in this PHWR can be best explained by noting that the life-span of these reactors can be divided into three different stages:

i) Initial stage: from 0 days to about 150 days

The reactor operation starts with all fresh fuel bundles inside the reactor core. Since all the fuel bundles are fresh, the initial excess reactivity of the core is about 20 to 25 mk in hot operating condition. With this excess reactivity, available in the form of neutron poison in moderator, the reactor can operate up to about 150 FPD (full power days) without refueling of any fresh fuel bundle. The average burn-up in the core is low.

ii) Pre-equilibrium stage: from 150 days to about 600 days

At the completion of initial excess reactivity of the core, a proper fuel channel is selected and refueled. The 8 or 4 Bundle Shift Scheme (BSS) is used. This period is called pre-equilibrium stage of reactor operation. In the pre-equilibrium stage of reactor operation, since the relatively lower than design discharge burnup fuel bundles are thrown out of the core, the feed rate remains quite high.

iii) Equilibrium stage: from 600 days upto the life span of about 2 decades

After completion of about 600 FPD, the reactor enters the equilibrium stage of operation. The feed rate becomes constant. Almost every day, one of the channels is fuelled. The reactor operates about 95% of its life time in equilibrium phase.

The excess reactivity and average core burn-up for the three stages are graphically shown in Fig. 2.2 and 2.3 below.

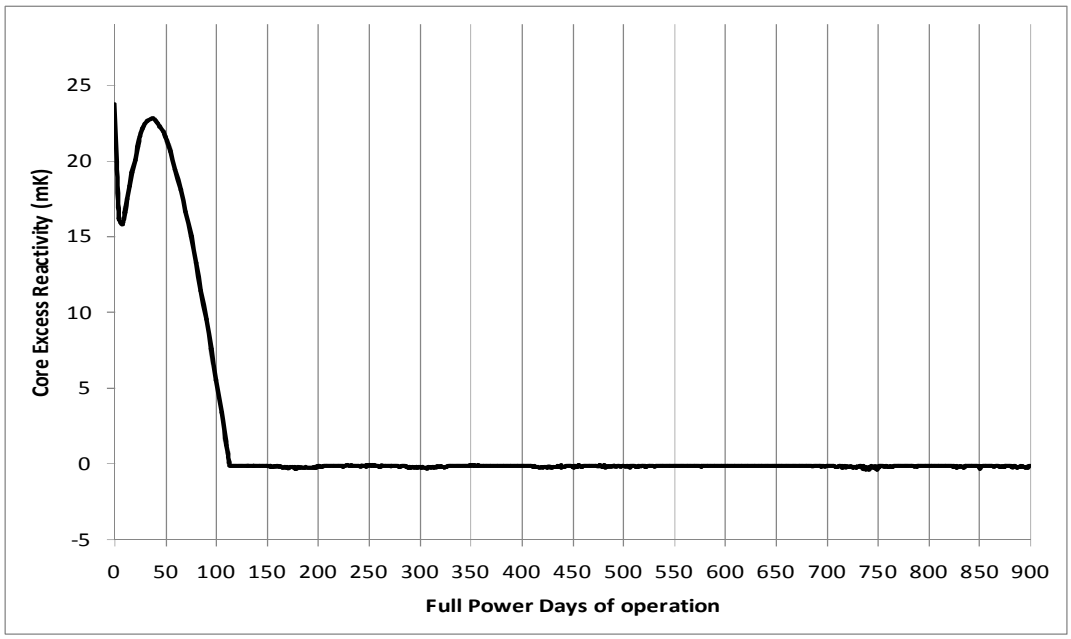

Figure 2.2: The core excess reactivity vs FPD

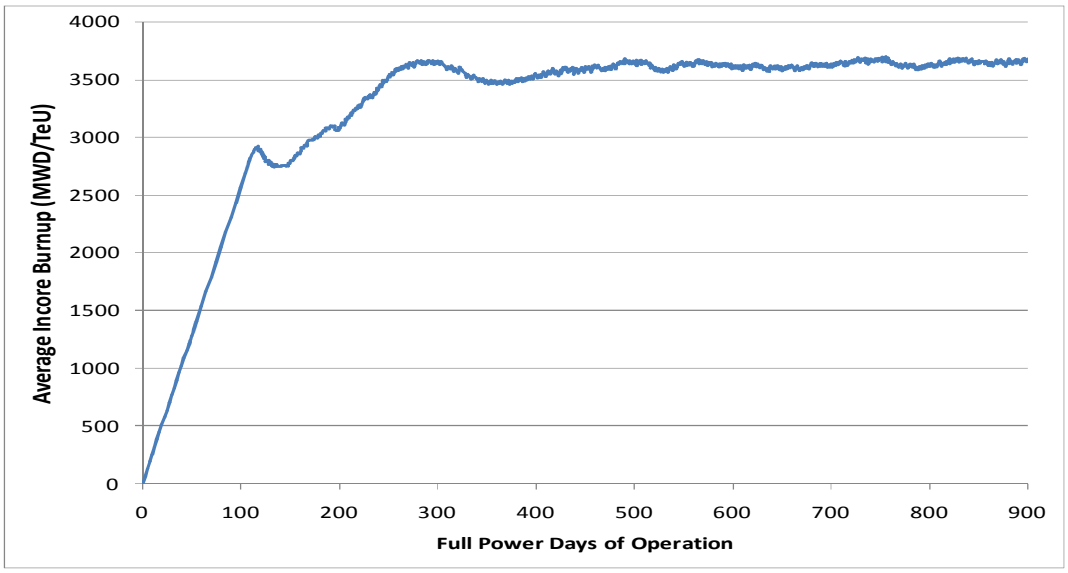

Figure 2.3: The average in-core burnup vs FPD

An important feature of the equilibrium core is flattening of the power shape in both radial as well as axial direction. The axial flattening is achieved by fuelling adjacent channels in opposite directions. The radial flattening is achieved by considering two or three radial zones. The fuel discharge burn-up of inner region is higher than that of the outer region or in other words, fuelling is more frequent

in inner zone channels than outer zone channels. This helps in radial power/flux flattening so that more power can be extracted from the core than if the burn-up had been uniform throughout.

2.3. Specific Optimization Problems Studied in the Thesis

Different type of optimization problems are encountered during design and operation of PHWRs. At initial stage of reactor core, suitable loading pattern using fresh fuel bundles is needed for full power operation. With this loading the reactor can operate up to about 100 to 150 FPDs. In order to keep the reactor critical, it is necessary to do on-power fuelling in pre-equilibrium and equilibrium stage of PHWR. The fuelling is done in such a way that the flux/power remains flattened, so that the reactor can be operated at full power. The optimum choice of fuelling channel has to be made. Certain rejection rules are used to reduce the number of fuel channel candidates among which a suitable fuel channel has to be chosen. For example one can set a criterion that if the fuel channel discharge burnup is more than 75% of the design value, it will be considered for refueling. This is not a very large-sized problem and is being done at site on daily basis. Other problems related to PHWRs are design of TPMS and a suitable algorithm for FMS. The problems studied in thesis are listed below.

2.3.1. Loading pattern for initial stage of PHWR

The initial stage starts with the fresh reactor loaded with fresh NU fuel and needs no refueling for about 150 Full Power Days (FPD). However, during this period, the power peaking is much higher than in the equilibrium stage and hence the reactor has to be operated at lower power (~70%FP in 220 MWe, ~88%FP in 700 MWe). For economy, it is desirable to operate the reactor at close to Full Power. For this, some Thorium or Depleted Uranium (DU) bundles are loaded in the core. Thorium has zero fission cross section for thermal neutrons. DU has lower (from ~0.6wt% to ~0.3wt% U^{235}) fissile content than NU (0.7115wt% U^{235}). The locations of Thorium or DU bundles have to be chosen in such a way that following conditions are fulfilled:

1) Power peaking is reduced and maximum power can be drawn.

2) K-effective is maximized as far as possible.

3) Bundle power and channel power remain within limits.

4) The sufficient reactivity worth is possessed in the shut-down devices.

The main difficulty in deciding best fresh core loading pattern is that the total number of possible arrangements of NU and Thorium/DU bundles can be extremely large. For example: there are 306 fuel

channels and each channel contains 12 fuel bundles. Thus there are 306×12=3672 fuel bundle locations. Suppose one uses 30 Thorium bundles to obtain the desired level of flux/power flattening, this can be done in $^{3672}C_{30}$ ways (approximately 10^{75}). In order to choose the best configuration, a brute force approach of trying all possible combinations is absolutely impossible because such a large number of diffusion calculations cannot be carried out even with the best supercomputer in the world.

The problem of determining fresh core loading pattern is solved here using a novel approach based on evolutionary algorithms.

2.3.2. Selection of instrumented channels for thermal power measurement system

There are 392 horizontal fuel channels in 700 MWe PHWR. It is necessary to select ~44 fuel channels (out of 392) for keeping instrumentation to measure flow and temperature of coolant. The selection of instrumented channels is to be made such that the average of power values measured by them in terms of per unit basis represents the true zone-wise and global powers fairly accurately. This should be possible for a large number of reactor configurations that can occur because of the movement of reactivity devices in the core. This capability is useful to make the TPMS more accurate means to measure the reactor bulk power and zone powers. The selection of 44 fuel channels for instrumentation is an optimization problem which has to satisfy the following constraints:

(1) Total 44 numbers of channels should be selected and thus 11 numbers of channels should be there in each of the four sets of fuel channels.

(2) The channels which have been selected for instrumentation should not be symmetric about X-axis.

(3) Nowhere a gap of 4 pitch × 4 pitch or more should be left without a instrumented channel.

(4) Each Zone Control Detector (ZCD) should have minimum two ICs at nearby location.

The problem of selecting instrumented channels for Thermal Power Measurement System is solved here using evolutionary algorithm.

2.3.3. Optimization of flux mapping algorithm for flux map generation

There are 102 vanadium self powered neutron detectors (SPNDs) in 700 MWe PHWR. They are well distributed inside the reactor core. With the help of these detector readings, one has to continuously estimate the detailed power distribution inside the reactor. This is achieved by the so-called Flux Mapping System (FMS). Apart from detector readings, the FMS makes use of the fact that flux shape is

governed by neutron diffusion theory. A detailed flux map is created by FMS every two minutes. It is used to calibrate the zonal detectors so that they correctly reflect the zonal powers. The maximum bundle power and channel power are also estimated to take corrective action if necessary.

The objective of FMS can be achieved by various algorithms. The computation by FMS has to be carried out every 2 minutes. Hence, the calculation should be fast enough. The resultant flux map is used for reactor regulation and to monitor channel powers and bundle powers. Hence, the calculation should be fairly accurate. These two requirements conflict with each other. Hence, an optimum choice has to be made from amongst the various computational algorithms suggested for this purpose. Some of the algorithms are based on modal method. In such methods, the number of modes needs to be optimized.

Here, apart from studying existing algorithms, a hybrid algorithm is suggested as an optimum choice.

CHAPTER 3

SIMULATION OF PHWR CORE

In order to solve optimization problems discussed in chapter 2, it is necessary to simulate the neutronic behaviour in a PHWR for any specified configuration and obtain important parameters such as effective multiplication factor and power distribution. The computational methods employed for this purpose are discussed in this chapter.

3.1. Introduction

The subject of reactor physics is an art of applying the suitable method for analyzing and performing the computations associated with the nuclear system. The reactor physics in a single statement can be described as the estimation of neutrons and their reaction rates with target nuclei. In reactor core calculation for all kind of reactors, we are mainly interested in determining reaction rates for individual reactions and leakage from the core. Strictly speaking, the neutron population and related quantities will have fluctuations. Usually our interest is to determine the average behavior. The average behavior of neutrons is rigorously described by the Boltzmann Transport equation. In transport theory, in the most general case, the directional flux $\Psi(r,\Omega,E,t)$ at position r, with energy E, in direction Ω at time t; is the unknown variable to be determined. In most practical cases, the equation has to be solved numerically. The independent variables have to be discretised. The energy variable is usually replaced by groups. The r and Ω are also discretised in some way. The computational effort and memory requirements are prohibitively large for a numerical solution for 3-dimensional fine energy-group problems. The most common approach is to use transport theory for small repetitive structures (called lattices) occurring in the reactor in 2-D using fine energy group structure from which few group homogenized cross-sections for the full lattice are obtained. The full-core calculations are done in few energy groups using the homogenized cross-sections by the so-called “diffusion theory” which is an approximation to transport theory. In diffusion equation, the directional variable is absent and is much easier to solve than the transport equation.

In what follows, the time-dependent neutron transport equation is described. Thereafter, the static K-eigenvalue form is presented. Later, the simpler diffusion equation is presented. The levels at which transport and diffusion theories are used are explained.

3.2. Neutron Transport Equation

The transport theory was first proposed in 1800's for kinetic theory of gases in the form of Boltzmann equation. The neutron transport equation is a simpler form in which non-linear collision term is absent. After the invention of chain-reacting nuclear reactors in 1940s, the neutron distributions were found in simple geometries using elegant approximations and analytic solutions. However, as computational power has increased, numerical approaches to neutron transport have become prevalent. The following assumptions are made in the derivation of the neutron transport equation [3]:

(i) Neutron is considered as a classical point particle. The De Broglie wave length of neutron is small compared to the inter-atomic distances between collisions. Hence, it can be adequately described by a point location and velocity.

(ii) Neutrons travel in straight line between two collisions: Neutrons have no charge, and therefore, long-range electrical and magnetic forces do not alter their straight-line trajectories.

(iii) Neutron - neutron collisions may be neglected: In nuclear reactors and radiation shields, the neutron densities are small compared with atomic densities and so neutron - neutron collisions can be neglected.

(iv) Collision may be considered instantaneous: After a collision, the emerging particles are emitted immediately for all practical purposes. The only exception is the fission reaction in which a small fraction of neutrons are being emitted by fission products. These delayed neutrons are incorporated as a separate term in the neutron transport equation.

(v) The material properties are assumed to be isotropic: This assumption is valid for reactor media.

(vi) The properties of the nuclei and the composition of materials under consideration are assumed to be known.

(vii) The expected or mean value of the particle density distribution is considered. Fluctuation about the mean is not considered.

Based on above assumptions, the neutron transport equation is derived by considering the rates at which neutrons of different energies moving in different directions enter and leave a small phase space element. The integro-differential form of the neutron transport equation can be written as:

$$\frac{1}{v}\frac{\partial}{\partial t}\psi(r,\Omega,E,t)+\Omega\nabla\psi(r,\Omega,E,t)+\Sigma_t(r,E)\psi(r,\Omega,E,t)=q_f(r,\Omega,E,t)+q_s(r,\Omega,E,t)+S(r,\Omega,E,t) \qquad (3.1)$$

where $\psi(r,\Omega,E,t)$ is neutron flux at r having energy E and moving in direction Ω at time t. The fission source $q_f(r,\Omega,E,t)$ denotes sum of prompt source $q_p(r,\Omega,E,t)$ and delayed neutrons source $q_d(r,\Omega,E,t)$. The rate at which prompt neutrons are produced can be expressed as

$$q_p(r,\Omega,E,t)=\frac{1}{4\pi}\chi_p(r,E)(1-\beta)\int\int dE'\,d\Omega'\ \nu\Sigma_f(r,E')\psi(r,\Omega',E',t) \qquad (3.2)$$

The delayed neutrons arise from the decay of a variety of fission products. For neutron kinetics considerations these are usually divided into six groups, each with a characteristic decay constant λ_i. The net yield β is summation over all six group-yields β_i. If the concentration of the fission product precursors for any delayed group is $C_i(r,t)$, then the rate at which delayed neutrons are produced can be expressed as

$$q_d(r,\Omega,E,t)=\frac{1}{4\pi}\sum_i \chi_d^i(r,E)\lambda_i C_i(r,t) \qquad (3.3)$$

The source of neutrons due to scattering with other nuclei can be expressed as

$$q_s(r,\Omega,E,t)=\int dE'\int d\Omega'\Sigma(r,E'\to E,\Omega'\to\Omega)\psi(r,\Omega',E',t) \qquad (3.4)$$

An additional equation is also required for each group precursor concentration for solving the neutron transport equation. The net rate of change in the precursor concentration is

$$\frac{\partial}{\partial t}C_i(r,t) \quad = \quad \beta_i\int dE\,\nu\Sigma f(r,E)\psi(r,E,t) - \quad \lambda_i C_i(r,t) \qquad (3.5)$$

The notations used to describe neutron transport equation are the following:

$\psi(r,\Omega,E,t)$: Neutron flux at location (r) with energy (E) along direction (Ω) at time (t)

$\Sigma_t(r,E)$: Total macroscopic cross section at location (r) for a neutron of energy (E)

$S(r,\Omega,E,t)$: All neutron sources other than scattering and fission, i.e. external source

$\Sigma(r,E'\to E,\Omega'\to\Omega)$: Macroscopic differential scattering cross section, describing the transfer of neutrons with initial coordinates (r,E',Ω') to (r,E,Ω)

$\nu \sum_f (r, E)$: Fission production macroscopic cross section at location (r) for neutron of energy E

We are mainly concerned with steady state K-eigenvalue problem that can be written as

$$\Omega.\nabla \psi(r,\Omega,E) \quad + \sum_t (r,E)\psi(r,\Omega,E) - q_s(r,\Omega,E) = \frac{1}{K} q'_f(r,\Omega,E) \tag{3.6}$$

where $$q'_f(r,\Omega,E) = \frac{1}{4\pi}\chi_p(r,E)\int \int dE' d\Omega' \ \nu \sum_f (r,E')\psi(r,\Omega',E') \tag{3.7}$$

Neutron balance is enforced by dividing fission source by K. There is no distinction between prompt and delayed neutron source.

The cross sections are the quantities which define the neutron interaction probabilities. The cross sections of each material are highly dependent on the energy of the incident neutron. At reasonably low energies of incident neutrons, cross sections are quite smooth in energy. However, as the energy increases, the cross sections are dominated by resonance peaks that result from unstable state of compound nucleus formed by the collision. In the off-resonance region, the variation in cross section shows $1/E^{1/2}$ or 1/v dependence. The deterministic neutron transport codes usually use appropriately generated multi-group cross section libraries.

The neutron transport equation is usually solved for finite region or space, in which cross-sections are known. There exist an infinite number of possible solutions of the neutron transport equation within any spatial region and hence, appropriate neutron angular density at the boundary of the region is needed to determine which of the solution corresponds to that physical problem. At the external boundary of a reactor, there are no incoming neutrons and free surface boundary conditions are used:

$$\psi(r,\Omega,E) = 0 \qquad if \quad n.\Omega < 0 \tag{3.8}$$

where n is unit vector normal to external surface. If transport theory is used to simulate the repetitive lattice structure, reflective or white boundary condition is used.

3.3. Neutron Diffusion Equation

Because of its relative simplicity and range of applicability, the diffusion approximation to the Boltzmann neutron transport equation is widely used for reactor core simulation. Diffusion theory is sufficiently accurate to provide a quantitative understanding of many physics features of nuclear reactors and is, in fact, the workhorse computational method of nuclear reactor physics. The problem for which

very high accuracy is not required, or the calculation on large systems, in which the important regions are several neutron mean free paths in thickness, diffusion theory is used.

The angular flux and scattering function is expanded in terms of spherical harmonics. The term up to linearly anisotropic scattering are retained leading to the P_1 approximation. The P_1 approximation to the one-speed transport theory is equivalent to ordinary diffusion theory in a source free medium regardless of whether the scattering is isotropic or anisotropic. In multi-group theory, however, scattering from higher groups constitutes an anisotropic source and then diffusion theory and P1 approximation are not equivalent.

The essential postulate of diffusion equation is Fick's law, which assumes that the neutron current J(r,E) is given by a diffusion coefficient D(r,E) multiplied by the gradient of the flux; thus,

$$J(r,E) = -D(r,E)\frac{\partial \phi(r,E)}{\partial r} \tag{3.9}$$

The leakage term is $\nabla . J(r,E)\ or\ -\nabla D(r,E)\nabla\phi(r,E)$.

Three major approximations which lead to neutron diffusion equation are as follows [4]:

(1) The first major approximation leading to diffusion theory is made that the flux is assumed to be sufficiently slowly varying in space.

(2) The second major approximation that integral of in-scattering of neutrons from all energies to energy E is equal to the integral of out-scattering of neutrons from energy E to all other energies. When there is a weak absorber ($\Sigma_a \ll \Sigma_s$), these two quantities balance each other.

(3) The third assumption that the neutrons are scattered isotropically.

The diffusion theory will not be valid near and inside an absorber like shut-off rod. It is also not accurate near external boundary of the reactor. However, usually the reactor is large-sized with a thick reflector. The flux is small at the periphery and it is a good approximation zero neutron flux as a boundary condition on the external surface.

The mathematical formulation of neutron diffusion theory is obtained by using the Fick's law:

$$-\nabla . D\nabla\phi(r,E) + \sum_t (r,E)\phi(r,E) = \int dE' \sum_s (r,E' \to E)\phi(r,E') + \frac{\chi(E)}{K}\int dE'\ \nu\sum_f (r,E')\phi(r,E') \tag{3.10}$$

The angular fluxes are collapsed as $\phi(r,E) = \int \psi(r,E,\Omega)d\Omega$

The (time-independent) multigroup neutron diffusion equations in K-eigenvalue form are a system of coupled elliptic partial differential equations of second order and can be written, as follows

$$-\nabla D_g(r)\nabla\phi_g(r) + \Sigma_g^r(r)\phi_g(r) - \sum_{g'\neq g}\Sigma_{g'\to g}(r)\phi_{g'}(r) = \frac{1}{K}\chi_g\sum_{g'}\nu\Sigma_{g'}^f(r)\phi_{g'}(r) \quad ; \quad g = 1,2,3.. \tag{3.11}$$

The following group-dependent boundary conditions is used

$$D_g(r)\frac{\partial\phi_g(r)}{\partial n} + \alpha_g(r)\phi_g(r) = 0 \quad ; where \quad r \in \Gamma \tag{3.12}$$

Here g represents the energy group of the neutron and n is the normal outwardly directed to the boundary surface Γ. The notations $D_g(r)$, $\Sigma^r_g(r)$, $\upsilon\Sigma^f_g(r)$ represent diffusion coefficient, removal cross section and υ times fission cross sections at location r respectively.

3.2.1. Discretization of neutron diffusion equation

The neutron diffusion equation is solved for practical problems using standard numerical analysis techniques such as finite-difference method. The continuous diffusion equation problem is converted to discrete representations by using meshes. The mesh centered finite difference approximation is used to convert the analytical diffusion equation to a system of linear coupled algebraic equations.

The two energy group analytical neutron diffusion equation can be written as

$$-\nabla D_1(r)\nabla\phi_1(r) + \Sigma_1^r(r)\phi_1(r) = \frac{1}{K}[\nu\Sigma_1^f(r)\phi_1(r) + \nu\Sigma_2^f(r)\phi_2(r)] \tag{3.13}$$

$$-\nabla D_2(r)\nabla\phi_2(r) + \Sigma_2^r(r)\phi_2(r) - \Sigma_{1\to 2}^s(r)\phi_1(r) = 0 \tag{3.14}$$

In the above equation the up scattering cross-section $\Sigma^s_{2\to 1}(r)$ is assumed to be zero. In 3-D Cartesian geometry the mesh will be chosen such that the different lattice interfaces coincide with mesh surfaces while the mesh points are at centre of mesh volumes. It is called mesh centered finite difference scheme [5].

The integration is carried out over the mesh volume ΔV_k. The volume integration to the first term (leakage term) of diffusion equation transforms it into a surface integral owing to the divergence theorem.

$$\int -\nabla.(D\nabla\phi)dV = \oint -(D\nabla\phi).ndS = \oint \left(-D\frac{\partial\phi}{\partial n}\right)dS = \sum_{j=1}^{6} J_{kj}\Delta S_{kj} \tag{3.15}$$

Here, $J_{kj}$are net currents from mesh volume k to mesh volume j, averaged over their common surfacesΔS_{kj}. Replacing the volume averaged quantities by midpoint value of diffusion equation terms give

$$\sum_j J_{kj}\Delta S_{kj} + \sum_k^r \phi_k \Delta V_k \quad = Q_k \Delta V_k \tag{3.16}$$

Where, Q represents the fission and scattering neutron source. If $\phi_{kj}$is the redundant flux on the surface $\Delta S_{kj}$and $J_{kj}$the net current from k to j, the new quantities can be defined using diffusion coefficient using mesh size i.e. $\Delta_x, \Delta_y, \Delta_z$ as:

$$\mathrm{d_x} = \frac{\mathrm{D}}{\Delta_\mathrm{x}}; \quad \phi_{kj} = \frac{d_k\phi_k + d_j\phi_j}{d_k + d_j}; \quad d_{kj} = \frac{2d_k d_j}{d_k + d_j}; \quad J_{kj} = d_{kj}(\phi_k - \phi_j) \tag{3.17}$$

The seven point discrete diffusion equation becomes

$$\sum_j \Delta S_{kj} d_{kj}(\phi_k - \phi_j) + \sum_k^r \phi_k \Delta V_k \quad = Q_k \Delta V_k \tag{3.18}$$

3.2.2. Solving neutron algebraic equation

The two energy group linear coupled algebraic neutron diffusion equation can be written as

$$\sum_j \Delta S_{kj} d_{kj}(\phi_{1,k} - \phi_{1,j}) + \sum_{1,k}^r \phi_{1,k}\Delta V_k \quad = \frac{1}{K}\{\nu\sum_{1,k}^f \phi_{1,k} + \nu\sum_{2,k}^f \phi_{2,k}\}\Delta V_k \tag{3.19}$$

$$\sum_j \Delta S_{kj} d_{kj}(\phi_{2,k} - \phi_{2,j}) + \sum_{2,k}^r \phi_{2,k}\Delta V_k \quad - \sum_{1\to 2,k}^s \phi_{1,k}\Delta V_k = 0 \tag{3.20}$$

For 3-D Cartesian geometry flux in each mesh point is directly related only to the flux in its six neighbors. If diffusion equation is solved for a system having Im×Jm×Km meshes in x, y and z direction respectively, then the two energy group coupled algebraic neutron diffusion equation can be represented in matrix form as

$$M\phi = \frac{1}{K}F\phi \tag{3.21}$$

The matrix M represents capture, leakage and group-to-group transfers. The matrix F is fission source operator. Both M and F are square matrices of dimension {2×Im×Jm×Km} and ϕ is a vector with dimension {2×Im×Jm×Km}. Here, K stands for eigenvalue. The above equation has a large number of eigenvalues K_i and corresponding eigenfunctions ϕ_i. All K eigenvalues are real positive and they can be arranged as $K_1 > K_2 \geq K_3$ .. etc. The largest value K_1 is the fundamental eigenvalue usually denoted by K_{eff}.

The corresponding mode is the fundamental mode. One is usually interested in finding the fundamental mode. The most common method to obtain the fundamental mode is the power iteration method and it is implemented via the so-called inner and outer iterations as described below. Equation (3.21) can be written as,

$$M^{-1}F\phi = K\phi \tag{3.22}$$

Thus the problem is to find largest eigenvalue and corresponding eigenvector of $M^{-1}F$. The basic idea in Power Iteration method is that if an arbitrary guess vector is repeatedly multiplied by M^{-1} F (and normalised), it will approach the fundamental eigenvector. In practice, the multiplication by $M^{-1}F$ is implemented (without explicitly finding M^{-1} F) by carrying out certain inner and outer iterations [6]. One starts with a guess value for K and the fission source vector Fϕ which are denoted by k^1 and $F\phi^1$. The superscript 1 indicates the outer iteration number. The successive outer iterations can be shown as:

$$M\phi^{i+1} = \frac{1}{K^i}F\phi^i \tag{3.23}$$

$$K^{i+1} = K^i \frac{||F\phi^{i+1}||}{||F\phi^i||} \tag{3.24}$$

The main task is to solve Eq.(3.23) to evaluate ϕ^{i+1} (which equals $M^{-1}F\phi^i/K^i$). Usually, this is done by solving the problem group wise. Starting from the 1st energy group, an external fixed source problem is solved for each group. The fixed source consists of two types of contributions: one from fission source on R.H.S. of Eq.(3.23) and second from scattering of neutrons in other groups which is contained in matrix M. Such an equation for group g can be written as:

$$\nabla \cdot D_g \nabla \phi_g - \Sigma_g^R \phi_g = Q_g \tag{3.25}$$

where Q_g is the external source. If n=2×Im×Jm×Km, the CPU time required for a non-iterative method (i.e. direct methods) to solve Eq. (3.25) and find group fluxes scales in general as n^3. The direct methods like Gauss Elimination suffer from what is called fill-in (many zero elements becoming non-zeros). Hence, for large size system, iterative methods (like Gauss-Seidel iteration) offer better performance. For Gauss-Seidel iteration it is explained as follows:

Eq.(3.25) can be written in matrix form as:

$$A\,\phi_g = Q_g \tag{3.26}$$

A is a symmetric diagonally dominant matrix of order Im×Jm×Km. A is split into a diagonal, strictly lower triangular and strictly upper triangular parts giving:

$$(D - L - U)\,\phi_g = Q_g \tag{3.27}$$

The Gauss-Seidel (or inner) iterations can be shown as:

$$(D\text{-}L)\,\phi^{j+1}{}_g = U\phi^{j}{}_g + Q_g \tag{3.28}$$

where j is iteration number. The convergence criterion for inner iterations is (for all energy groups separately):

$$\frac{|\phi^{i+1} - \phi^{i}|}{\phi^{i}} < \epsilon 1 \tag{3.29}$$

It is possible to have over-relaxation in above iterations.

Eq.(3.28) is solved by using Gauss-Seidel iterations for all the groups. The convergence of the Jacobi method depends upon the spectral radius of $D^{-1}(L+U)$. The Gauss-Seidel method is an improvement over Jacobi method, where inverse of $(D-L)$ is considered. In case of upscattering, one may have to repeat these within-group calculations till group-to-group scattering sources converge. These calculations give the flux vector ϕ^{i+1} containing all group fluxes, which is solution of Eq.(3.21). Using the computed ϕ^{i+1}, the fission source vector $F\phi^{i+1}$ is computed and K^{i+1} is evaluated by using Eq.(3.22). The outer iterations are continued till successive values of K and fission source vector are close within a convergence criterion. Most of the well-established reactor physics codes are based on this method. The computer code 'DOLP' has been developed based on this approach. The power iteration method converges slowly if the dominance ration K_2/K_1 is close to unity.

The convergence criteria for multiplication factor K can be written as:

$$\frac{|K^{i+1} - K^{i}|}{K^{i}} < \epsilon 2 \tag{3.30}$$

In similar way the convergence criteria for fission source can also be written. Acceleration of the power iteration method and use of alternative efficient schemes has been an active field of research for a long time. One of the most popular acceleration schemes has been the Chebyshev acceleration scheme [7]. There exists another quite efficient approach based on Orthomin(1) algorithm [8] to solve the eigenvalue problem $M\phi = \lambda F\phi$. The residual vector $r = M\phi - \lambda F\phi$ is determined. The function $f(\phi) = (r, r)$ is minimized in Orthomin(1) algorithm. The algorithm used for chebyshev acceleration

and Orthomin(1) are shown in Fig.3.1 and Fig.3.2 respectively. A comparison of CPU time is made between power iteration, Chebyshev method and Orthomin(1) algorithm for a typical case. It is presented in Fig.3.3.

Chebyshev Extrpolation

In the two parameter Chebyshev method, the first n^* (=3) iterations are carried out as simple power iterations. Subsequently parameters α and β are computed and used to extrapolate the fission source vector as shown below.
Each outer-iteration fission source vector is extrapolated as

$$\underline{S}^{(n^*+p)} = \underline{S}^{(n^*+p-1)} + \alpha_p [S^{(n^*+p)} - \underline{S}^{(n^*+p-1)}] + \beta_p [\underline{S}^{(n^*+p-1)} - \underline{S}^{(n^*+p-2)}]$$

Where, $\underline{S}$ denotes the extrapolated vector. And S denotes un-extrapolated vectors. The superscript of S is outer iteration number. The parameters α and β are given as

$$\alpha_p = \frac{1}{\frac{2-d}{2} - \frac{d^2 \alpha_{p-1}}{16}}$$

$$\beta_p = \frac{(2-d)\alpha_p}{2} - 1$$

$\alpha_1 = \frac{2}{2-d}$; $\beta_1 = 0.0$; d is dominance ratio and is estimated using latest source vectors.

Figure 3.1: Chebyshev acceleration method

Orthomin(1) algorithm to solve Ax= λBx

1. Choose x_0
2. $\lambda_0 = \frac{(Ax_0, Bx_0)}{(Bx_0, Bx_0)}$
3. $r_0 = \lambda_0 Bx_0 - Ax_0$
4. $s_0 = r_0$
5. For i=0,1,2,…….until convergence, Do:
6. $\alpha_i = \frac{\{(r_i, As_i) - \lambda_i (r_i, Bs_i)\}}{\{(As_i, As_i) - 2\lambda_i (As_i, Bs_i) + \lambda_i^2 (Bs_i, Bs_i)\}}$
7. $x_{i+1} = x_i + \alpha_i s_i$
8. $\lambda_{i+1} = \frac{(Ax_{i+1}, Bx_{i+1})}{(Bx_{i+1}, Bx_{i+1})}$
9. $r_{i+1} = \lambda_{i+1} Bx_{i+1} - Ax_{i+1}$
10. $\beta_i = \frac{-[(Ar_{i+1}, As_i) - \lambda_{i+1}\{(Ar_{i+1}, Bs_i) + (As_i, Br_{i+1})\} + \lambda_{i+1}^2 (Br_{i+1}, Bs_i)\}}{\{(As_i, A s_i) - 2\lambda_{i+1} (As_i, Bs_i) + \lambda_{i+1}^2 (Bs_i, Bs_i)\}}$
11. $s_{i+1} = r_{i+1} + \beta_i s_i$
12. End Do

Figure 3.2: Orthomin(1) algorithm

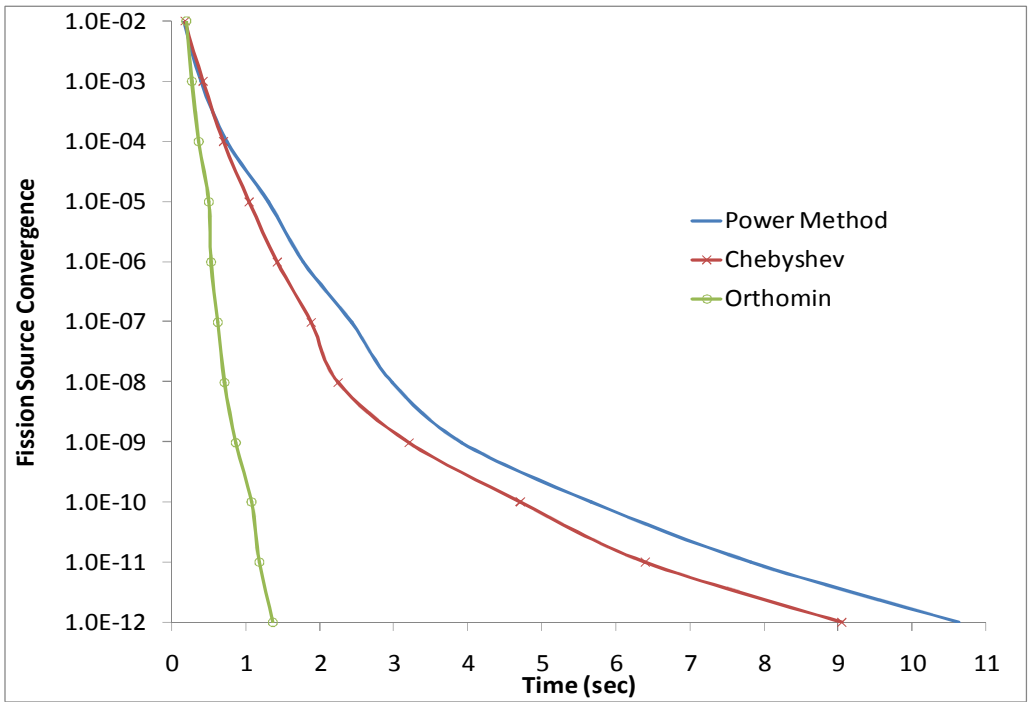

Figure 3.3: Comparison of power iteration, Chebyshev and Orthomin(1) CPU time

The comparison of CPU time among power iteration, Chebyshev acceleration method and Orthomin(1) algorithm indicated that Orthomin(1) algorithm is an efficient method to solve the K-eigenvalue problem.

3.3. Reactor Core Simulation

The relative geometric arrangement of fuel bundles, pressure tubes, coolant materials, calandria tubes, moderating material follows regular patterns inside the core. These patterns are referred to as lattices. At lattice level, the local flux varies strongly and resonance effect, interaction at boundaries of different materials etc are important. The Evaluated Nuclear Data File (ENDF/B-VI.8) collapsed in multi-group is used as the main source of nuclear cross sections of different materials. The lattice cell calculation is carried out to condense the vast amount of basic nuclear data relating to its constituent materials into a relatively small number of parameters that can be used subsequently during the full core simulation. Therefore, to cope with the complexity of the problem, full core simulation is broken down in to smaller problems that are treated separately as lattice cell simulation and full core simulation. The lattice cell may be regarded as the smallest part of the reactor that has the properties of a self-sustaining chain reacting assembly. It is assumed that the complete reactor core is comprised of numerous unit

lattice cells. An important feature in reactor core analysis which is taken care in lattice calculation is that the cross-sections for typical heavy nuclides exhibit resonances. The flux drops substantially in the resonance energy range. Self shielding calculation is done to recover effective microscopic cross sections for a resonant reaction.

Two energy group homogeneous cross-sections are generated for a lattice by solving neutron transport equation. The computer code CLUB [9] is used for this purpose. The lattice geometrical details and ENDF/B-VI.8 cross section library serves as input and two energy group homogeneous lattice cross-sections are derived as output.

There are various reactivity devices in the core, which are located in between fuel channels. The presence of these devices, alter the 2 groups cross-section of the lattice cell. Thus a super cell calculation is required for the lattices, which are affected by the reactivity devices. This calculation is performed, by using the transport theory code BOXER [10]. This code gives the homogenized 2 group incremental cross-sections of the lattice cell affected by the particular reactivity device.

These two energy group homogeneous lattice cross sections are used in solving the neutron diffusion equation over full reactor core. Diffusion theory is a simple and less expensive scheme for modeling neutron transport. A computer code has been developed for this purpose. The differential equation has been discretised by finite-difference methods. Orthomin(1) algorithm is available for fast convergence. A flow chart diagram for reactor core simulation is presented in Fig.3.4.

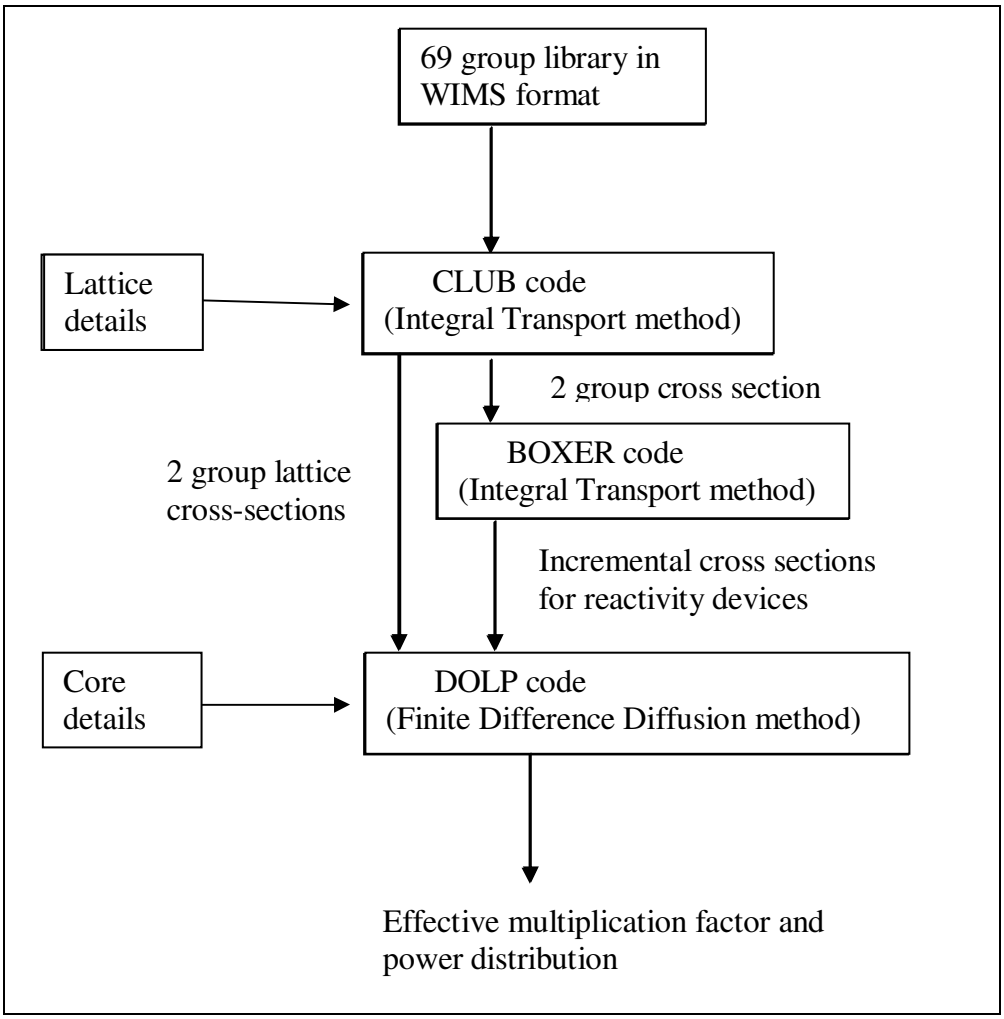

Figure 3.4: Flow chart diagram for reactor core simulation

CHAPTER 4

OPTIMIZATION TECHNIQUES IN PERSPECTIVE

Optimization means maximization or minimization of one or more functions with any possible constraints. In this chapter different types of optimization techniques are described briefly with emphasis on those that are used in the present dissertation.

4.1. Introduction

The origin of optimization methods can be traced from 300 BC when Euclid identified the minimal distance between two points to be length of straight line joining the two. He also proved that a square has the greatest area among the rectangles with given total length of edges. Heron proved in 100 BC that light travels between two points through the path with shortest length when reflecting from a mirror. Before the invention of calculus of variations, the optimization problems like, determining optimal dimensions of wine barrel in 1615 by J. Kepler, a proof that light travels between two points in minimal time in 1657 by P. De Fermat were solved. I. Newton (1660s) and G.W. von Leibniz (1670s) created mathematical analysis that forms the basis of calculus of variation. L. Euler's publication in 1740 began the research on general theory of calculus of variations.

The method of optimization for constrained problems, which involve the addition of unknown multipliers, became known by the name of its inventor, J. L. Lagrange. Cauchy made the first application of the gradient method to solve unconstrained optimization problems in 1847. G. Dantzig presented Simplex method in 1947. N. Karmarkar's polynomial time algorithm in 1984 begins a boom of interior point optimization methods. The advancement in solution techniques resulted several well defined new areas in optimization methods.

The linear and non-linear constraints arising in optimization problem can be easily handled by penalty method. In this method few or more expressions are added to make objective function less optimal as the solution approaches a constraint.

4.2. An Optimization Problem

The main components of an optimization problem are:

Objective Function

An objective function expresses one or more quantities which are to be minimized or maximized. The optimization problems may have a single objective function or more objective functions. Usually the different objectives are not compatible. The variables that optimize one objective may be far from optimal for the others. The problem with multi-objectives can be reformulated as single objective problems by either forming a weighted combination of the different objectives or by treating some of the objectives as constraints.

Variables

A set of unknowns, which are essential are called variables. The variables are used to define the objective function and constraints. One can not chose design variable arbitrarily, they have to satisfy certain specified functional and other requirements. The design variables can be continuous, discrete or Boolean.

Constraints

A set of constraints are those which allow the unknowns to take on certain values but exclude others. They are conditions that must be satisfied to render the design to be feasible.

Once the design variables, constraints, objectives and the relationship between them have been chosen, the optimization problem can be defined.

Statement of an optimization problem

An optimization problem can be stated as follows: To find $x = \begin{bmatrix} x_1 \\ x_2 \\ \vdots \\ x_n \end{bmatrix}$, which minimizes or maximizes $f(x)$;

Subject to the constraints

$$g_i(x) \leq 0; \;\; i = 1,2,3 \ldots m$$

$$h_j(x) = 0; \;\; j = 1,2,3 \ldots p$$

Where x is an n-dimensional vector called design variable, $f(x)$ is called the objective function, and $g_i(x)$ and $h_j(x)$ are known as inequality and equality constraints respectively. This type of problem is called constrained optimization problem. This problem can be represented in the following way,

Given: a function $f: A \to R$ (from some set A to set R)

Sought: an elements x_0 in A such that $f(x_0) \leq f(x)$for all x in A ("minimization") or such that $f(x_0) \geq f(x)$for all x in A ("maximization").

Typically, A is some subset of Euclidean space R^n, often specified by a set of constraints, equalities or inequalities that the members of A have to satisfy. The elements of A are called candidate solutions or feasible solutions. The function f is called an objective function, or cost function. A feasible solution that minimizes (or maximizes) the objective function is called an optimal solution. The domain A of f is called the search space. When the feasible region or the objective function of the problem does not present convexity, there may be several local minima and maxima, where a local minimum x* is defined as a point for which there exist some $\delta > 0$ so that for all x such that $\|x - x^*\| \leq \delta; \quad and \quad f(x^*) \leq f(x)$

i.e., on some region around x^* all the function values are greater than or equal to the value at that point. In a similar manner local maxima can be defined.

A large number of algorithms for solving non-convex problem are not capable of making a distinction between local optimal solutions and global optimal solutions.

4.2. Classification of Optimization Problems

Optimization problems can be classified based on the type of constraints, nature of design variables, nature of the equations involved and type & number of objective functions. These classifications are briefly discussed below.

- ***Based on existence of constraints***

A problem is called constrained optimization problem if it is subject to one or more constraints otherwise it is called unconstrained.

- ***Based on the nature of the equations involved***

Based on the nature of equations for the objective function and the constraints, optimization problems can be classified as linear and nonlinear programming problems. The classification is very useful from a

computational point of view since many predefined special methods are available for effective solution of a particular type of problem.

(i) Linear Programming problem

If the objective function and all the constraints are 'linear' functions of the design variables, the optimization problem is called a *linear programming problem* (LPP). In such case objective function $f(x)$, inequality constraints $g_i(x)$ and equality constraints $h_j(x)$ are linear.

(ii) Quadratic programming problem

If the objective function is a quadratic function and all constraint functions are linear functions of optimization variables, the problem is called a quadratic programming problem. It is possible to solve Quadratic Programming problems using extensions of the methods for LPP.

(iii) Nonlinear programming problem

If any of the functions among the objectives and constraint functions is nonlinear, the problem is called a *nonlinear programming* (NLP) *problem*. This is the most general form of a programming problem and all other problems can be considered as special cases of the NLP problem.

- ***Based on the permissible values of the decision variables***

(i) Integer programming problem

If some or all of the design variables of an optimization problem are restricted to take only integer (or discrete) values, the problem is called an *integer programming problem.* For example, the optimization is to find number of articles needed for an operation with least effort. Thus, minimization of the effort required for the operation being the objective, the decision variables, i.e. the number of articles used can take only integer values. Other restrictions on minimum and maximum number of usable resources may be imposed.

(ii) ***Real-valued programming problem***

A real-valued problem is that in which it is sought to minimize or maximize a real function by systematically choosing the values of real variables from within an allowed set. When the allowed set contains only real values, it is called a real-valued programming problem.

- ***Based on the number of objective functions***

Under this classification, objective functions can be classified as single-objective and multi-objective programming problems.

(i) ***Single-objective problem:*** Problem in which there is only a single objective function.

(ii) ***Multi-objective problem:*** A multi-objective programming problem can be stated as follows:

Find x which minimizes $f_1(x), f_2(x), \ldots f_k(x)$; Subject to $g_j(x) \leq 0$, $j = 1, 2, \ldots, m$

where $f_1, f_2, \ldots f_k$ denote the objective functions to be minimized simultaneously. There are m number of constraints also. For multi-objective optimization problems one tries to find good trade-offs rather than a single solution as in single objective problems. The most commonly used notion of the 'optimum' proposed by Pareto is depicted as follows. A vector of the decision variable x is called Pareto Optimal (efficient solution) if there does not exist another y such that $f_i(y) \leq f_i(x)$ for $i=1,2,3...k$ with $f_j(y) < f_i(x)$ for at least one j. In other words a solution vector x is called optimal if there is no other vector y that reduces some objective functions without causing simultaneous increase in at least one other objective function.

4.3. Solution of Optimization Problems

The choice of suitable optimization method depends on the type of optimization problem. Various classical methods were there to solve such problems. The major advances in optimization occurred only after the development of fast digital computers. Now days various advanced optimization techniques are used to solve the design and operation related nuclear reactor problems.

4.3.1. Classical optimization techniques

The classical optimization techniques are useful for single as well as multi dimensional optimization problems. Few popular classical optimization techniques are described below.

4.3.1.1. Direct methods

Direct methods are simple brute force approaches to exploit the nature of the function. These methods do not require evolution of derivatives at any points. For one-dimensional problem golden-section search or quadratic interpolation method can be used whereas, for multi-dimensional problem random search or univariate search method can be used.

The golden-section search [11] is a simple, general-purpose, single-variable search technique. The method starts with two initial guess (i.e. lower and upper bound points). The interior point is chosen

according to the golden ratio ($\frac{\sqrt{5}-1}{2}$). The function is evaluated at new points and accordingly lower or upper bound point is changed.

Quadratic interpolation method [11] is based on the fact that there will be only one quadratic connecting three points and a quadratic polynomial often provides a good approximation to the objective function shape near an optimum.

As the name implies, the random search method repeatedly evaluates the function at randomly selected values of independent variables. If a sufficient number of samples are used, the optimum will eventually be located. This method works well even for the discontinuous and non-differentiable functions and it always finds global rather than local optimum point. The main drawback of this method is that it does not account the behavior of function at already evaluated points. Hence if the number of independent variables grows, the required amount of effort increases enormously. Hence it is not an efficient method. In univariate search method, change is made in one variable at a time to improve the approximation while the other variables are held constant. The univariate search method is more efficient than random search method. The advanced optimization methods provide more sophisticated search because they utilize the information gathered at previously solved points.

4.3.1.2. Gradient methods

The optimization method that uses knowledge of derivative information to locate optimum point is called gradient method. The first derivatives provide slope of the function being differentiated and at optima it become zero. The slope or gradient of the function tells what direction to move locally. For one-dimensional problem Newton's method use the following technique to find optimum of *f(x)*

$$x_{i+1} = x_i - \frac{f'(x_i)}{f''(x_i)}$$

The gradient of n-dimensional function $f(x_1, x_2, x_3, \dots x_n)$ can be represented as $\nabla f^T = [\frac{\partial f}{\partial x_1}, \frac{\partial f}{\partial x_2}, \frac{\partial f}{\partial x_3} \dots .]$. The iterative scheme followed in gradient method is $x_{k+1} = x_k + \propto_k . D_k$, where $\propto_k$ and D_k are step size and direction vector respectively. In the method of steepest descent ∇f is chosen as direction vector whereas, in conjugate gradient method the direction vector is chosen such that two successive direction vectors are conjugate to each other (they can never be in same direction). The appropriate step size is determined accordingly [11].

4.3.1.3. Linear programming methods

In Linear Programming the term linear connotes that the mathematical functions representing both the objective and constraints are linear. The term Programming connotes 'scheduling' or 'setting an agenda'. For two or three dimensional linear programming problem graphical solution method can be used. The feasible solution region is determined by plotting equality and inequality constraints. The objective function can be plotted by another line for a particular point lying in feasible region. The point in feasible region for which objective function is optimum can be determined in this graphical representation method. This method has very limited practical utility. Simplex method [11] provides optima in an extremely efficient manner for linear programming problems. In the simplex method an external (slack) variable is added to convert the inequality constraints into equality constraints. The basic solution for m linear equations with n unknowns is developed by setting n-m variables to zero, and solving the m equations for m remaining unknowns. The zero variables are formally referred to as nonbasic variables, whereas the remaining m variables are called basic variables. If all the basic variables are non-negative, the result is called basic feasible solution. The optimum will be one of them.

4.3.1.4. Interior point methods

The interior point methods were popular during 1960s for solving nonlinearly constrained optimization problems because of the total dominance of simplex method for linear programming problems. After the Karmarkar's fast interior method for linear programming, interior methods are playing a growing role in the study of all kind of optimization problems. Khatchian's ellipsoid method and Karmarkar's projective scaling method [12] are the interior point method which produce solution to a linear programming problem by moving through the interior of the feasible region. The time required to solve an linear programming problem of size *n* by the simplex method is of the order 2^n (known as exponential time algorithm) where, the time consumed by interior point method is of the order of n^i (i=2 or 3, known as polynomial time algorithm). The polynomial time algorithms are computationally superior to exponential algorithms for large linear programming problems.

4.3.2. Advanced optimization techniques

Most of the real world optimization problems involve complexities like discrete, continuous or mixed variables, multiple conflicting objectives, non-linearity, discontinuity etc. The search space may be so large that the global optimum can not be found in reasonable time. The classical methods may not

be efficient to solve such problems. Various stochastic methods like simulated annealing or evolutionary optimization algorithms can be used in such situations.

4.3.2.1. Simulated annealing

The name and inspiration came from annealing process in metallurgy, a technique involving heating and controlled cooling of a material to increase the size of its crystals and reduce their defects. The heat causes the atoms to become unstuck from their initial positions (a local minimum of the internal energy) and wander randomly through states of higher energy; the slow cooling gives them more chances of finding configurations with lower internal energy than the initial one. In the simulated annealing method [13, 14], each point of the search space is compared to a state of some physical system, and the function to be minimized is interpreted as the internal energy of the system in that state. Therefore the goal is to bring the system, from an arbitrary initial state, to a state with the minimum possible energy.

4.3.2.2. Evolutionary optimization algorithms

Evolutionary algorithms (EAs) are developed to arrive at near-optimum solutions to a large scale optimization problem. The problem having very large number of decision variables and non-linear objective functions are often solved by EAs. EAs mimic the metaphor of natural biological evolution or social behavior like how ants find the shortest route to a source of food and how birds find their destination during migration. The behavior of such species is guided by learning and adaptation. A flow chart diagram is shown in Fig.4.1. The evolutionary algorithms are based on population based search procedures that incorporate random variation and selection. The first evolutionary-based optimization technique was the genetic algorithm (GA) [15]. GA was developed based on the Darwinian principle of the survival of the fittest and the natural process of evolution through reproduction. There are so many algorithms like Particle Swarm Optimization (PSO) [16], Ant Colony Optimization (ACO) [17] and Estimation of Distribution Algorithm (EDA) [18] etc. have been introduced during the past 10 years.

EAs start from a population of possible solutions (called individuals) and move towards the optimal by incorporating generation and selection. Objects forming possible solution sets to the original problem are called phenotype and the encoding (representation) of the individuals in the EAs are called genotype. The way by which mapping of phenotype to genotype is done and the EA's operators are applied to genotype affects the computational time. An individual consist a genotype and a fitness function. Fitness

represents the quality of the solution and forms the basis for selecting the individuals. A flow chart indicating the steps of a simple evolutionary algorithm is shown below.

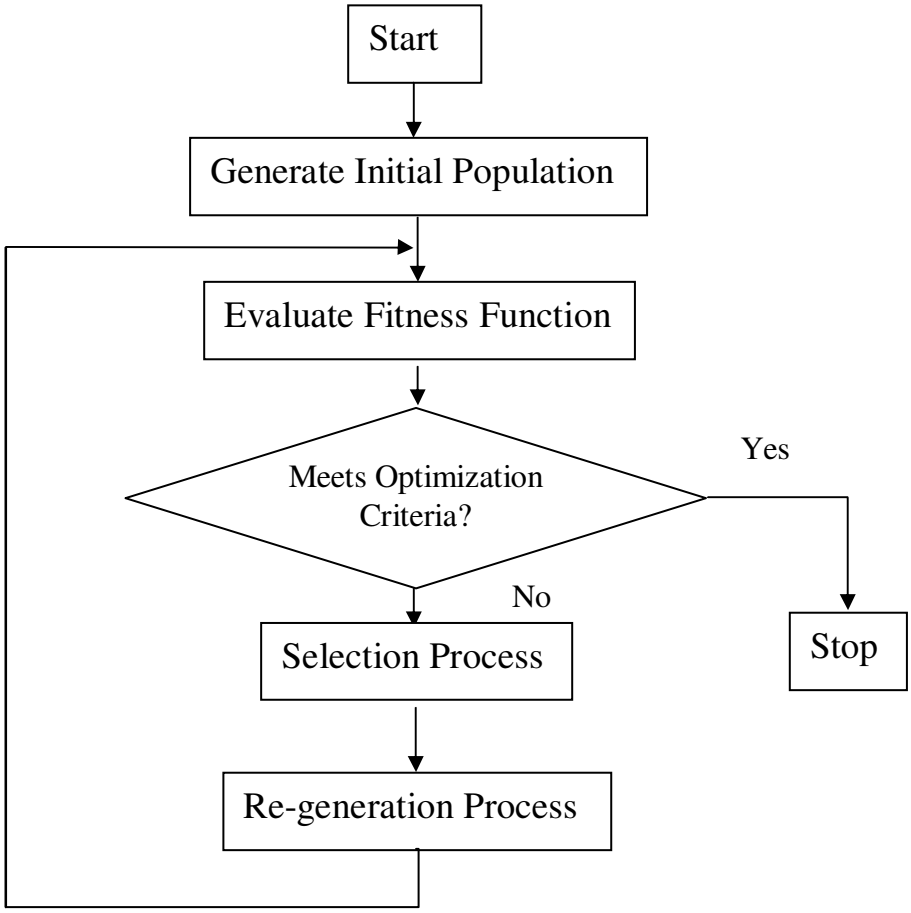

Figure 4.1: Evolutionary algorithm flow chart

• Genetic algorithms (GA)

Genetic algorithm (GA) [15] improves fitness through evolution. A solution to a given problem is represented in the form of a string, called 'chromosome', consisting of a set of elements, called 'genes' that holds a set of values for the optimization variables. GAs works with a random population of solutions. The fitness of each chromosome is determined by evaluating it against an objective function. To simulate the natural survival of the fittest process, best chromosomes exchange information (through crossover) to produce offspring chromosome. There are many methods to select the best chromosomes, for example roulette wheel selection, Boltzman selection, tournament selection, termination selection

and others. The chromosome is then mutated by changing a few genes to create a new individual. The newly generated individuals are evaluated and used to evolve the population if they provide better solutions than weak population members. This process is continued for a large number of generations to obtain a near-optimum solution. Four main parameters affect the performance of GAs are population size, number of generations, crossover rate and mutation rate.

• Estimation of distribution algorithm (EDA)

EDAs [18] are motivated by the idea of discovering and exploiting the interaction between variables in the solution. In EDAs, the two GA operations of recombination and mutation are replaced by estimation of distribution and sampling. In each generation, N individuals are generated by sampling probability distribution. The fitness is evaluated for each of them and the best M individuals are selected to estimate probability distribution. The probability distribution function is updated slowly. The performance of an EDA highly depends on how well it estimates and samples the probability distribution.

• Some other algorithms

The Particle Swarm Optimization (PSO) [16] is inspired by the social behavior of a flock of migrating birds trying to reach an unknown destination. In PSO, each solution is a bird in the flock and is referred to as a particle. A particle is analogous to a chromosome in GAs. As opposed to GAs, the evolutionary process in the PSO does not create new birds from parent ones. Rather, the birds in the population only evolve their social behavior and accordingly their movement towards a destination. Each bird looks in a specific direction, and then when communicates together, they identify the bird that is in the best location. Accordingly, each bird speeds towards the best bird using a velocity that depends on its current position. Each bird, then investigates the search space from its new local position, and the process repeats until the flock reaches a desired destination.

Similar to PSO, ACO [17] population evolves not by their genetics but by their social behavior. In the real world, ants (initially) wander randomly, and upon finding food return to their colony while laying down pheromone trails. If other ants find such a path, they are likely not to keep traveling at random, but instead follow the trail laid by earlier ants, returning and reinforcing it, if they eventually find any food. Over time, however, the pheromone trail starts to evaporate, thus reducing its attractive strength. The more time it takes for an ant to travel down the path and back again, the more time the pheromones have to evaporate. A short path, by comparison, gets marched over faster, and thus the

pheromone density remains high as it is laid on the path as fast as it can evaporate. Thus, when one ant finds a good (short) path from the colony to a food source, other ants are more likely to follow that path, and such positive feedback eventually leaves all the ants following a single path.

There are other evolutionary algorithms like shuffled frog leaping, cellular automata, virtual bee algorithms for solving optimization problems. In this thesis the two optimization algorithms i.e. genetic algorithm and estimation of distribution algorithm are used to solve the PHWR physics optimization problems.

• Some interesting characteristics of evolutionary algorithms

The evolutionary algorithms are based on selection of fitter individuals from the population and regeneration of new individuals guided by previous fitter individuals. In general if selection pressure is high (often called exploitation), the convergence of algorithm is fast. However, one may end up with an inferior result. On the other hand, if selection pressure is low (also called exploration), one is likely to get a superior result though convergence is poor. Here some kind of optimization is needed based on experience to decide selection pressure and diversity in population.

Another interesting property is the "no free lunch theorem" [15, 16, 17]. According to this, one algorithm can not be superior to other algorithms in all kinds of cases. Hence, for the class of problem being studied, one has to find out which algorithm is better. As will be seen later in present studies, we found that EDA is better than GA for problem at hand.

CHAPTER 5

OPTIMIZATION OF FRESH CORE LOADING FOR 220 MWe PHWR

At the beginning of the core life, when the entire core is loaded with fresh NU bundles, the power distribution is highly peaked in the centre due to lack of radial flux flattening. It is possible to flatten the power distribution by loading some depleted uranium or Thorium bundles in the central region of the core. This chapter presents suitable optimization algorithm to generate fresh core loading pattern for 220 MWe Indian standard PHWRs.

5.1. Introduction

Use of NU bundles as fuel in PHWR leads to lower excess reactivity of the core. Regular on-power fuelling becomes the need to operate the PHWR on continuous basis. Fuelling is done on-power by pushing eight fresh bundles in the selected channel almost everyday. The fuelling direction is opposite in adjacent channels. It helps in axial flux flattening. For the radial flux flattening, the core is treated as consisting of two radial zones for the purpose of fuelling: inner and outer. The fuel discharge burnup of inner region is higher than that of the outer region or in other words, fuelling is less frequent in inner zone channels than outer zone channels. This helps in radial power/flux flattening so that more power can be extracted from the core than if the burnup had been uniform throughout. This is true for an equilibrium core. However, at the beginning of the core life, when the entire core is loaded with fresh NU fuel, the power distribution is highly peaked in the centre due to lack of radial flux flattening. Hence, it will not be possible to get the full rated power from the core right from beginning unless some other way of achieving power flattening is followed. It is possible to flatten the power distribution by loading some depleted uranium or Thorium bundles in the central region of the core. Since Thorium has higher capture cross section than Natural Uranium (NU) or Depleted Uranium (DU), it causes stronger flux depressions in its vicinity. Therefore, to get similar flattening, the number of Thorium bundles needed is less as compared to the number of DU bundles. Strong flux depression in the vicinity of Thorium bundles affects the reactivity worth of the shutdown systems and thus Thorium bundles are

kept away from shutdown devices. The locations of Thorium or DU bundles have to be chosen in such a way that following conditions are fulfilled:

1) Power peaking is reduced and maximum power can be drawn.
2) K-effective is maximized as far as possible.
3) Bundle power and channel power remain within limits.
4) Sufficient reactivity worth is retained in the shut-down devices.

5.2. Earlier Studies

Simulated Annealing, Genetic Algorithm, Particle Swarm Optimization and Ant Colony Optimization have been extensively used to solve light water reactor fuel management and control design problems [18, 19, 20, 21, 22]. As far as PHWRs are concerned, the problem of obtaining an optimum distribution of Thorium bundles which satisfies above criteria was solved successfully about two decades ago by Balakrishnan and Kakodkar [23] and a suitable distribution consisting of 35 Thorium bundles was arrived at. A gradient based method was used to find the solution. Few decision variables are chosen to characterize a given Thorium bundle distribution. For instance the mean distance of all shutoff rods from all Thorium bundles is a decision variable. An objective function was defined which characterizes flux flattening, shutoff devices worth etc. One starts with a guess distribution of Thorium bundles. The gradient of objective function with respect to decision variables is estimated and used to gradually update the Thorium distribution till an optimum is reached. The loading pattern thus obtained was subsequently loaded in the Indian PHWR at Kakrapar (KAPS-1), which went critical in September 1992. The optimum Thorium bundle configuration obtained by Balakrishnan and Kakodkar [23] is explicitly shown in Figure 5.1. There are 35 Thorium bundles in 35 different channels. The figure shows all the 306 channels. In the channel containing Thorium bundle, a number in Arabic numerals is written. This number indicates axial position of the Thorium bundle in active part of that channel. This number lies between 1 to 10. The serial number of bundle is counted in the direction of coolant flow in that channel which is also direction of fuelling. The channels in Fig.5.1 where no number is written are fully occupied by NU bundles. The maximum allowed power with this configuration was 95.5 %FP and it satisfied all other constraints. It can be seen that the Thorium bundles are widely distributed in radial as well as axial directions.

The nuclear cross sections available at that time were used to derive the lattice average parameters. Those parameters were used and 35 locations for Thorium bundles were determined. In the present work ENDF/BVI.8 69 group library is used to generate lattice average parameters (two energy

group macroscopic cross-sections) using code CLUB [9]. These macroscopic cross sections are supplied to the recently developed code 'DOLP'. The published results [23] and results derived by DOLP are compared in Table5.1.

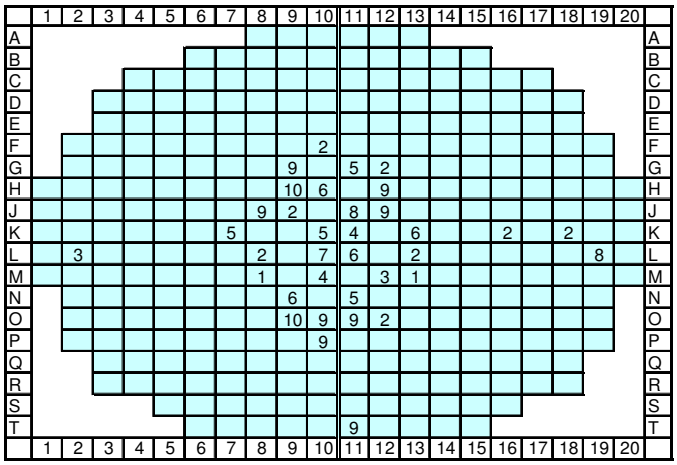

Figure 5.1: Loading derived by gradient method [Ref. 23]

Table 5.1: Comparison of result published by B&K [Ref 23] and DOLP

Sr. No.	Characteristics	B&K	DOLP
1	No. of Thorium Bundles	35	35
2	Maximum Channel Power (MW)	3.01	3.02
3	Maximum Bundle Power (kW)	440.0	445.6
4	Maximum Coolant Outlet Temperature	298.2	297.9
5	Allowed Reactor Power (%FP)	95.5	95.5
6	Reactivity Load due to Thorium (mK)	13.6	12.2
7	Worth of SDS#1 (mK)	32.9	33.1
8	Worth of SDS#2 (mK)	33.1	33.2

5.3. Nature of Present Studies

The optimization algorithm to generate fresh core loading pattern is developed. The developed algorithm determines suitable locations for two types of fuel bundles in the core. Therefore, a loading pattern which provides required amount of flattening can be generated using NU and Thorium or NU and DU fuel bundles by using the algorithm. Genetic Algorithm with random correction and penalty method are compared with Estimation of Distribution Algorithm. Evolutionary algorithms have been abundantly used for obtaining loading pattern in light water reactors. However, their use for PHWR loading pattern generation seems to be new.

It may be mentioned that the reactor core (Fig.5.1) has left-right symmetry hence we may choose a pair of channels in which Thorium/DU is to be loaded consistent with this symmetry. However, the coolant flow as well as fuelling direction is opposite to each other in this pair of channels. Hence the location of Thorium bundle in this pair of channels is chosen to be anti-symmetric in Z-direction. Therefore, left right symmetry is utilized in the algorithm to reduce the search space.

5.4. Fresh Core Loading Pattern with Thorium Bundles

The optimization problem of generating fresh core loading pattern using Thorium bundles along with natural Uranium bundles is defined as follows:

Objective To maximize the effective multiplication factor (K_{eff})

Constraints The following constraints are considered:

(1) Total numbers of Th bundles are restricted within a pre-determined interval.

(2) The reactor power should be close to 100 % Full Power (FP).

(3) The maximum channel power (MCP) should be less than 3.08 MW.

(4) The maximum bundle power (MBP) should not cross the operating limit 440 KW.

(5) The maximum channel outlet temperature (MCOT) should not be more than 299^{o}C.

(6) The reactivity worth of two independent shutdown systems i.e. SDS-1 and SDS-2 should not be less than 30 mk.

Penalty method is used for handling the constraints. The penalty method penalizes infeasible (or unfavorable) individuals. In general, it transforms a constrained optimization problem to an unconstrained problem by defining penalty function [25]. Here, the objective function to be maximized has been defined to take care of constraints as follows:

$$\text{Fitness} = \text{Keff} - F1 - F2 - F3 - F4 - F5 - F6 \tag{5.1}$$

where

F1 = (FP0-FP)*__Afp__ if FP < FP0 and zero otherwise

F2 = (CP-CP0)*__Acp__ if CP > CP0 and zero otherwise

F3 = (COT-COT0)*__Acot__ if COT > COT0 and zero otherwise

F4 = (BP-BP0)*__Abp__ if BP > BP0 and zero otherwise

F5 = (PSS0-PSS)*__Apss__ if PSS < PSS0 and zero otherwise

F6 = (SSS0-SSS)*__Asss__ if SSS < SSS0 and zero otherwise.

The notation used is as follows:

FP0=100, corresponding to full rated Power.

FP is the maximum allowable power in a given configuration.

CP0= 3.08, corresponding to maximum permitted channel power.

CP is the maximum channel power in a given configuration.

COT0=299, corresponding to maximum permitted channel outlet temperature.

COT is the maximum channel outlet temperature in a given configuration.

BP0=440, corresponding to maximum permitted bundle power.

BP is the maximum bundle power in a given configuration.

PSS0=32, a slightly higher value than minimum worth of PSS in millik.

PSS is the worth of PSS in a given configuration.

SSS0=32, a slightly higher value than minimum worth of SSS in millik.

SSS is the worth of SSS in a given configuration.

Afp, Acp, Acot, Abp, Apss and Asss are suitably chosen constants to give a weightage to each of the factors. The procedure to decide these constants is somewhat arbitrary. About 1000 random configurations containing 36 Thorium bundles were generated. The K-eigenvalue and flux distribution were calculated for each of them. The fluxes were normalized to get the maximum channel power equal to the CP0 (=3.08). The PSS and SSS worth were also found for each configuration. From these results, the typical extent of deviations of FP, COT, BP, PSS and SSS from the limiting values FP0, COT0, BP0, PSS0 and SSS0 were estimated. The constants Afp, Acot, Abp, Apss and Asss were found such that the penalty caused by each factor for such deviation is of the order of Keff (which is of order unity). The constant Acp is arbitrary, since the term containing Acp in Eq.(5.1) always vanishes. It may be mentioned that one can obtain the constants in some other way also and Eq.(5.1) is a general expression.

5.4.1. Genetic algorithm (GA)

Pseudo model of Genetic Algorithm used to solve the above problem is shown in Figure 5.2. For the tournament selection [15] [item 4 in Fig 5.2], the number M was chosen to be 2. There are two primary factors to be considered: population diversity and selective pressure. An increase in selective pressure decreases the diversity of the population and vice versa. Too much selective pressure gives a faster but premature convergence. As M increases, selective pressure increases. The value of M = 2 has been found to be good in several applications [25] and was used by us. Our selection of genotype is not based on binary strings. As mentioned by [26], the representation should be as natural as possible. In the

PHWR, there are 306 channels, each containing 12 bundles. For each channel, we generate a uniformly distributed integer number, say p, between 1 to 12. As a result of cross-over, the offspring has 1 to p bundles identical to first parent and (p+1) to 12 bundles identical to the second parent for that particular channel.

1. Initialize the population (Size=N) randomly
2. Evaluate the fitness of each individual based on their K_{eff}, maximum permissible reactor power, channel power, channel outlet temperature, bundle power and the worths of PSS and SSS as obtained by diffusion code DOLP.
3. Either continue for new generation calculations or terminate the execution.
4. Selection of a pair of individuals based on tournament selection method (tournament between M<N candidates and best one wins).
5. Generate new individual by using uniform crossover operator on the selected pair of individuals with Pc crossover rate. The newly generated individual may not have desired number of NU or Th bundles. Hence a correction operator is applied. The fuel type which is more in number than the specified value is randomly changed into other type.
6. Steps 4 and 5 are repeated to generate N new individuals.
7. The newly generated N individuals are subjected to mutation operator with Pm mutation rate. The shuffle type mutation operator has been used. The fitness of new N individuals is found out as in step 2.
8. We have N old and N new individuals with known fitness. Out of these, N individuals with better fitness are retained.
9. Go to step 3.

Figure 5.2: Pseudo GA model used for optimization

5.4.2. Estimation of distribution algorithm (EDA)

Pseudo model of Estimation of Distribution Algorithm used to solve the above problem is shown in Fig. 5.3. The probability that a given location is occupied by NU or Thorium bundle is estimated from the selected M individuals. The performance of an EDA highly depends on how well it estimates and samples the probability distribution. Univariate Marginal Distribution Algorithm (UMDA) assumes no interaction among variables. The probability distribution is estimated using UMDA [18] in the present case. The Probability Distribution Function (PDF) was generated using 30% dominated individuals [item 4 in Fig 5.3] of the population size. Alpha [item 5 in Fig 5.3] is chosen 0.05.

1. Initialize the population (Size=N) randomly.
2. Evaluate the fitness of each individual based on their K_{eff}, maximum permissible reactor power, channel power, channel outlet temperature, bundle power and the worths of PSS and SSS as obtained by diffusion code DOLP.
3. Either continue for new generation calculations or terminate the execution.
4. Select M<N candidates based on termination selection method (the best fit M individuals among total N individuals).
5. Calculate Probability Distribution Function (PDF) using selected M individuals. At any generation (t) the PDF has been estimated as given below for each location.

$$PDF\ (t+1) = PDF\ (t)\ .(1-\alpha) + \alpha\ .\frac{1}{M}\ .\sum_{m=1}^{M} X_m(t)$$

where α is constant between [0, 1]. X is binary representation of loading pattern.

6. Generate new population (Size=N) using this new probability distribution function (PDF).
7. The newly generated individuals may not have desired number of NU or Th bundles. Hence a correction operator is applied. The fuel type which is more in number than the specified value is randomly changed into other type.
8. The fitness of new N individuals is found out as in step 2.
9. Go to step 3.

Figure 5.3: Pseudo EDA model used for optimization

5.4.3. Parallelization of optimization algorithm

The evolutionary algorithms (GA and EDA) evolve population of candidate solutions. They take a great amount of computational time. The most time consuming part is the evaluation of "Fitness" corresponding to each individual of the population. This requires full core simulation by diffusion calculation from which objective function or "Fitness" can be computed. Hence, these diffusion calculations for different individuals in the population were carried out in parallel. The parallelization was achieved using the MPI Library functions [27] as follows. The rank 0 processor is called here as MASTER processor and others are SLAVE processors. The MASTER will generate population containing N individuals. If there are S SLAVE processors, each SLAVE is assigned the job of evaluating fitness of (N/S) individuals by diffusion calculations. The results are returned to the MASTER. The MASTER will generate new population and send (N/S) individuals to each slave for fitness evaluation. This is continued for all the generations. The computer code DOLP has been written to execute this using standard message passing interface (MPI) library functions in FORTRAN. The distributed memory parallel computer systems [28] AMEYA/ AJEYA at BARC and CRL computational facility at Pune were used. The detailed information about EKA is available at website: http://www.crlindia.com.

5.4.4. Performance of GA and EDA with different populations

At the outset, it was decided to try number of Thorium bundles nearly similar to the number (35) in the [23]. Thus the bundles were restricted to lie within 36±4 i.e. in the interval (32, 40). Owing to the left right symmetry of the core, only even number of Thorium bundles is considered. Thus, the possible numbers are 32, 34, 36, 38 and 40. Both GA and EDA methods were used. Analysis with GA and EDA was carried out for 4 sizes of population of configurations, namely, 1000, 4000, 6000, and 8000. The variation of Fitness function derived from GA and EDA (keeping total number of Thorium bundles 36±4) against generation number for population size 1000, 4000, 6000 and 8000 is presented in Fig. 5.4 and 5.5 respectively. The work was published in Annals of Nuclear Energy (ANE 36, 948-955). For GA, the evolution of fitness highly depends on the population size, whereas it is not true for EDA. Hence, with GA one needs to use large population size. On the other hand, with EDA, result is almost same for all population sizes 1000, 4000, 6000 and 8000. The CPU time (computational effort) is proportional to the product of population size and number of generations. Hence, use of population size 1000 is considered adequate in our studies in case of EDA.

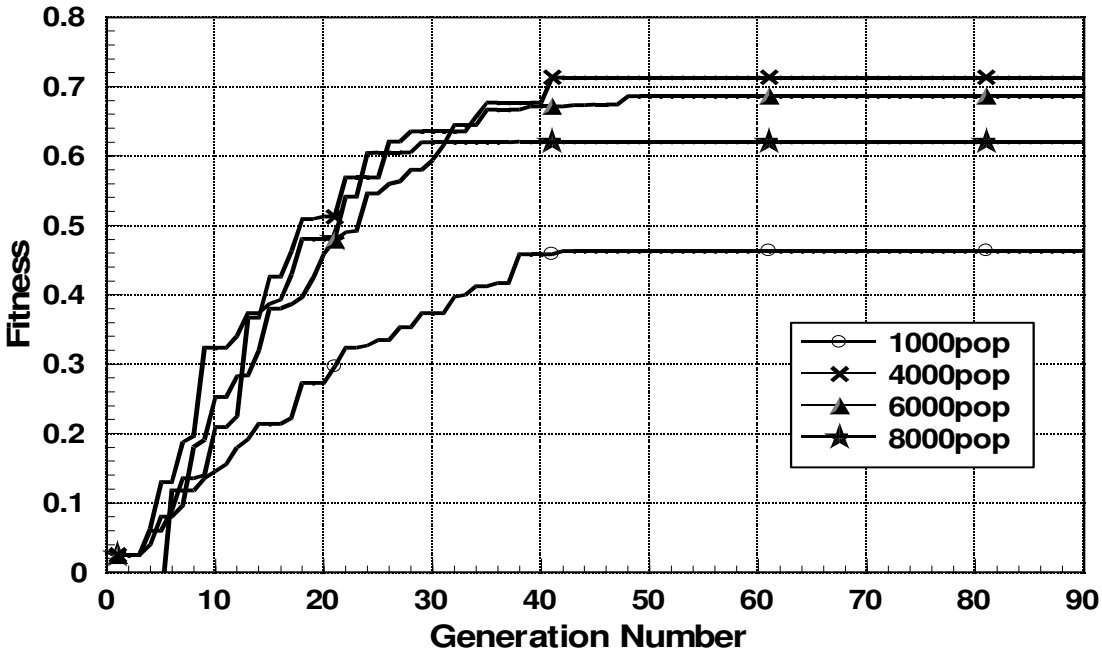

Fig 5.4: GA performance for different population size (pop) for 36±4 Thorium bundles

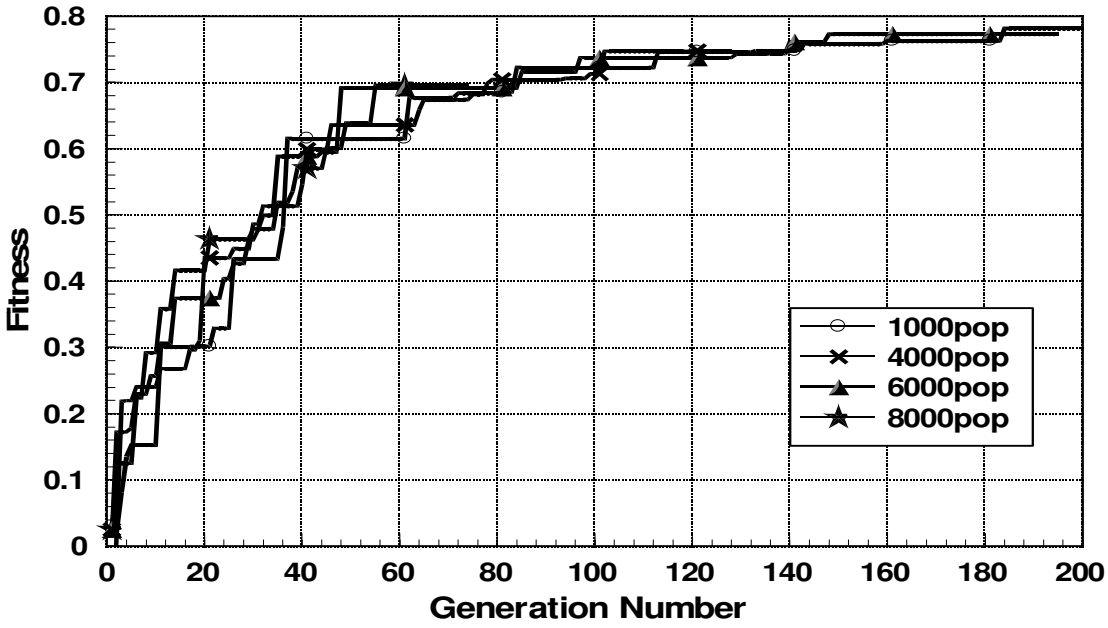

Fig 5.5: EDA performance for different population size (pop) for 36±4 Thorium bundles

5.4.5. Optimum number of Thorium bundles

Fresh core loading patterns using EDA with population size 1000 is generated for 8±4, 16±4, 20±4, 24±4, 28±4, 36±4 and 44±4 number of Thorium bundles. In order to keep the number of Thorium bundles in a predefined interval, random correction model is applied to EDA. The constraint parameters FP0=100, CP0=3.08, COT0=299, BP0=440, PSS0=30 and SSS0=30 is used for optimization. The work is published in International Conference on Peaceful Uses of Atomic Energy-2009 [46]. The obtained result is shown in Table 5.2.

Table 5.2: Optimization result with different number of Thorium bundles

Case	Net Th Bundles	Keff	Rx Power %FP	MCP (MW)	MBP (kW)	COT (^{0}C)	SDS#1 (mK)	SDS#2 (mK)
8±4	12	1.02904	91.8	3.08	438.4	297.0	32.0	30.9
16±4	20	1.02664	96.4	3.08	440.3	297.6	32.2	31.0
20±4	24	1.02621	96.0	3.07	439.9	296.5	32.4	31.7
24±4	28	1.02561	96.0	3.08	440.2	297.5	33.1	32.0
28±4	28	1.02622	96.3	3.08	440.0	297.2	32.8	32.0
36±4	36	1.02257	99.4	3.08	439.8	297.3	32.2	32.0
44±4	46	1.02169	100.0	3.05	439.3	296.7	32.4	32.1

Here it can be seen from above table that in few cases the bundle powers are crossing the limit 440 kW. The reason is follows. The code DOLP is executed with lower convergence criterion (Eigen value 1.0E-4 and Eigen vector 1.0E-3) to save computational time, but the results obtained by optimization algorithm are simulated with tighter convergence (Eigen value 1.0E-7 and Eigen vector 1.0E-6).

It is found that with 12 Thorium bundles the reactor can operate above 90%FP and about 46 Thorium bundles are needed to operate the reactor at 100%FP from day one onwards. The fresh core loading pattern having 12, 28 and 46 Thorium bundles (corresponding to the case 8±4, 28±4, 44±4 respectively) are shown in Figure 5.6, 5.7 and 5.8 respectively.

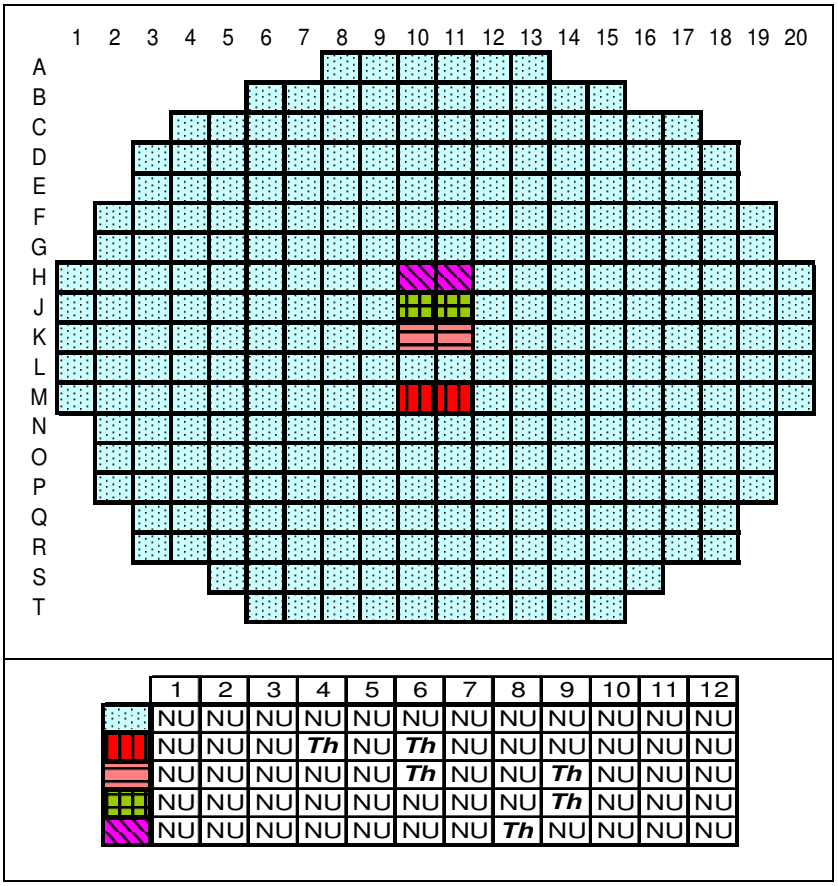

Figure 5.6: Fresh core loading pattern with 12 Thorium bundles

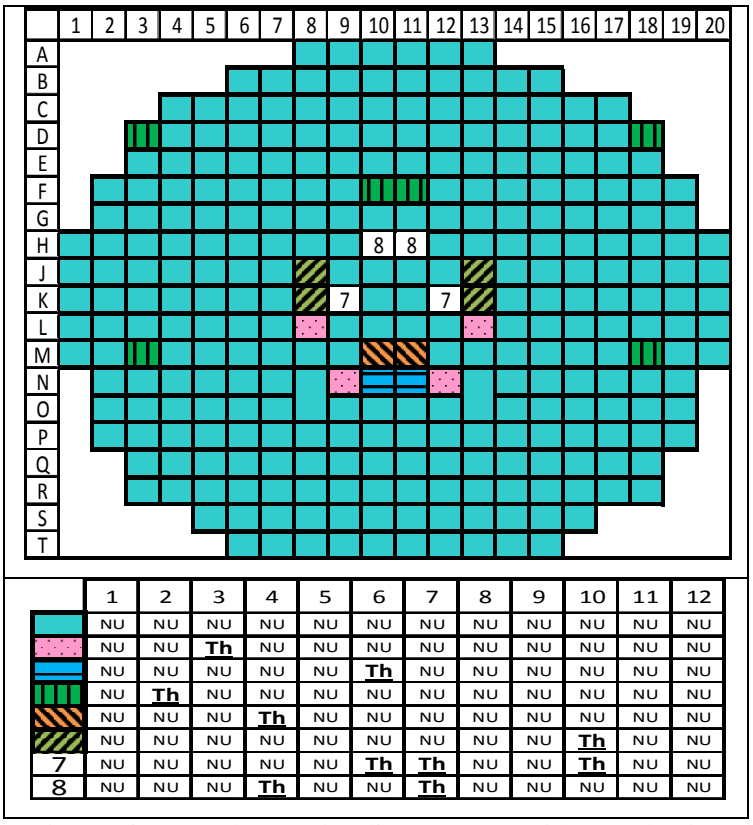

Figure 5.7: Fresh core loading pattern with 28 Thorium bundles

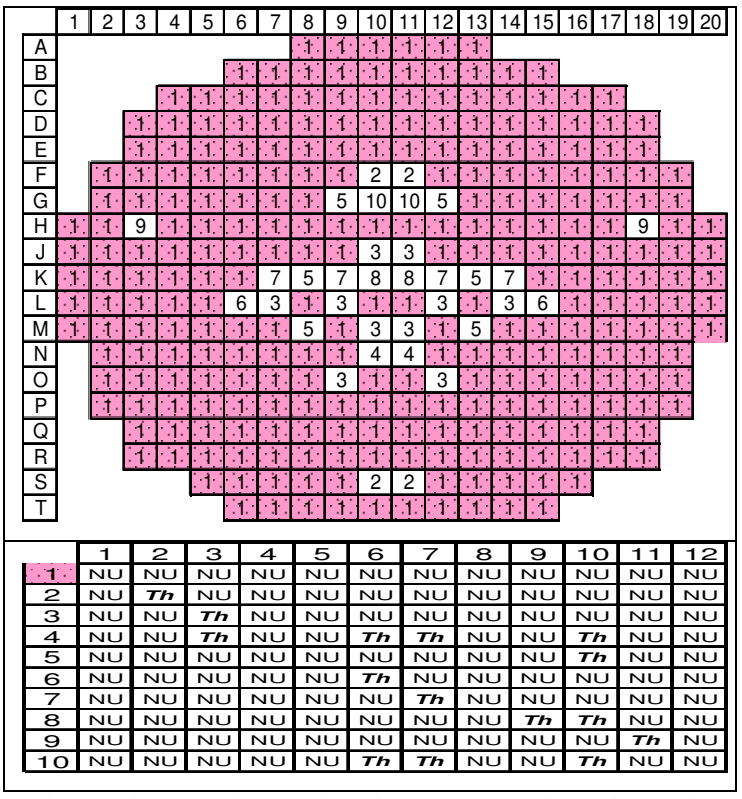

Figure 5.8: Fresh core loading pattern with 46 Thorium bundles

5.5. Fresh Core Loading Pattern with DU (0.6 wt% U^{235}) Bundles

There are many differences between Thorium and Depleted Uranium (DU) loading. Thorium has relatively larger neutron capture cross-section than DU. While a few tens of Thorium bundles are enough for flux flattening, a few hundreds of DU bundles are needed for the same purpose. The neutron flux gets sharply depressed around the Thorium bundle location due to higher capture. This affects the worth of PSS and SSS shutdown systems adversely. This problem is generally less significant in DU loading. Another point to be noted is that in contrast with Thorium bundles, DU bundles are fissionable. Hence, there exists a possibility of loading a very large number of DU bundles (a few thousands) in the core. A fresh core loading pattern for DU bundles obtained purely on the basis of manual trials & intuition was loaded at MAPS#1. The DU bundles having enrichment of 0.60wt% U^{235} was considered. The central 32 channels were loaded with DU bundles (total 384 bundles). It gives 93% FP without reducing the worth of PSS and SSS. The excess reactivity is about 21 mK.

Fresh core loading pattern with an optimum distribution of DU bundles (0.6% U-235 content) which allows 100%FP of reactor operation is generated. The work was published in Annals of Nuclear Energy (ANE 37, 208-217). The first aim of the optimization work was to assure that the pattern generated on manual intuition can be improved upon. The idea is to check whether we can get better K_{eff} and higher power level (or better flattening) than for 384 DU pattern with a similar number (few hundreds) of DU bundle loading. The second aim is to find out whether the number of DU bundles loaded in the core can be further increased. As mentioned earlier, this will minimize the NU bundles requirement, extract more power from DU bundles and thus provide better fuel utilization. In general, as number of loaded DU bundles is increased, the maximum possible K_{eff} is expected to reduce. It is necessary to find best possible arrangements of DU bundles which flatten the flux sufficiently to get 100% FP and also maximize the K_{eff} as far as possible.

5.5.1. Exploitation of symmetry of the core

There are total 306 fuel channels (from A-T in Y-direction and 1-20 in X-direction). These channels are horizontal and extend in Z-direction up to about 500 cm (12 fuel bundles). There is no top-bottom symmetry in the core. There is however, left-right symmetry. Thus there is reflective symmetry along X-direction. In addition, there is reflective symmetry along Z-direction also. Reflective symmetry along both X and Z directions are exploited. In that case, one has to choose locations of DU bundles in only one-fourth core which contains 153 channels and six bundle locations in half channel length. Some

of these locations have to be loaded with DU bundles. The symmetry in Z-direction implies that there must be only even number of DU bundles in any channel containing DU. It was felt that this will restrict the distribution of DU bundles in radial plane. Hence, in addition to the one-fourth core, optimization of DU bundles was done which respects only symmetry in X-direction or half core symmetry. The results obtained by EDA with population size 1000 for X-symmetry and XZ-symmetry in the core are compared.

5.5.2. Random correction versus penalty model

We try to optimize the loading pattern with the number of DU bundles lying within a certain pre-decided range or interval. In EDA, the total number of DU or NU bundles does not remain constant while going to next generation by the process of estimation of distribution and sampling. Hence, the number of DU bundles may fall outside the pre-decided interval. To keep the total number of DU bundles within the pre-decided interval, random correction method is applied. The excess bundles (of NU or DU) are randomly chosen and converted to other type. Let the interval be denoted by (N_d -250, N_d +250). The optimization study is carried out for all these ranges or intervals. As a result, certain members of population are prevented from participating in the evolution and one may get sub-optimal results. This possibility is absent if we use Penalty model. An additional penalty term F7 is subtracted from RHS of Eq.(5.1). The F7 term is defined as follows:

$$F7 = \text{abs}\,(N_d - N_a) * \mathbf{A_{DU}}$$

Where N_d is pre-decided number of DU bundles, N_a is the actual number of DU bundles in the individual under consideration in EDA and $\mathbf{A_{DU}}$ is an appropriately chosen positive constant. 'abs' stands for absolute value. The values of N_d considered are: 250, 750, 1250, 1750, 2250, 2750 and 3250.

The results obtained using X-symmetry (half core) and random correction model are shown in Table 5.3. The results obtained using X and Z-symmetry (quarter core) and random correction model are shown in Table 5.4. The results obtained using X and Z-symmetry (quarter core) and penalty model are shown in Table 5.5.

Some sample curves showing change of fitness with generation number are shown in Fig.5.9. The fitness or objective function increases rapidly up to 200 to 300 generations and then gradually approaches optimum value. The XZ-symmetric case with Random correction approach converges faster than X-symmetric case with same approach as expected.

Table 5.3: Properties of configurations obtained by EDA (X-Symmetry, Random correction)

Case	#DU bundles	Keff	%FP	MCP	MBP	COT	PSS worth	SSS worth
250±250	438	1.0244	100	3.05	439.8	297.3	32.6	32.0
750±250	554	1.0244	100	3.06	439.9	296.8	32.5	32.0
1250±250	1082	1.0241	100	3.07	440.0	297.6	33.2	32.0
1750±250	1500	1.0236	100	3.06	437.7	296.6	33.3	32.0
2250±250	2000	1.0169	100	3.07	439.2	297.6	34.5	33.2
2750±250	2502	1.0057	100	3.07	441.1	296.7	34.8	35.2
3250±250	3000	0.9878	98.5	3.08	440.8	295.9	33.9	32.1

Table 5.4: Properties of configurations obtained by EDA (XZ-Symmetry, Random correction)

Case	#DU bundles	Keff	%FP	MCP	MBP	COT	PSS worth	SSS worth
250±250	472	1.0236	100	3.07	439.5	297.4	32.6	32.0
750±250	628	1.0239	100	3.06	439.6	297.5	32.6	32.0
1250±250	1036	1.0241	100	3.07	440.0	297.2	33.2	32.0
1750±250	1500	1.0236	100	3.08	440.0	297.2	33.4	32.1
2250±250	2000	1.0164	100	3.08	439.4	297.1	34.1	33.0
2750±250	2500	1.0056	100	3.07	440.4	297.0	34.3	35.6
3250±250	3000	0.9876	98.8	3.08	440.2	297.5	33.2	32.0

In general, as the number of DU bundles increases, the maximum possible K_{eff} will reduce (Tables 5.3, 5.4 and 5.5). The EDA tries to maximize the K_{eff} as far as possible by optimizing the distribution of DU bundles. In Figure 5.10, the K_{eff} is plotted against total number of DU bundles present in the core for Tables 5.3, 5.4 and 5.5. It is seen that the results given by Table 5.3, 5.4 and 5.5

have similar trend. It is clear from Fig. 5.10 that the number of DU bundles can not exceed 2500 because K_{eff} falls below 1.0 and reactor can not be operated.

Table 5.5: Properties of configurations obtained by EDA (XZ-Symmetry, Additional Penalty)

Case	#DU bundles	Keff	%FP	MCP	MBP	COT	PSS worth	SSS worth
250	280	1.0247	97.7	3.08	440.1	297.1	32.0	32.0
750	748	1.0227	100	3.04	439.8	295.7	32.5	32.0
1250	1248	1.0222	100	3.04	439.1	297.5	32.9	32.0
1750	1748	1.0200	100	3.08	439.2	297.3	33.7	32.1
2250	2248	1.0107	100	3.06	440.2	296.8	34.2	34.0
2750	2748	0.9964	99.8	3.08	439.5	295.7	32.8	32.2
3250	2956	0.9887	100	3.06	439.7	297.6	33.0	32.1

The random correction approach and penalty approach were applied to the cheaper XZ-model. It was observed that the random correction approach applied on XZ-model is more economic.

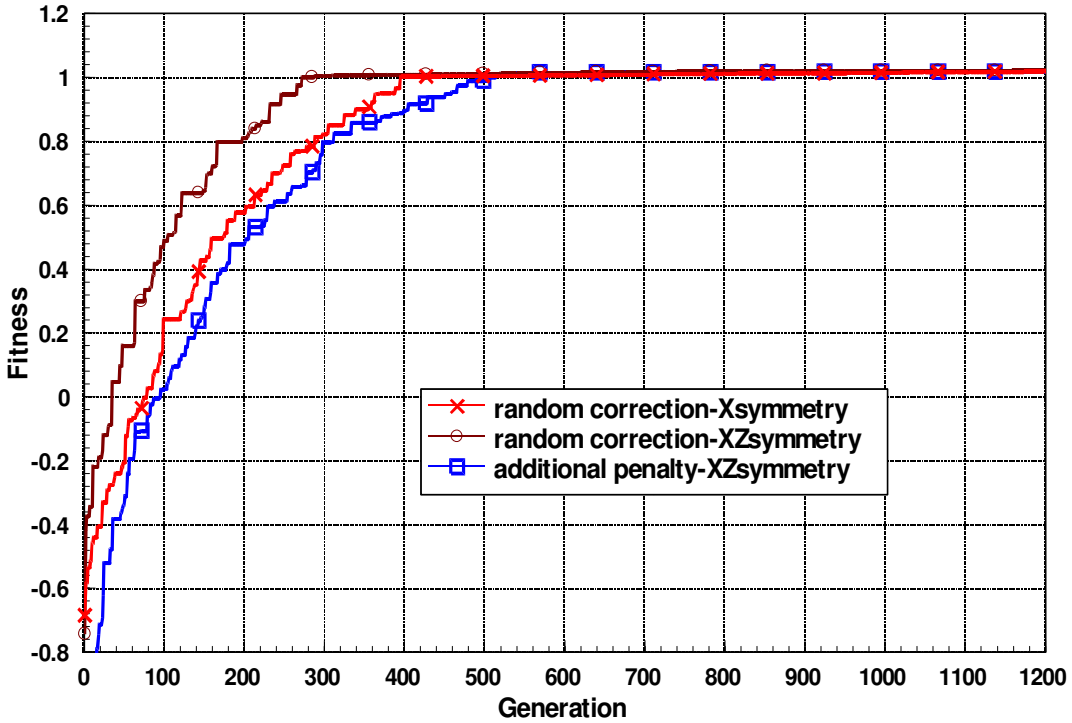

Figure 5.9: Fitness evolution with generation

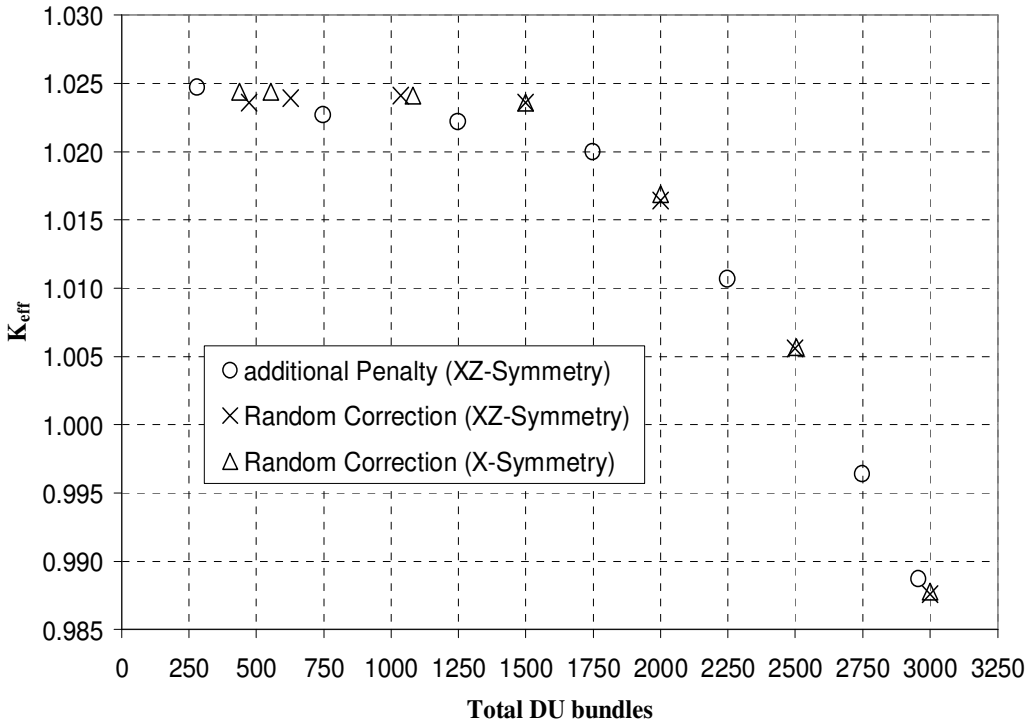

Figure 5.10: K_{eff} versus total DU bundles by various methods (Tables 5.3, 5.4 & 5.5)

5.6. Loading Pattern with DU (0.3 wt% U-235) Bundles for KAPS#1

Random correction applied on EDA with population size 1000 seems to be more economic approach. A fresh core loading pattern using NU and DU (0.3wt% U-235 content) fuel bundles has been determined using EDA with random correction. The search space for DU bundle along a channel was limited from 5^{th} position to 10^{th} position. This allows the DU bundle to get removed from the core in first refueling itself. The pattern as shown in Fig. 5.11 is derived and it has been loaded at KAPS#1 in December 2010 which went through EMCCR (EnMass Coolant Channel Replacement). The variation in core excess reactivity with full power day of operation is shown in Fig. 5.12. The variation in PSS and SSS reactivity worth with full power day of operation is shown in Fig. 5.13 & 5.14

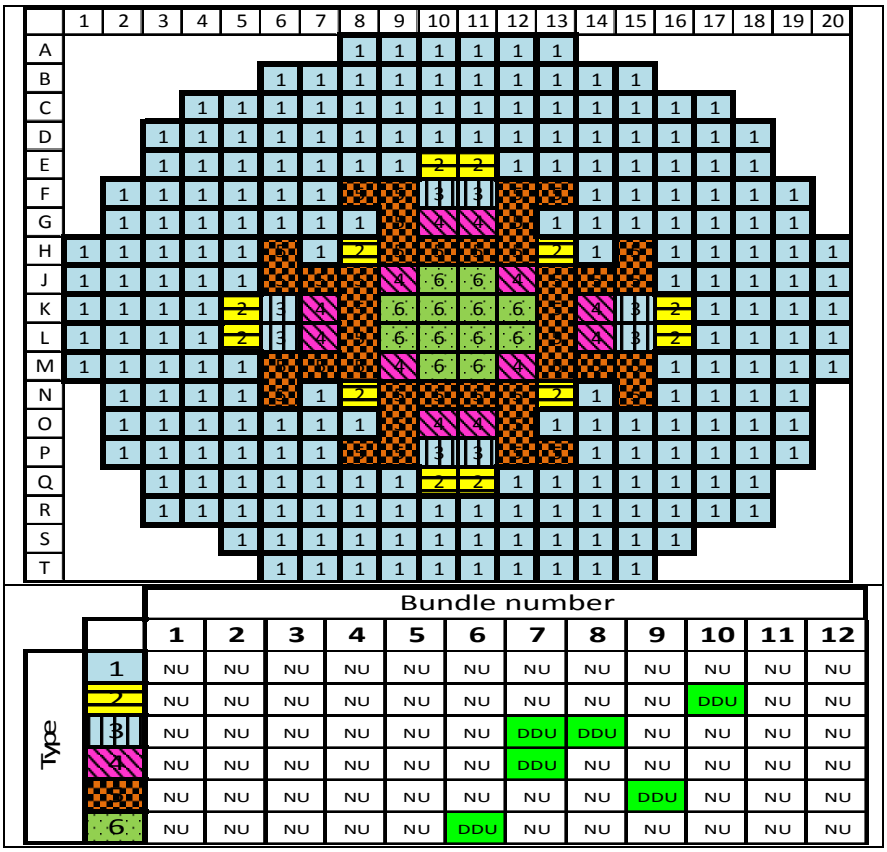

Type	Bundle number 1	2	3	4	5	6	7	8	9	10	11	12
1	NU	NU	NU	NU	NU	NU	NU	NU	NU	NU	NU	NU
2	NU	NU	NU	NU	NU	NU	NU	NU	NU	DDU	NU	NU
3	NU	NU	NU	NU	NU	NU	DDU	DDU	NU	NU	NU	NU
4	NU	NU	NU	NU	NU	NU	DDU	NU	NU	NU	NU	NU
5	NU	NU	NU	NU	NU	NU	NU	NU	DDU	NU	NU	NU
6	NU	NU	NU	NU	NU	DDU	NU	NU	NU	NU	NU	NU

Figure 5.11: Loading pattern using 92 DU (0.3wt% U^{235}) bundles

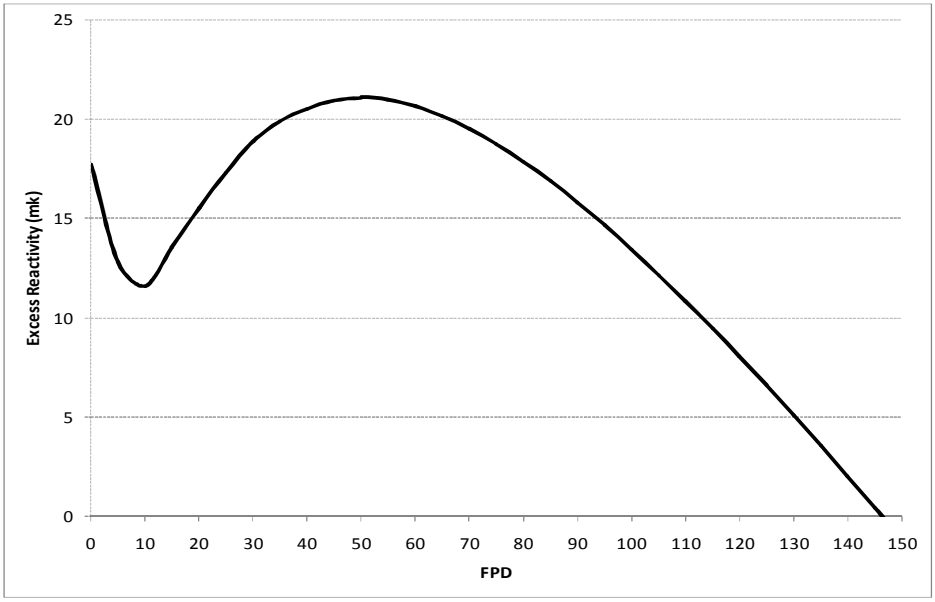

Figure 5.12: Variation of core excess reactivity

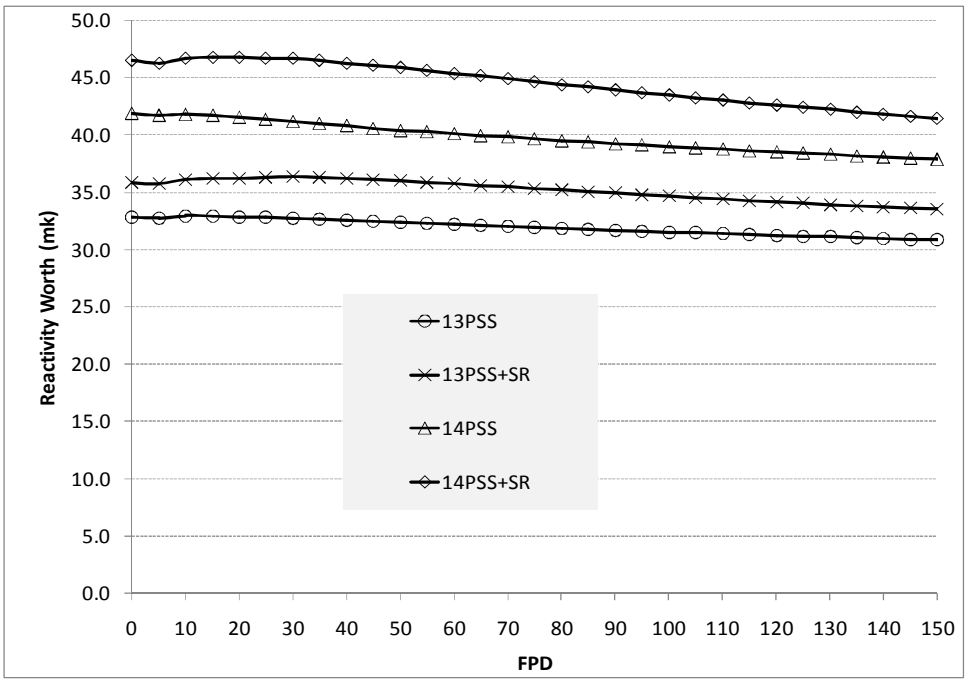

Figure 5.13: Reactivity worth in PSS and PSS+SR

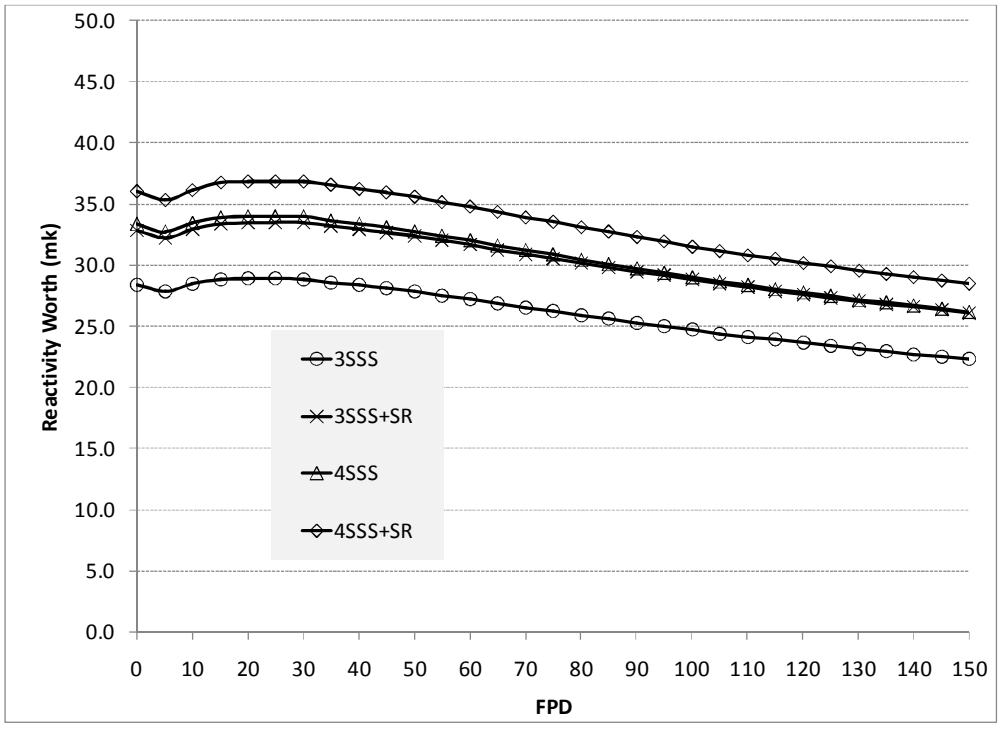

Figure 5.14: Reactivity worth in SSS and SSS+SR

CHAPTER 6

OPTIMIZATION OF FRESH CORE LOADING FOR 700 MWe PHWR

The optimization studies for fresh core loading pattern in chapter 5 were concerned with the small sized 220 MWe Indian PHWR. Similar to 220 MWe, in 700 MWe PHWR also, one has to load some bundles of either Thorium or Depleted Uranium to get full power. The present chapter describes suitable optimization algorithm to generate fresh core loading pattern using 0.3 wt% U^{235} Depleted Uranium (DU) bundles for 700 MWe PHWR.

6.1. Introduction

The construction of 220 MWe PHWRs has come to an end with the first criticality of KGS#4 in Dec. 2010. There are now totally 15 units of 220 MWe PHWRs operating in India. Six units have undergone EMCCR (En-Mass Coolant Channel Replacement) and some units may undergo EMCCR in future. Future PHWR programme of India is solely based on the construction of the new design of 700 MWe PHWRs. As is well-known, a large-sized reactor with higher power output is more economical than smaller units. Hence, currently there is a trend to build large reactors. The 700 MWe is an upgraded version of the 540 MWe Indian PHWRs. Larger power is obtained by permitting slight boiling of the coolant. In the near future, four units (two at Kakrapar, Gujarat and two at Rawatbhata, Rajasthan) are expected to become operational. Just like 220 MWe PHWR, full power cannot be drawn from the 700 MWe reactors if the initial core is loaded with Natural Uranium alone. Hence, one has to load some bundles of either Thorium or Depleted Uranium to get full power. At present, it has been decided to load 0.3 wt% U235 enriched Depleted Uranium (DU) bundles. In view of this, optimization study is carried out with such DU bundles. The EDA algorithm, successfully used for 220 MWe PHWR, will be used. However, the present study is different in many ways from the earlier studies on 220 MWe PHWR. The prime difference between 220 MWe and 700 MWe PHWRs is the neutronic coupling. The 700 MWe reactor, being large sized, is loosely coupled. As a result, there are substantial differences in the control and regulating systems in the two types of reactors.

6.2. Comparison of 220 MWe Core with 700 MWe Core

The 700 MWe reactor core consists of 392 horizontal pressure tubes arranged along a square lattice of 28.6 cm pitch. The 37 element fuel bundles in the form of a string of 12 bundles lie in each fuel channels. All the 12 bundles are in the active portion of the core. The 12 bundle locations are numbered as 1, 2, 3, ….., 12; in the direction of fuelling. For the purpose of reactor regulation there are 14 Zone Control Compartments (ZCC), 17 Adjuster Rods (AR) symmetrically grouped into eight banks and 4 Control Rods (CR) as shown in Fig 6.1. There are two independent shutdown systems called Shutdown System-1 (SDS#1) and Shutdown System-2 (SDS#2) for reactor protection. The SDS#1 consists of 28 shutoff rods dropping from the top of the core. The SDS#2 consists of six perforated horizontal tubes allowing large amount of neutron poison to get mixed in the moderator. In addition, there is a Regional Over power Protection (ROP) system which senses excess power in any local region of the core by means of two sets of detectors and trips the reactor (by sending signal to SDS#1 or SDS#2) to avoid the on-set of coolant dry out or fuel centre line melting. More detailed description can be found in reference [1]. The optimum DU distribution is expected to preserve the worth of SDS#1. The SDS#2 has very large worth and need not be checked. Moreover, the DU loading should provide sufficient operating margin and do not cause spurious trip by ROP. The channel power peaking factor (i.e. CPPF defined as maximum of ratio of instantaneous channel power to time averaged channel power) is used to limit the channel power for 700 MWe core. Lower CPPF value provide more operating margin from ROP trip.

There is one interesting difference between 220 MWe and 700 MWe optimization. In case of 220 MWe PHWR, when different DU bundle compositions are tried, the worth of 13 PSS rods (with the maximum worth rod missing) does not change much because the reactor is tightly coupled. In case of 700 MWe PHWR, for different DU bundle compositions, the two rods with maximum worth keep changing. In order to decide these to rods, one may have to do many trial calculations. To avoid too many calculations, the best locations for DU bundle have been obtained using EDA algorithm without any calculation for stuck-rod criterion. Later on, to meet the required reactivity worth in 26 SRs (2 missing out of 28 SRs) few more DU bundles are loaded using heuristic information. The final pattern arrived at using EDA and heuristic information satisfies all criteria.

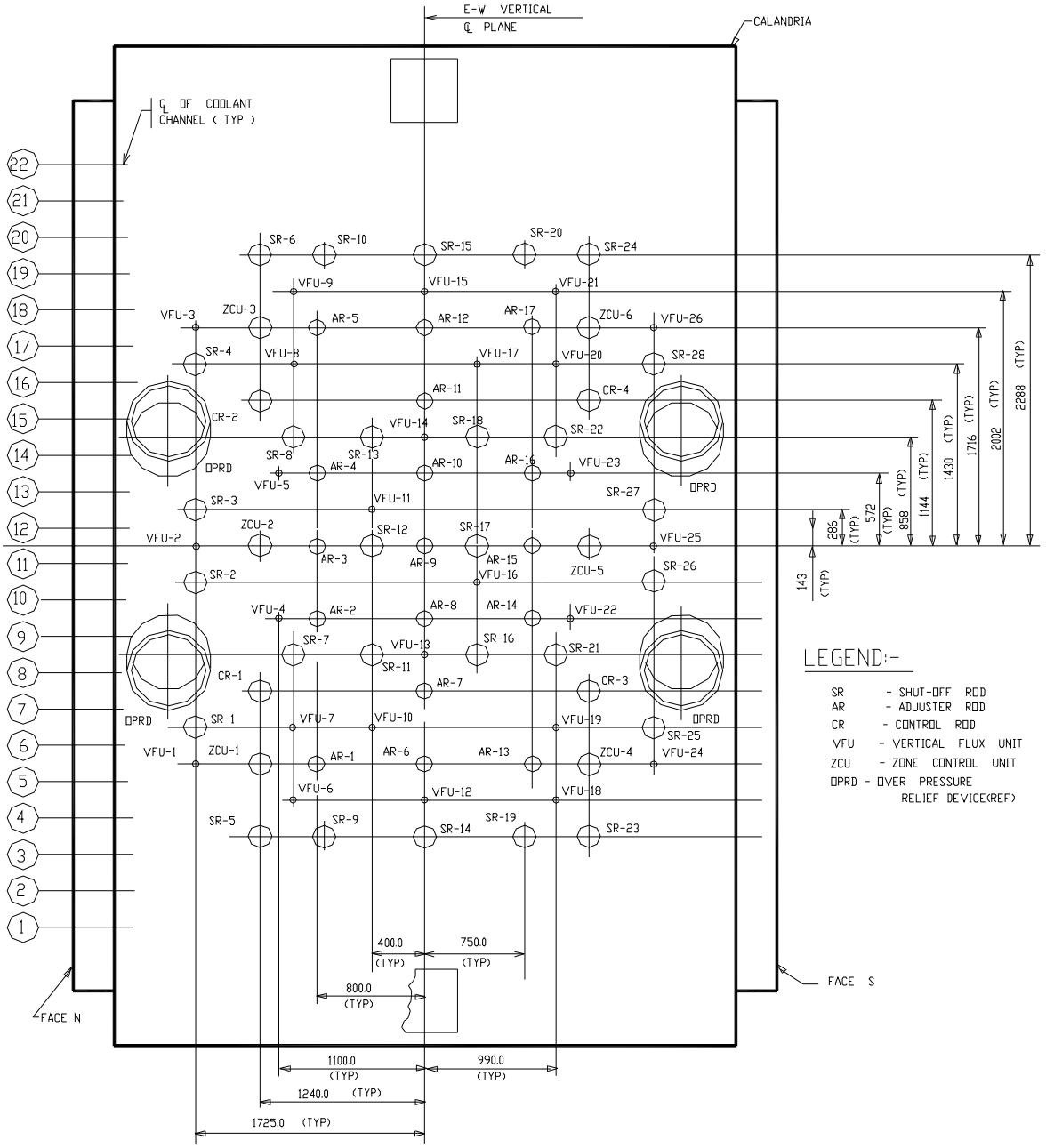

Figure 6.1: Location of reactivity devices in 700 MWe core

Table 6.1: Comparison of features of 220 MWe and 700 MWe PHWR

Feature	**220 MWe**	**700 MWe**	**Effect on optimization of 700 MWe**
Meshes	26×26×20	28×28×24	Problem size becomes bigger
Symmetry	Only in X-direction	Both X & Y direction	Reduces search space if symmetry is used
Monitoring individual channel power	Restriction on Channel Outlet Temperature	Restriction on Channel Power Peaking Factor	Lower CPPF give more operating margin, The variation in CPPF with burnup should be small
SDS#2	Small worth (~30 mK)	Huge worth (>300 mK)	Too high worth, No concern at all
Stuck rod Criterion	One rod	Two rods	Maximum worth rods change with core configuration
ROP System	Absent	present	Additional concern

6.3. Reduction of Search Space

The optimum distribution using DU bundles (0.3 wt% U^{235}) is determined for 700 MWe Indian PHWR with some restrictions on locations. The 700 MWe PHWR is larger and has more bundle locations than 220 MWe PHWR. However, it has more symmetry properties. Exploitation of symmetry and restrictions on DU locations mentioned earlier help to reduce the search space. In the XY-plane, the core has reflective symmetry along both X and Y directions. There is also symmetry with respect to rotation in XY plane by 90^0 as shown in Figure 6.2. We assume that the DU bundle locations also follow these symmetries. Thus it is enough to determine locations of DU bundles in the 53 channels.

A simple loading pattern can be generated if DU bundles are chosen to lie at a fixed bundle position (say 7^{th} bundle position in axial direction). The locations in other channels are determined by symmetry. There are 12 bundles in each channel. The numbering of bundles in z-direction is along direction of fuelling and adjacent channels are fuelled in opposite direction. Hence, the DU bundles will lie only in two planes perpendicular to z-axis. The generated loading pattern will be simple and easier for actual loading.

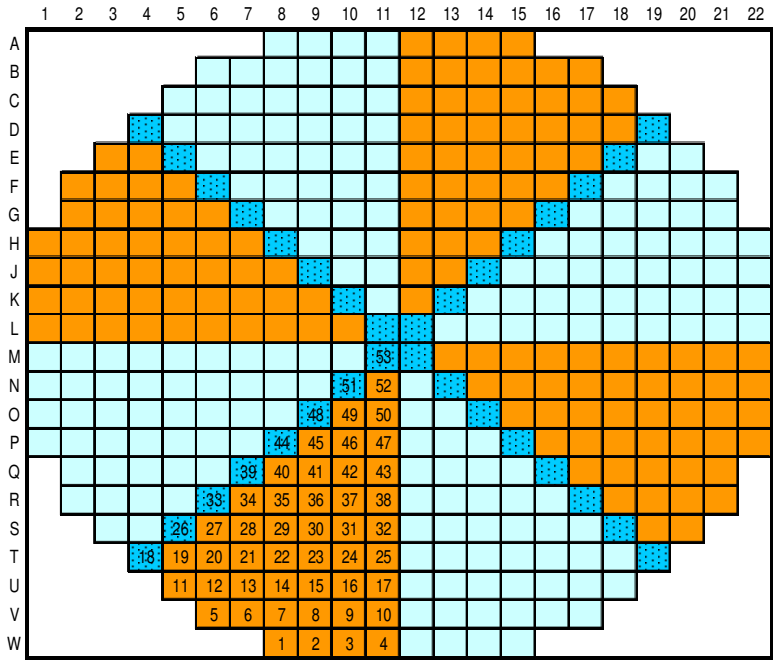

Figure 6.2: 1/8th symmetric 700 MWe core

Four types of optimization studies are carried out: DU bundles are placed at only one axial location which can be 7th, 8th, 9th or 10th location. This is shown schematically in Figure 6.3 as cases A, B, C and D. The Four cases analyzed are named as follows:

Case A: The DU bundles can be loaded only in two radial planes at 7th bundle location along the direction of fuelling.

Case B: The DU bundles can be loaded only in two radial planes at 8th bundle location along the direction of fuelling.

Case C: The DU bundles can be loaded only in two radial planes at 9th bundle location along the direction of fuelling.

Case D: The DU bundles can be loaded only in two radial planes at 10th bundle location along the direction of fuelling.

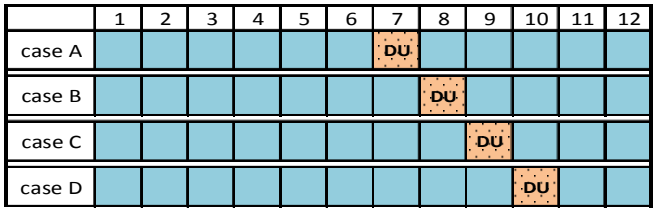

Figure 6.3: Possible locations of DU in various cases

The search space reduces drastically due to various symmetries and restrictions on DU loading and hence parallel computing was not necessary. The optimization could be carried out on a serial computer.

6.4. The Optimization Problem

The optimization problem is defined as follows.

***Objective**:* To maximize the effective multiplication factor (K_{eff}).

***Constraints**:* Following constraints are imposed.

- The reactor power (FP) should not be less than FP0 (100% FP).
- The maximum channel power (MCP) should be less than MCP0 (7.2 MW).
- The maximum bundle power (MBP) should be less than MBP0 (917 KW).
- The maximum channel power peaking factor (CPPF) should be less than CPPF0. The maximum CPPF0 which allow 100%FP operation is about 1.12 but here we have considered CPPF0=1.10.
- The reactivity worth of shut down system (SDS) should not be less than SDS0 (70 mk).

The objective function to be maximized has been defined using penalty to take care of constraints as follows:

$$Fit = K_{eff} - F1 - F2 - F3 - F4 - F5 \quad (6.1)$$

Where

F1 = (FP0-FP)*Afp if FP < FP0 and zero otherwise

F2 = (CP-CP0)*Acp if CP > CP0 and zero otherwise

F3 = (CPF-CPF0)*Acpf if CPF > CPF0 and zero otherwise

F4 = (BP-BP0)*Abp if BP > BP0 and zero otherwise

F5 = (SDS0-SDS)*Asds if SDS < SDS0 and zero otherwise.

The notation used is as follows:

FP0=100, corresponding to 100%FP.

FP is the maximum allowable power in a given configuration.

CP0 is corresponding to maximum permitted channel power i.e. 7.2 MW.

CP is the maximum channel power in a given configuration.

CPF0 is corresponding to the permitted channel power peaking factor i.e. 1.10.

CPF is the maximum channel power peaking factor in a given configuration.

BP0 is corresponding to maximum permitted bundle power i.e. 917 KW.

BP is the maximum bundle power in a given configuration.
SDS0 is the minimum worth of Shut-down System i.e. 70 mk.
SDS is the worth of SDS in a given configuration.

Afp, Acp, Acpf, Abp and Asds are suitably chosen constants to give a weightage to each of the factors. The procedure to decide these constants is somewhat arbitrary and is based on experience.

6.5. Estimation of Distribution Algorithm

EDA is used to determine the suitable loading pattern. The Probability Distribution Function (PDF) was generated using 30% dominated individuals of the population size (i.e. 100). Alpha is chosen 0.05. To keep the total number of DU bundles within the pre-decided interval, random correction model is applied. The large interval (80±64) is chosen. The possible number of DU bundles in the pattern can be from 16 to 144. The probability of random correction is small since a very large interval is considered in the simulation. In random correction the excess bundles (of NU or DU) are randomly chosen and converted to other type.

6.6. Loading Pattern with DU (0.3wt% U^{235}) for 700 MWe PHWR

In all, four types of DU loadings (cases A, B, C and D) described in section 6.3 were separately optimized using the EDA algorithm. The properties of optimum DU configuration obtained in each of the four cases are shown in Table 6.1.

It is seen that the configurations corresponding to case A, B and C can give 100%FP with sufficient excess reactivity, while keeping bundle power, channel power and CPPF within limits. The worth of 28 rods of SDS#1 is also adequate. In case D, the CPPF is somewhat higher than the prescribed limit and hence it is not accepted.

Table 6.1 gives maximum power and safety parameters in the fresh core. It is necessary that the power level and constraints are satisfactory at later times also. To further study suitability of DU loadings, time dependent burnup simulation was carried out for all the four cases up to the pre-fueling period. A time-step of 2.5 FPD (full power days) was used. The change in excess reactivity with FPD is shown in Figure 6.4 for all the four cases. It is seen that excess reactivity becomes zero after about 116 FPD, which marks beginning of refueling.

The variation of CPPF with time is shown in Figure 6.5 for all the four cases. The CPPF varies in narrow range for case A (DU at 7^{th} location). The ROP detectors are calibrated with CPPF regularly.

Case A permits more operating margin (lower CPPF) before the ROP trip as well as better safety (less variation in CPPF). Hence, the DU configuration in case A are considered as a better choice.

Table 6.2: The 700 MWe core properties for different type of loading

Case	#DU bundles	Reactor Power (%FP)	Excess Reactivity (mK)	MBP (kW)	MCP (mW)	CPPF	SDS#1 Worth (mK)
All NU	0	88	32.0	742.0	7.03	1.100	79.9
Case A	124	100	23.5	829.8	6.85	1.108	75.2
Case B	120	100	21.7	769.1	6.78	1.088	74.2
Case C	108	100	22.6	826.9	6.80	1.101	76.7
Case D	80	100	26.3	862.0	6.86	1.145	78.9

The configuration in case A needs further changes. There are 28 shut-off rods (SRs) in SDS#1. The DU bundle at 7th location gives sufficient reactivity worth in SDS#1 (28 SRs). In case, two rods with maximum worth fail to drop in the core during shutdown, the realized reactivity worth of SDS#1 (26 SRs) is found to be less than 50 mk. In order to increase the worth of 26 SRs, some additional DU bundles are placed at 11th and 12th bundle locations in few channels. These channels are selected manually. DU bundles are kept at 7th location in the four fuel channels (F10, F11, F12 & F13) to reduce the non-uniformity in zone powers due to zone control compartments (ZCCs). The final loading pattern is shown in Figure 6.6.

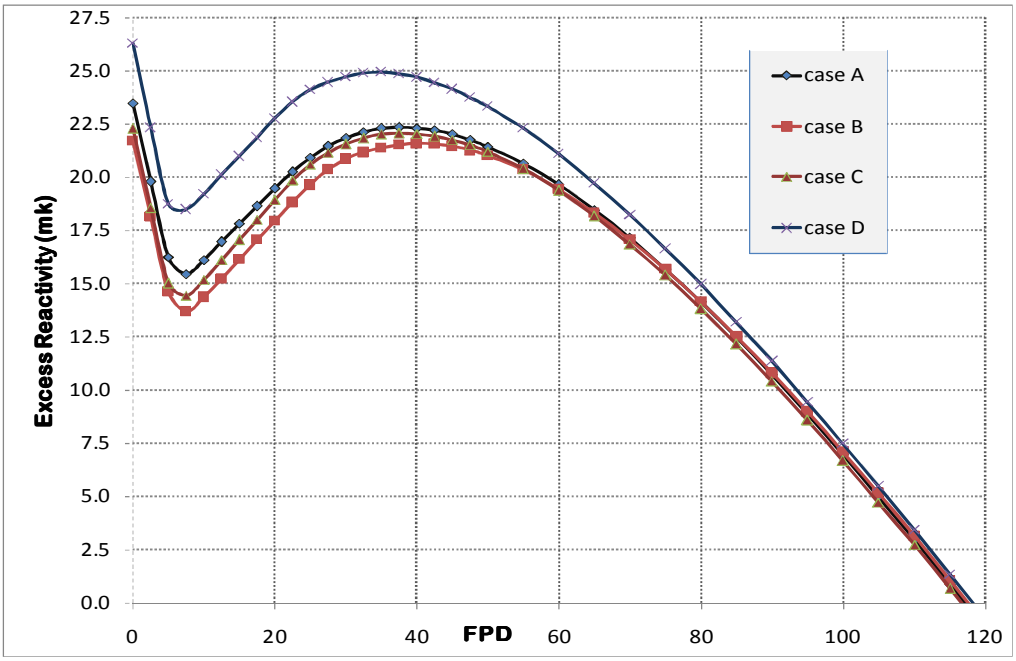

Figure 6.4: Variation in excess reactivity

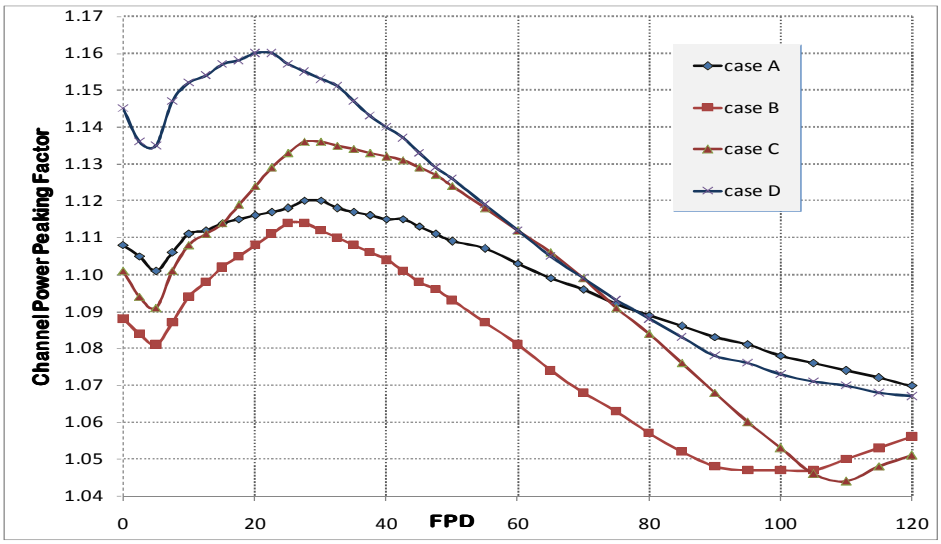

Figure 6.5: Variation in channel power peaking factor

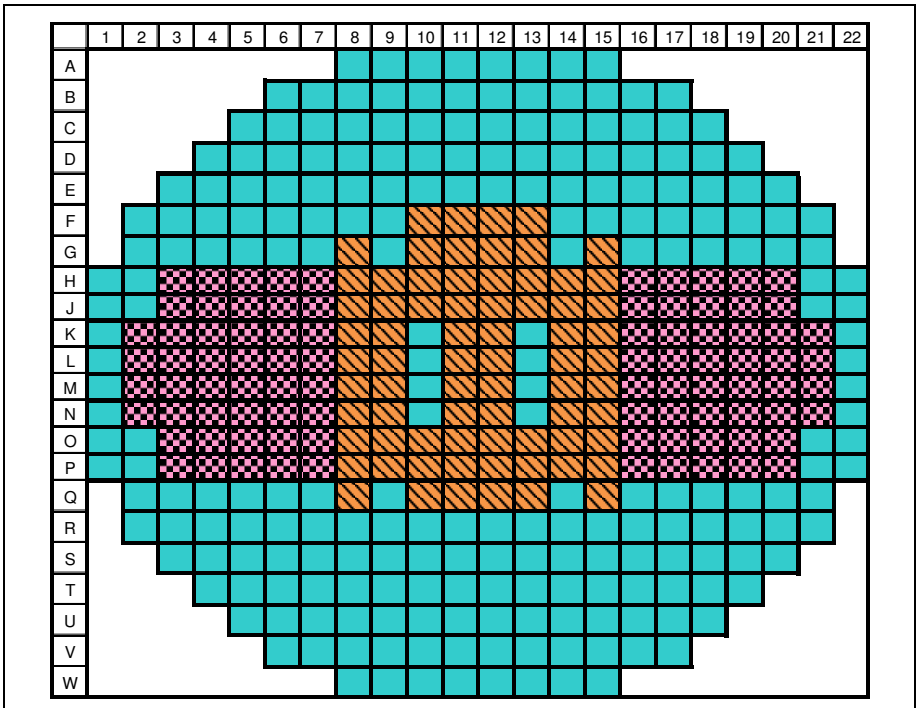

Fuel Bundle Location												
	1	2	3	4	5	6	7	8	9	10	11	12
	NU	NU	NU	NU	NU	NU	NU	NU	NU	NU	NU	NU
	NU	NU	NU	NU	NU	NU	**DU**	NU	NU	NU	NU	NU
	NU	NU	NU	NU	NU	NU	NU	NU	NU	NU	**DU**	**DU**

Figure 6.6: The Loading pattern with 248 DU (0.3wt%U^{235}) bundles

CHAPTER 7

OPTIMIZATION OF INSTRUMENTED CHANNELS FOR THERMAL POWER MEASUREMENT SYSTEM IN 700 MWe PHWR

A study for the design of Thermal Power Measurement System (TPMS) for the forthcoming 700 MWe Indian PPHWR is presented in this chapter. The selection of 44 channels out of 392 for instrumentation is to be made such that the average of power values measured by them in terms of per unit basis represents the true zone-wise and global powers fairly accurately. This should be possible for a large number of reactor configurations that can occur because of the movement of reactivity devices in the core. The selection of fuel channels for instrumentation is an optimization problem in which the error in zonal and global power measurement is to be minimised. There are several constraints on the selection of instrumented channels. Therefore, a constrained combinatorial optimization problem has to be solved.

7.1. Necessity of TPMS

The medium and large sized PHWRs are neutronically loosely coupled and hence, are prone to spatial flux tilts and xenon oscillations. As a result, they need a sophisticated regulation and protection system. For the purpose of regulation, the core is conceptually divided into 14 spatial zones. Each zone is equipped with one Zone Control Compartment (ZCC). The light water level in each compartment can be changed to control the flux shape. Apart from ZCCs, the reactor is equipped with two more regulating devices: There are 17 Adjuster Rods (ARs) symmetrically grouped into eight banks and 4 Control Rods (CRs) symmetrically grouped into two banks [1]. The objective of reactor regulating system is to operate the reactor keeping bundle, channel power within prescribed limit and to keep zonal power close to the design value. Each zone contains a Zone Control Detector (ZCD) to assess the power in that zone. The surrounding fuel channels corresponding to each ZCD are shown as dark circles in Fig.7.1. The regulating devices are operated based on the zone power measured by corresponding ZCD. The ZCDs measure point flux at nearby location, therefore the power measured by these detectors needs

to be corrected. The correction is usually carried out using the power measured by more accurate systems. There is Thermal Power Measurement System (TPMS) to measure reactor bulk power. Reactor zone powers are measured by TPMS and on-line flux mapping system (OFMS). In OFMS, there are 102 vanadium self powered neutron detectors (SPNDs). They are well distributed inside the reactor core. With the help of these vanadium detector readings and modal expansion method, detailed flux distribution in side core is obtained by flux mapping algorithm. In case of unavailability of OFMS, the zone power correction is also carried out using the TPMS.

Reactor bulk power is also estimated using measurement of primary side (D_2O coolant) and secondary side (feed water) parameters. Primary side parameter is the delta-T of D_2O coolant across Steam Generator (SG-ΔT). The bulk power estimation by SG-ΔT is prone to error when there is a change in coolant flow, frequency of induction motor (Primary Coolant Pump) and frequency of Boiler Feed Pump (BFP). For the estimation of reactor bulk power using secondary side parameters heat balance across the steam generator (feed water in SG) is carried out. But for better accuracy one has to know the steam pressure, feed flow rate & temperature, rate of blow down and heat loss from insulation accurately. In contrast, TPMS is an accurate and direct means of measuring reactor bulk and zone power on per unit basis.

In the TPMS, certain selected fuel channels are equipped with instruments to measure temperature, flow etc. of that channel. TPMS determines the reactor bulk power and zone powers based on the power measured by these instrumented channels (ICs). The 14 zones shown in Fig. 7.2 can be reduced to 7 new zones by combining zones with same channels. Thus,

$$\begin{bmatrix} \text{zone A} = \text{zone1} + \text{zone8}; & \text{zone B} = \text{zone2} + \text{zone9} \\ \text{zone C} = \text{zone3} + \text{zone10}; & \text{zone D} = \text{zone4} + \text{zone11}; \quad \text{zone E} = \text{zone5} + \text{zone12} \\ \text{zone F} = \text{zone6} + \text{zone13}; & \text{zone G} = \text{zone7} + \text{zone14} \end{bmatrix}$$

Hereafter, “zonal power” refers to power in zones A to G defined above. The zonal power is calculated using average of per unit thermal power of ICs in the corresponding zone. The reactor thermal bulk power calculation is based on average of per unit thermal power of all ICs.

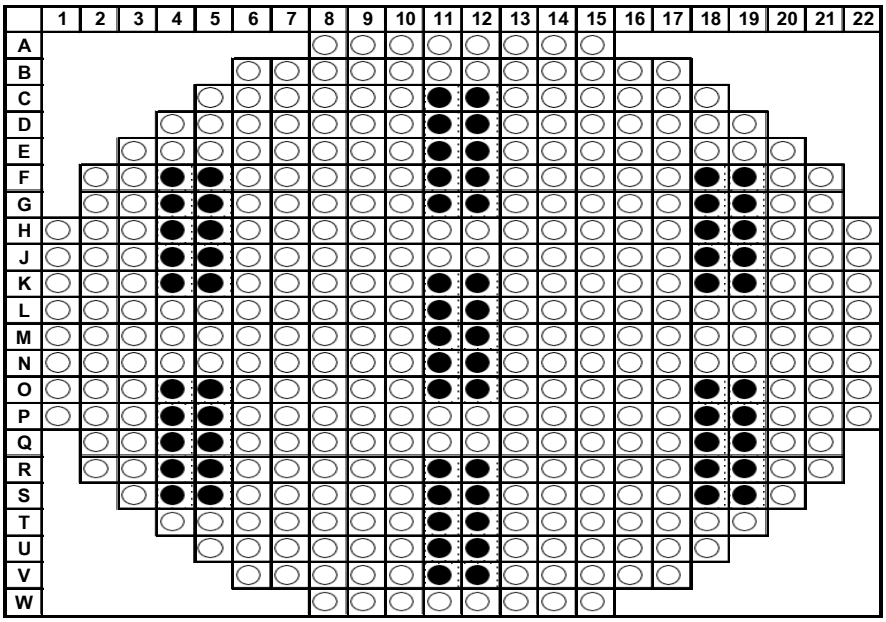

Fig. 7.1: Reactor core having 392 fuel channels (open circle: normal fuel channel; filled circle: fuel channels surrounding ZCD)

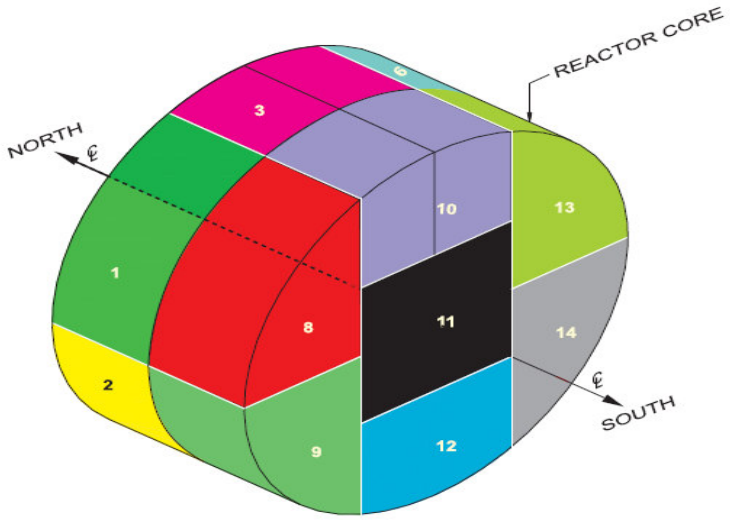

Fig. 7.2. Reactor core having 14 zones (7 front and 7 rear)

7.2. Selection of Fuel Channels for TPMS

Optimization studies to identify the best possible fuel channels for instrumentation which minimizes the errors in prediction of the seven zonal powers and global power is carried out. During operation, the reactor configuration changes due to movement of reactivity devices. The error in the

measurement should be minimized for all these core configurations. The equilibrium state of the core with 357 possible device configurations is considered for the optimisation. There are several restrictions on the selection of fuel channels for instrumentation. Thus, one has to solve a constrained optimization problem. There are several methods to solve such problems such as gradient methods and simulated annealing. There are yet other techniques based on Genetic Algorithms (GA), particle swarm optimization (PSO) and ant colony optimization (ACO). These population based algorithms can be found in references [15, 19, 20, 25, 26, 31, 32]. In the present work such a technique [18] based on the "Estimation of Distribution Algorithm" (EDA) has been used.

7.3. Constraints of the Optimization Problem

The two ends of fuel channels (as shown in Fig.7.2) are designated as "north" and "south" face of the reactor core. The 392 fuel channels can be logically divided in 4 sets depending on its loop and header of coolant:

(1) Set 1: The fuel channels having coolant flow from north side inlet header to south side outlet header in loop 1
(2) Set 2: The fuel channels having coolant flow from south side inlet header to north side outlet header in loop 1
(3) Set 3: The fuel channels having coolant flow from north side inlet header to south side outlet header in loop 2
(4) Set 4: The fuel channels having coolant flow from south side inlet header to north side outlet header in loop 2

This design of coolant system with two loops is chosen because it reduces the reactivity gain due to void in coolant. As is known, the reduction in coolant density leads to positive reactivity addition in a PHWR and is a safety concern. To reduce the effect of coolant voiding, 700 MWe PHWR consists of two Primary Heat Transport (PHT) loops implied with checkerboard type distribution in the reactor core. There are two inlet and two outlet headers in each loop of the PHT system.

The first constraint is that all the four sets of fuel channels contain an equal number of instrumented channels.

The change in power/flux at any location in the core is realized up to about 3 lattice pitch away from that location. Hence, any given channel whose power/flux is undergoing a change should not be more than 3 lattice pitches away from an instrumented channel. Therefore the selection of IC is made such

that nowhere a core of size 4×4 pitches be left without an instrumented channel. This is the second constraint. This constraint is useful to estimate the total number of ICs needed. Let the 392 fuel channels be divided into 3×3 pitch regions each containing 9 fuel channels and suppose the central channel in each 3×3 pitch region is instrumented. Then, distance between 2 IC's would be 3 pitches and fulfill the constraint. Since there can 44(≈392/9) such regions, a minimum of 44 ICs should give adequate coverage of the whole core. Thus 11 ICs in each fuel channel set (as per first constraint) should get instrumented.

The third constraint arises from symmetry. The core has reflective symmetry along the X-axis whereas the reactivity devices disturb reflective symmetry along Y-axis. The symmetry of ICs about X-axis is avoided for better coverage and less redundancy.

There are 14 ZCDs to measure the zone powers. The fourth constraint in the design of TPMS is that each ZCD should be surrounded by minimum of two ICs. The ICs at ZCD nearby location are useful for intercomparison purpose.

7.4. Optimization Method

Channel power distribution has been generated using diffusion theory code for 100%FP reactor operation using equilibrium time average fuel burnup distribution for the nominal state (Nominal state means ZCCs at 50%FL, ARs fully IN, CRs fully OUT). All the channel powers (including the ICs), zonal powers and total power were noted. Later, the power distribution was found for various reactivity device configurations. Total 357 reactivity device configurations are considered. The sequential withdrawal of AR banks at different ZCC levels is covered up to case number 124. From case no.125 to 147, CR insertion cases are covered. From cases 148 to 236, single ZCC drain is represented. Beyond case number 236, less probable configurations such as draining of multiple ZCCs are considered. In the present analysis it is assumed that ICs read the corresponding channel powers.

The bulk power and zone powers are measured using TPMS in per unit basis. The channel power of selected IC per unit basis is the ratio of channel power measured by that IC in any configuration to the channel power in nominal device configuration. Reactor bulk power per unit basis is obtained by averaging the power per unit basis measured by all ICs. Similarly zone power per unit basis is obtained by averaging the power per unit basis of corresponding zone ICs.

The reactor bulk power and zone powers are estimated for all 357 core configurations using power in ICs obtained by diffusion theory code. The reactor bulk power per unit basis measured by ICs should

be 1 in ideal case, since all 357 cases are corresponds to 100%FP. The % error in zone powers measured by ICs is determined.

It may be mentioned that an effort has been made to design TPMS by manual intuition. The designed TPMS satisfies all the above mentioned constraints but the error in estimated reactor bulk and zone powers for various reactivity configurations are about ±2.3% and ±5.7% respectively. A better design has been obtained using EDA [45].

7.4.1. The optimization problem

The optimization problem is defined as follows.

Objective The error in estimated bulk power should be less than ±0.5% and in zone power less than ±2%.

Certain fitness points are allotted if the pattern (individual) satisfies the criterion mentioned above.

Constraints The constraints are as follows:

1. Total 44 numbers of channels should be selected and thus 11 numbers of channels should be there in each of the four sets of fuel channels.
2. The channels which have been selected for instrumentation should not be symmetric about X-axis.
3. Nowhere a gap of 4 pitch × 4 pitch or more should be left without a instrumented channel.
4. Each Zone Control Detector (ZCD) should have minimum two ICs at nearby location.

Here, the objective function to be maximized has been defined as follows:

$$Fit = \sum_{case=1}^{357} (F0 + F1 + F2 + F3 + F4 + F5 + F6 + F7) \tag{7.1}$$

Where summation is carried out over all 357 configurations and the terms are as follows:

F0 = 3, if the measured bulk power (P) is above 99.5% and less than 100.5% and zero otherwise {in fraction the condition means, 0.995< P<1.005; P is fractional full power}

F1 = 1, if error in zone A power is less than ±2% and zero otherwise

F2 = 1, if error in zone B power is less than ±2% and zero otherwise

F3 = 1, if error in zone C power is less than ±2% and zero otherwise

F4 = 1, if error in zone D power is less than ±2% and zero otherwise

F5 = 1, if error in zone E power is less than ±2% and zero otherwise

F6 = 1, if error in zone F power is less than ±2% and zero otherwise

F7 = 1, if error in zone G power is less than ±2% and zero otherwise

The objective function (also called fitness function) given by Eq.(7.1) has to be evaluated to determine the fitness of any given set of selected channels. It can be seen from Eq.(7.1) that if all the errors are within specified limit for a power distribution the pattern (individual) is rewarded 10 points. There are total 357 power distributions and thus a suitable individual will acquire maximum 3570 points.

7.4.2. Optimization algorithm (EDA)

EDA belongs to the class of population based optimization algorithms. The two operators in EDA are estimation of distribution and sampling. In each generation, N individuals are generated by sampling probability distribution. They are generated (during initial and subsequent generations) in such a way that first three constraints are satisfied. The fitness is evaluated for each of them as described by Eq.7.1 and the best M (<N) individuals are selected to estimate probability distribution. The probability that a given fuel channel will get selected for instrumentation or not is estimated from the selected M individuals. However, the selection probabilities of the fuel channels which are adjacent to the ZCDs (as shown by dark circles in Fig.7.1) are kept 0.9 always. This takes care of the fourth constraint.

1. Initialize the population (Size=N) randomly such that they satisfy all the constraints.
2. Evaluate the fitness of each individual.
3. Either continue for new generation calculations or terminate the execution.
4. Select M<N candidates based on termination selection method (the best fit M individuals are chosen from among total N individuals).
5. Calculate Probability Distribution Function (PDF) using selected M individuals. At any generation (t) the PDF has been estimated as given below for each location.

$$PDF\ (t+1) = PDF\ (t)\ .(1-\alpha) + \alpha\ .\frac{1}{M}\ .\sum_{m=1}^{M} X_m(t)$$

Where α is constant between [0, 1]. X is binary representation of Instrumented/Non-instrumented fuel channels. For a particular fuel channel at generation t, $X_m(t)=0$ if channel is not instrumented and $X_m(t)=1$ if channel is not instrumented. Thus $\frac{1}{M}\ .\sum_{m=1}^{M} X_m(t)$ is probability that the location has been instrumented. The PDF at ZCDs nearby locations is kept 0.9 always.

6. Generate new population (Size=N) using this new probability distribution function (PDF) such that each individual satisfies the constraints.
7. The fitness of new N individuals is found out as in step 2.
8. Go to step 3.

Figure 7.3: Pseudo EDA model used for optimization

A pseudo model of the algorithm used for optimization is given in Fig.7.3. The Probability Distribution Function (PDF) was generated using 25% dominated individuals of the population size (i.e. 200). Alpha is chosen 0.10.

7.5. Result and Discussion

The evolution of fitness with generation number is shown in Fig.7.4. There are 200 individuals in each generation. After 3493 generations the maximum fit individual acquires 3570 points.

The core map representing selected instrumented channels is shown in Fig.7.5. The fuel channels numbered as "1" are not instrumented whereas, the fuel channels numbered as "2" are instrumented. The pattern satisfies all the constraints as mentioned above. There are 11 fuel channels in each set. The selected channels are not symmetric about X-axis and nowhere a gap of 4×4 pitches or more are left without an instrumented channel.

The reactor bulk power per unit basis estimated using all instrumented channels for all 357 cases is shown in Fig.7.6. The bulk power estimated by instrumented channels lies between 0.995 and 1.005. Thus error in bulk power is less than ±0.5%.

The %error in zone power estimation is shown in Fig.7.7. The %error in estimating reactor zone power lies between -2% and 2%. Thus the desired objectives have been achieved.

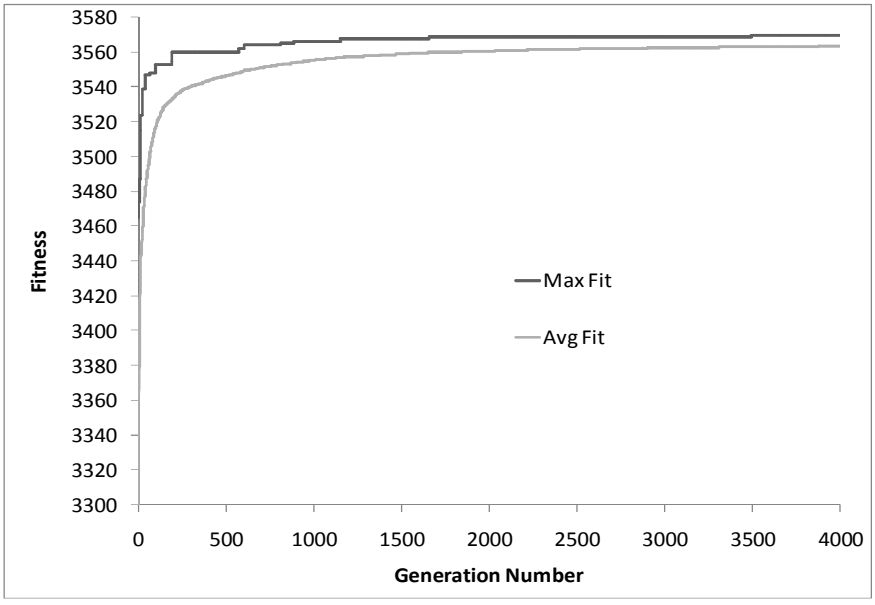

Figure 7.4: Fitness evolution for instrumented channel with generation number

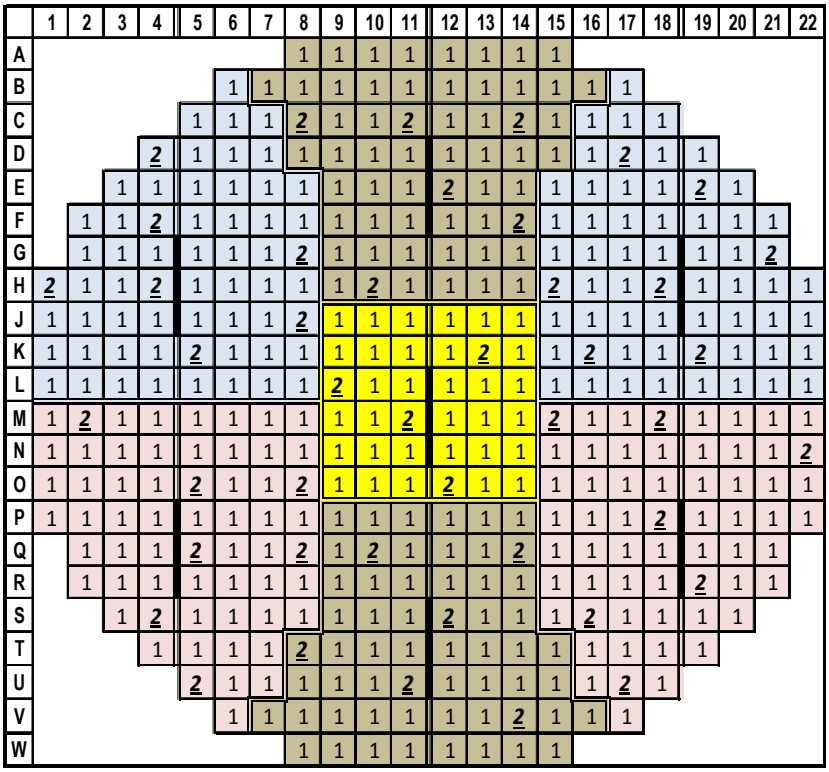

Figure 7.5: Reactor fuel channels instrumented/non-instrumented (1: non-instrumented; 2: instrumented)

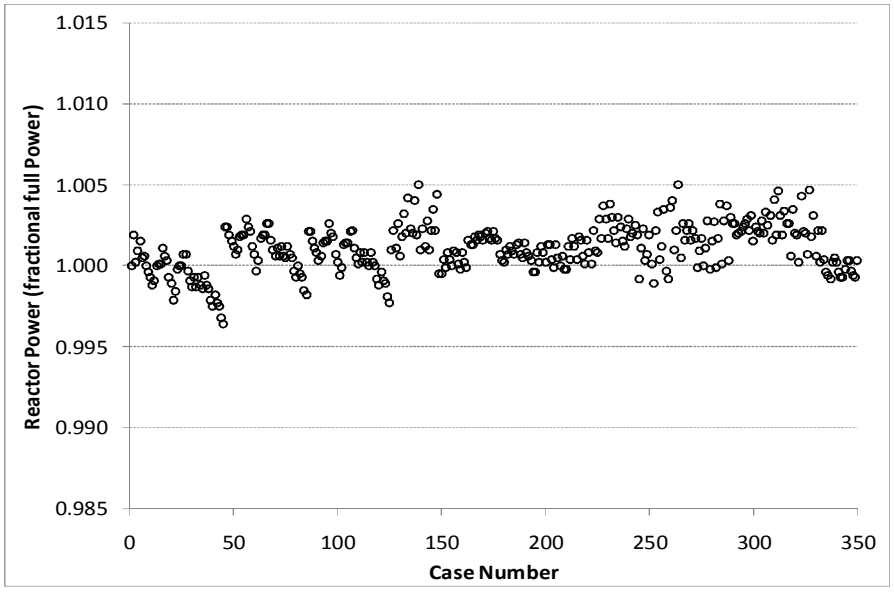

Figure 7.6: Reactor total power (fractional full power) estimated by instrumented fuel channels for various core configurations

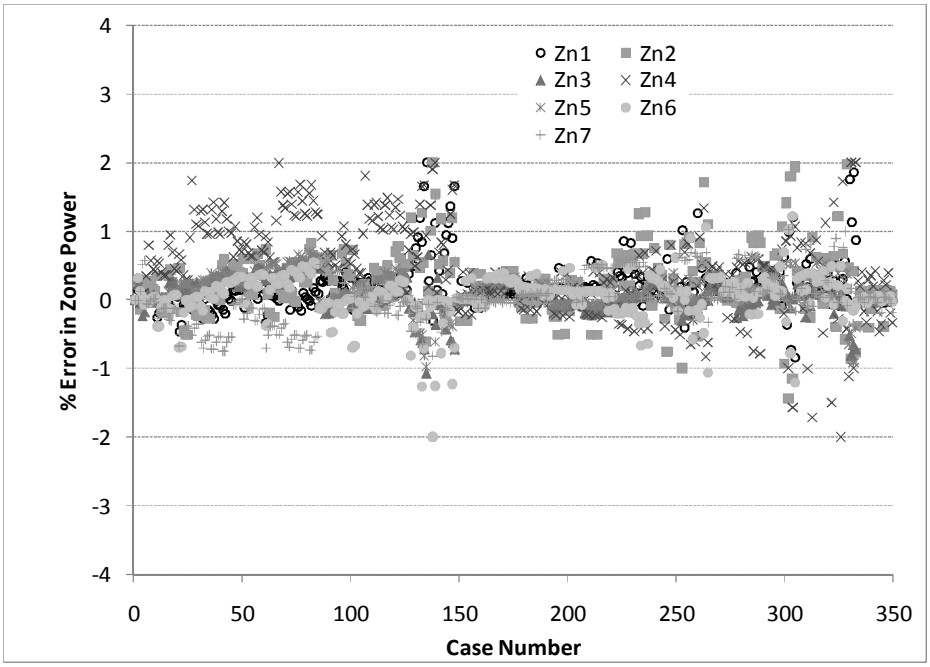

Figure 7.7: % Error in zonal power estimated by instrumented fuel channels for various core configurations

CHAPTER 8

OPTIMIZATION OF FLUX MAPPING ALGORITHM FOR 700 MWe PHWR

There are 102 vanadium self powered neutron detectors (SPNDs). They are well distributed inside the reactor core. With the help of these detector readings, one has to continuously estimate the detailed power distribution inside the reactor. This is achieved by the so-called on-line flux mapping system (OFMS). The comparison of four computational methods based on widely different principles for OFMS are presented in this chapter.

8.1. Introduction

The large sized PHWRs are neutronically loosely coupled and hence are prone to spatial flux tilts and xenon oscillations. As a result, they need a sophisticated regulation and control system [1]. For the purpose of regulation, the core is conceptually divided into 14 spatial zones (Fig. 7.2). Each zone is equipped with one Zone Control Compartment (ZCC). The light water level in each compartment can be changed to control the flux shape. Each zone contains one or two zonal detectors to assess the power in that zone. In addition, there are 102 vanadium self powered neutron detectors (SPNDs). They are well distributed inside the reactor core. With the help of these detector readings, one has to continuously estimate the detailed power distribution inside the reactor. This is achieved by the so-called on-line flux mapping system (OFMS). Apart from detector readings, the OFMS makes use of the fact that flux shape is governed by neutron diffusion theory. A detailed flux map is created by OFMS every two minutes. It is used to calibrate the zonal detectors so that they correctly reflect the zonal powers. The maximum bundle power and channel power are also estimated to take corrective action if necessary. The objective of reactor regulating system is to operate the reactor keeping bundle, channel power within prescribed limit and to keep zonal power close to the design value. For this, the neutron flux distribution in the reactor core has to be continuously estimated.

8.2. Computational Methods for OFMS

The purpose of OFMS is to estimate the flux (and power) distribution in the reactor at any time during its operation, as accurately as possible, using the measured flux values at the 102 fixed in-core locations. This task has to be accomplished every two minutes. The computational method used by OFMS should be fairly efficient and accurate. All the computational schemes developed for OFMS make use of multi-group neutron diffusion equation in some form.

Several computational methods have been proposed for finding flux distribution in the OFMS. Three computational methods based on widely different principles are studied to decide the optimum method. The three methods are:

(i) Flux Synthesis (FS) method

(ii) Internal Boundary Condition (IBC) method

(iii) Combined Least Square (CLSQ) method

8.2.1. Flux synthesis (FS) method

This is the oldest method [33, 34]. In this method, a "reference state" of the reactor has to be defined. In case of PHWR, after about 600 Full Power Days (FPD) of reactor operation, the core is operated in an equilibrium phase for rest of the life. For the flux mapping of equilibrium phase of PHWR, the "time-averaged" core [7, 35] can be a suitable reference state. In the reference state, the ARs are fully in, CRs are fully out and all the ZCCs water levels are 50 % of full level (FL).

The FS method is based on the assumption that the prevailing snap-shot flux shape at any time in an operating reactor with any configuration can be approximated by a linear combination of fundamental and next dominant K-modes of the reference state. The K-modes of reference state are found off-line only once and stored for use by OFMS during reactor operation. They are found numerically by solving the K-eigenvalue form of neutron diffusion equation for the reference state. This is generally done by solving finite-differenced two energy group diffusion equation in 3-D XYZ geometry. The mesh size is usually chosen to be equal to the pitch of fuel channels (28.6 cm) in X & Y direction. The mesh size is equal to half bundle length (~24.8 cm) in axial Z-direction. For the 700 MWe PHWR model, this leads to a 28×28×24 mesh structure. With total 18816 meshes and two energy groups, the eigenvalue problem involves 37632 unknowns. The fundamental mode can be found by power iteration method [6]. The higher modes can be found by using elimination method [36], Orthomin(1) method [37, 38] or sub-space

iteration method [39]. In some earlier studies, the modes of Helmholtz equation [34] have been used instead of K-modes.

The K eigenvalue equation for reference state can be schematically written as

$$M\phi_n^{ref} = \frac{1}{K_n} F\phi_n^{ref} \qquad n = 1, 2, 3, .. \qquad (8.1)$$

The operator M stands for leakage, absorption and group-to-group transfer and F is fission production operator in diffusion theory. The superscript "ref" indicates reference state; ϕ_n^{ref} is a vector containing flux in the 18816 meshes in both groups.

Let the K modes be ordered in such a way that $K_1 > K_2 \geq K_3 \geq \ldots\ldots$ Thus, ϕ_1^{ref} is fundamental mode. Suppose one finds I dominant modes $\phi_1^{ref}, \phi_2^{ref}, \phi_3^{ref}, \ldots, \phi_I^{ref}$. At any time during reactor operation, the prevailing (snap-shot) flux Φ can be approximated as

$$\Phi = \sum_{n=1}^{I} a_n \ \phi_n^{ref} \qquad (8.2)$$

where a_n are called combining coefficients. Let $r_1, r_2, \ldots, r_{102}$ denote the locations of the *102* in-core detectors. Let $\Phi(r_j)$ denote the flux given by Eq.(8.2) at j^{th} detector location. Let the measured flux at that location be denoted by Φ_{dj}, where $j = 1, 2, 3 \ldots, 102$. The conditions that the measured flux is equal to computed flux lead to the following set of *102* linear equations in the I unknowns $a_1, a_2, a_3 \ldots a_I$.

$$\Phi_{dj} = \sum_{n=1}^{I} a_n \, \phi_n^{ref}(r_j) \quad ; \quad j = 1, 2, 3 \ldots, 102 \qquad (8.3)$$

This is an over-determined system since, generally, the number of modes I (= number of unknowns a_n) is less than 102 (total number of detectors or number of equations). These equations can be written as a matrix equation:

$$H\ a = p \qquad (8.4)$$

where H is a rectangular matrix of order $102 \times I$, a is the unknown vector of size I and p is a vector of size *102* containing detector measured fluxes. Pre-multiplying Eq.(8.4) by H^T, we get

$$(H^T H)\ a = \ H^T\ p \qquad (8.5)$$

Since H^TH is symmetric positive definite matrix of order I, Eq. (8.5) has a unique solution that can be readily found. Once all the a_n are known, Eq. (8.2) gives an estimate of flux (or the flux map) at all points.

It may be noted that the solution of Eq. (5) minimizes the error L^2 , given by

$$L^2 = \sum_{j=1}^{102} [\, \Phi(r_j) - \ \Phi_{dj}]^2 \tag{8.6}$$

A subtle point regarding the detector location should be mentioned. The flux mapping detectors are located in the space between the fuel channels. A single mesh in the 28×28×24 mesh structure covers one fuel channel and associated moderator in XY plane (Fig. 8.1) and a distance of a half bundle length in Z-direction. The mesh centre is the same as the centre of a fuel channel. The detectors do not read the flux at the centre of any mesh. The flux at the detector can be expressed in terms of flux in the nearest meshes by Lagrangian Interpolation [40]. Thus, $\phi_n^{ref}(r_j)$ in Eq.(8.3) is obtained in terms of known values of ϕ_n^{ref} at the meshes nearest to r_j.

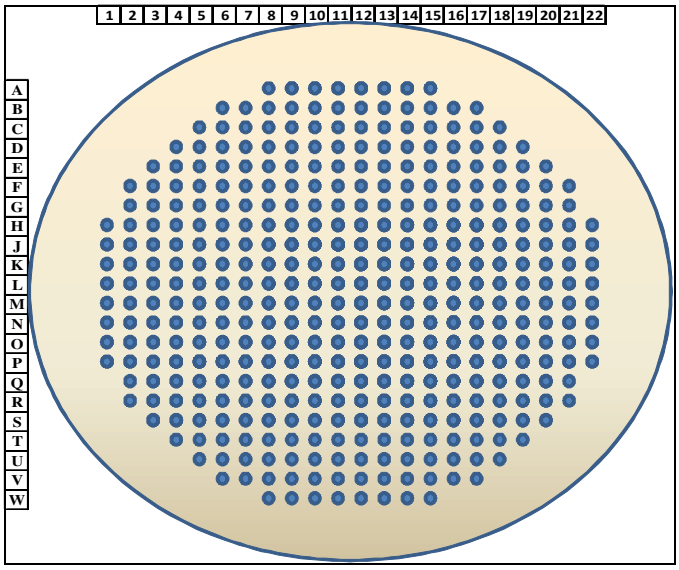

Fig. 8.1. Reactor core having 392 fuel channels surrounded by reflector

Perturbed shapes

The actual configuration of reactor during operation differs in many ways from the reference configuration for which K-modes are found. The fuel burn-up distribution would be different. The

position of adjuster rods may not be the same as in the reference state. The water levels in ZCCs can also differ from that in the reference state. Because of these differences, the flux obtained by a combination of K-modes of reference state can differ from the actual flux substantially at some places. The difference in reactivity device position produces local and global changes in flux shape. The global changes can be approximated by few higher modes of reference state but not the local changes. Hence, for an improvement in flux mapping, sometimes fundamental K-mode shapes for some configurations different from the reference configuration are also added to the expansion set. They are called perturbed shapes. If there are "p" number of perturbed shapes, Eq.(3) will contain total (I+p) basis functions and the square matrix H^TH in Eq.(5) would be of order (I+p). The "p" perturbed states have time averaged burn-up distribution like the reference state. In the present studies, the K-mode of these states are found by standard 28×28×24 mesh structure and two energy groups. There are 14 such configurations (p = 14). They are described in table 8.1

Table 8.1: The reactivity device configuration for 14 perturbed shapes

Shape No.	All ZCC level	AR bank position	CR bank position
1	5%FL	All bank 100%IN	Both bank 0%IN
2	95 %FL	All bank 100%IN	Both bank 0%IN
3	50%FL	Bank#1 0%IN, other 100%IN	Both bank 0%IN
4	50%FL	Bank#1&2 0%IN, other 100%IN	Both bank 0%IN
5	50%FL	Bank#1,2&3 0%IN, other 100%IN	Both bank 0%IN
6	50%FL	Bank#1,2,3&4 0%IN, other 100%IN	Both bank 0%IN
7	50%FL	Bank#1,2,3,4&5 0%IN, other 100%IN	Both bank 0%IN
8	50%FL	Bank#1,2,3,4,5&6 0%IN, 7&8 100%IN	Both bank 0%IN
9	50%FL	Bank#1,2,3,4,5,6&7 0%IN, 8 100%IN	Both bank 0%IN
10	50%FL	All bank 0%IN	Both bank 0%IN
11	50%FL	All bank 100%IN	bank#1 50%IN, bank#2 0%IN
12	50%FL	All bank 100%IN	bank#1 100%IN, bank#2 0%IN
13	50%FL	All bank 100%IN	bank#1 100%IN, bank#2 50%IN
14	50%FL	All bank 100%IN	Both bank 100%IN

.

8.2.2. Internal boundary condition (IBC) method

In this method [41], no reference state is considered like the FS method. Eq.(8.1) is solved for the fundamental mode of actual prevailing snap-shot configuration of the reactor during operation. The finite-differenced form of K-eigenvalue equation is solved by inner-outer iterations [6]. While carrying out inner iterations for the thermal group, the flux values around detector location are forced to get the exact measured fluxes. Thus, the fluxes measured at different locations act as internal boundary conditions [41]. After the convergence of inner and outer iterations, one gets flux distribution at all

points and the fluxes at detector locations match with the measured values. In the present studies, the standard 28×28×24 mesh structure and two energy groups are used in implementing the IBC method.

8.2.3. Combined least square (CLSQ) method

This is a novel approach proposed recently [40, 42] and has been shown to be useful for both PWR and PHWR. In this method, first the fundamental eigenvalue K_1 and corresponding mode ϕ_1 of the actual prevailing configuration of reactor during operation are computed by solving two-group diffusion equations given by Eq.(8.1). Thereafter, approximate solution of the following two simultaneous block equations is sought:

$$\begin{bmatrix} M - \frac{1}{K_1}F \\ D \end{bmatrix} \Phi = \begin{bmatrix} 0 \\ S \end{bmatrix} \qquad or \qquad A\Phi = b \tag{8.7}$$

The operators M and F are the same as in Eq.(8.1). The first block equation in Eq.(8.7), namely, $M\Phi - \frac{1}{K_1}F\Phi = 0$, is identical in form to Eq.(8.1), but since K_1 is known, it is not an eigenvalue equation. It represents $2N$ linear algebraic equations where N (=18816) is the number of meshes in the standard (28×28×24) mesh structure. The second equation (called the detector response equation), $D\,\Phi = S$, represents additional 102 equations that impose the condition that the 102 measured fluxes be equal to the calculated fluxes. The block vector S contains 102 elements that are the measured fluxes. In Eq. (8.7), there are totally $(2N+102)$ equations and only $2N$ unknowns. Hence, it cannot be solved exactly. A solution that minimizes the L_2 norm of $A\Phi - b$ can be obtained by solving

$$A^T A\,\Phi = A^T b \tag{8.8}$$

Since A^TA is a SPD (symmetric positive definite) matrix of order 2N, equation (8.8) can be solved exactly. The order of matrix A^TA is much higher than that in Eq.(8.5) of FS method. The solution of Eq.(8.8) needs substantial computational effort. Despite this, the CLSQ method is attractive because it has been shown [40] to give more accurate results than other methods. Moreover, the computation is expected to become manageable in future with continuous improvement in computers [40]. Eq.(8.8) is solved by using the CGNR algorithm [43] with diagonal preconditioning or bi-diagonal QR preconditioning. The CGNR is a Krylov sub-space method. In present studies, we have used diagonal pre-conditioner to implement this method.

This method is called here as '*combined*' least square method because the least square principle is applied jointly to both finite-differenced diffusion equations as well as the 102 detector response equations. On the contrary, in the FS method the least square principle is applied only to the 102 detector response equations.

8.3. Procedure for Testing the Methods

The OFMS is supposed to work in an operating reactor by making use of fluxes measured by the detectors. Here, the various OFMS methods are tested by numerical experiments which mimic this situation for the 700 MWe PHWR as explained below.

Ten different configurations of the 700 MWe PHWR which can occur frequently during its operation are identified which can act as test-cases for the methods. These cases have certain snap-shot fuel burn-up distribution during equilibrium regime which differs from the time-average distribution used in the reference state. The test cases are chosen to represent a variety of situations occurring in a real operating reactor. In some of the test cases, first few AR banks are partially or fully in. In some of the test cases, the water levels in the 14 ZCCs are 20%, 80%, 50% or are randomly distributed. The withdrawal of more than three AR banks and insertion of CR banks inside the core occur rarely and for very short time, hence they have been excluded from the test cases. The exact configurations i.e. ZCC levels and AR bank positions for the ten test cases are given in table 8.2. It should be noted that all the methods to be tested use the standard 28×28×24 mesh structure.

Table 8.2: The reactivity device configuration for 10 test cases

Test Case	ZCC levels	AR bank position
1	Individual random, average 50%FL	All banks 100%IN
2	All 20%FL	All banks 100%IN
3	All 80%FL	All banks 100%IN
4	All 44%FL	All banks 100%IN
5	All 50%FL	Bank#1 50%IN, Other banks 100%IN
6	All 50%FL	Bank#1 0%IN, Other banks 100%IN
7	All 50%FL	Bank#1 0%IN, Bank#2 50%IN & Other banks 100%IN
8	All 50%FL	Bank#1&2 0%IN & Other banks 100%IN
9	All 50%FL	Bank#1&2 0%IN, Bank#3 50%IN & Other banks 100%IN
10	All 50%FL	Bank#1,2&3 0%IN & Other banks 100%IN

It is necessary to simulate the 102 detector readings (to be used by OFMS) for each of the ten test cases. One should also know corresponding flux in all meshes to check the accuracy of fluxes estimated by OFMS. This is achieved by carrying out a fine mesh two-group K-eigenvalue calculation in diffusion

theory for the test cases using fine 224×224×144 mesh structure. The fundamental K-mode fluxes are found for all the 10 test cases using this fine mesh structure. The fluxes in the coarse 28×28×24 meshes are found from the fine mesh fluxes. These fluxes are supposed to be the 'true' fluxes for the test case. From these 'true' fluxes, the fluxes at the 102 detector locations are found by interpolation and they are stored for use by the OFMS as experimentally measured fluxes. The bundle, channel and zone powers are also stored for verifying OFMS performance. This method of checking OFMS performance has been used in earlier studies [40].

The RMS error in Bundle Power (BP), Channel Power (CP) and Zonal Power (ZP) for each test case will be computed using following formula:

$$RMS\ error(\%)\quad \varepsilon_x = \sqrt{\frac{1}{N_m}\sum_{1}^{N_m}\left(\frac{(X - X_{true})}{X_{true}} \times 100\right)^2} \tag{8.9}$$

The notation is as follows:

X : BP, CP or ZP estimated by various methods using 28×28×24 mesh structure.

X_{true} : BP, CP and ZP found using the finer 224×224×144 mesh structure K-calculation for test cases.

N_m : number of bundles, channels or zones as the case may be.

Different computational methods will be compared using the RMS error in predicting the BP, CP and ZP for each test case.

8.4. Fixing Number of K-modes in FS Method

In the FS method, one can use different number (I) of higher K-modes. It is useful to get an idea of the number of modes required. Strictly speaking, this number can vary with the actual state of reactor. Test case 1, which contains different levels of water in the 14 ZCCs, is considered to study the effect of varying number of modes on OFMS performance.

The RMS errors in BP, CP and ZP are estimated using FS method by changing the number of K-modes from 1 to 50 for test case 1. The RMS error in BP, CP and ZP are shown in Fig. 8.3. It is seen that errors are small for about 23 modes and also around 40 to 45 modes.

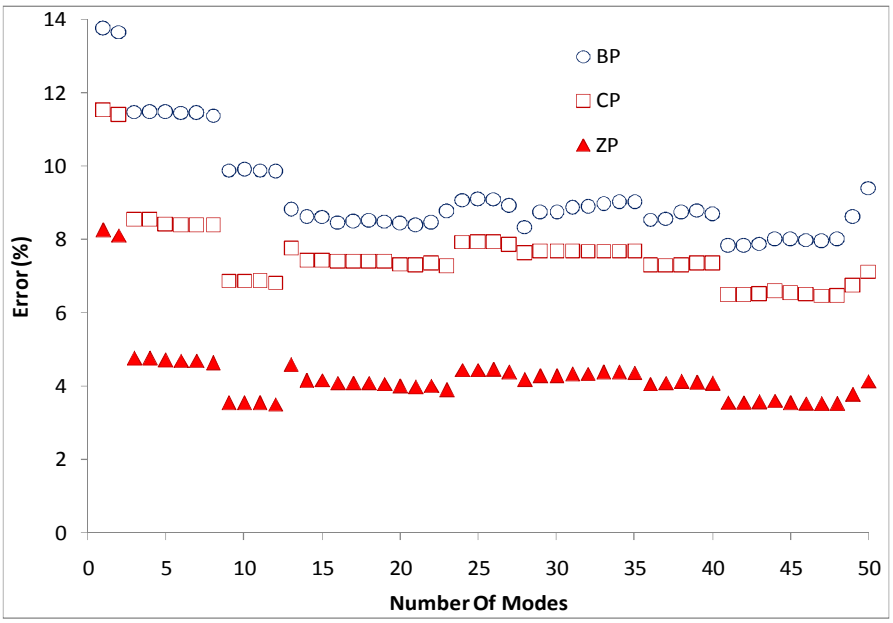

Fig. 8.2. RMS error in BP, CP and ZP by FS method against number of K-modes used

Certain perturbed shapes are useful to improve the FS method. Total 14 perturbed shapes (p=14) are considered as listed in Table 8.1. The effect of varying number of K-modes on FS method is studied with the 14 perturbed shapes included for the test case 1. The errors in BP, CP and ZP are presented in Fig. 8.4. It is seen that errors are reduced compared to the case without perturbed shapes in Fig. 8.3. About 23 K-modes seem to give better results.

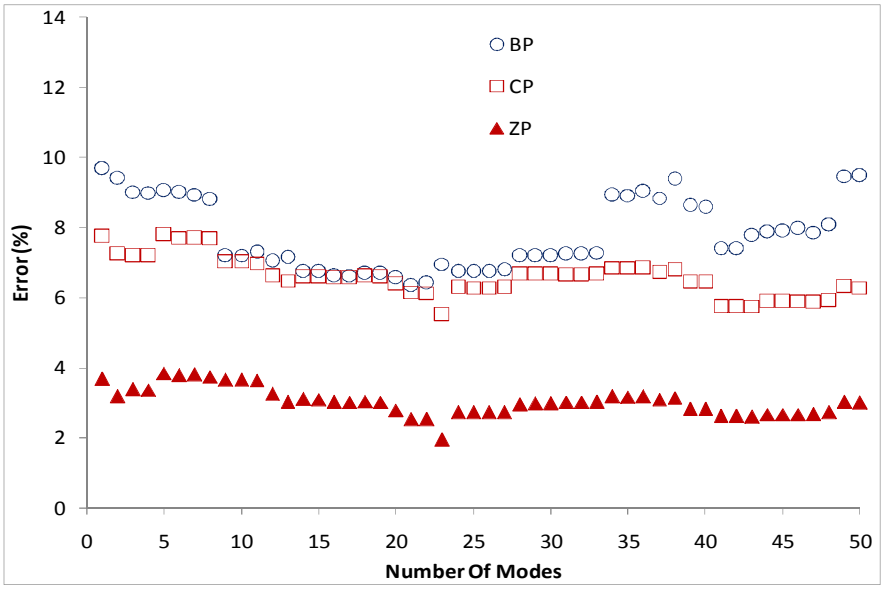

Fig. 8.3. RMS error in BP, CP and ZP by FS method using
14 perturbed shapes against number of K-modes

8.5. Modified Flux Synthesis (MFS) method

It should be noted that the FS method needs minimum computational effort. It requires solution of few tens of linear equations (Eq.8.5). It does not make use of the knowledge of snap-shot configuration of operating reactor at the time of flux-mapping. It is based only on the fundamental and higher K-modes of reference state and fundamental modes of some perturbed states which are computed a-priori and stored.

On the other hand, the IBC method and CLSQ method need significant computational effort. Both of them need a fundamental K-mode calculation for the snap-shot configuration with 28×28×24 meshes and two groups. The CLSQ method needs an additional more difficult calculation by CGNR algorithm (solving Eq.8.8) to minimize errors in neutronic and detector equations. This involves solution of 37734 simultaneous equations. As will be seen later, the CLSQ method, which needs maximum computational effort, is much more accurate than FS method and IBC method.

It is desirable to have a method that is reasonably accurate and yet does not need too much computational effort. In view of this, in this paper a hybrid method [44] is suggested that combines useful features of FS and CLSQ methods. In this method, one first finds the fundamental mode ϕ_1 of the prevailing state as is done in the CLSQ method. In addition, some higher modes of the reference state are used. They are estimated a priori only once and preserved. They are denoted by ϕ_2^{ref}, ϕ_3^{ref}, ϕ_4^{ref}.... ϕ_I^{ref}, with the superscript "ref" indicating reference state. Then the flux in reactor Φ is approximated by

$$\Phi = a_1\phi_1 + \sum_{n=2}^{I} a_n \phi_n^{ref} \tag{8.10}$$

The coefficients $a_1, a_2,\ldots a_I$ are found in a way similar to the FS method by invoking the condition that the calculated fluxes match with the measured fluxes at 102 locations. This requires solution of I simultaneous linear equations. Once the a_n's are known, Eq. (8.10) gives the detailed flux Φ.

Fixing K-modes in MFS method

The results obtained for test case 1 using MFS method by changing the number of K-modes from 1 to 50 is shown in Fig. 8.5. The RMS error in BP, CP and ZP are shown. It is seen that errors are small for about 23 modes and also for around 40 to 45 modes. The MFS method will be studied using both 23 and 44 K-modes.

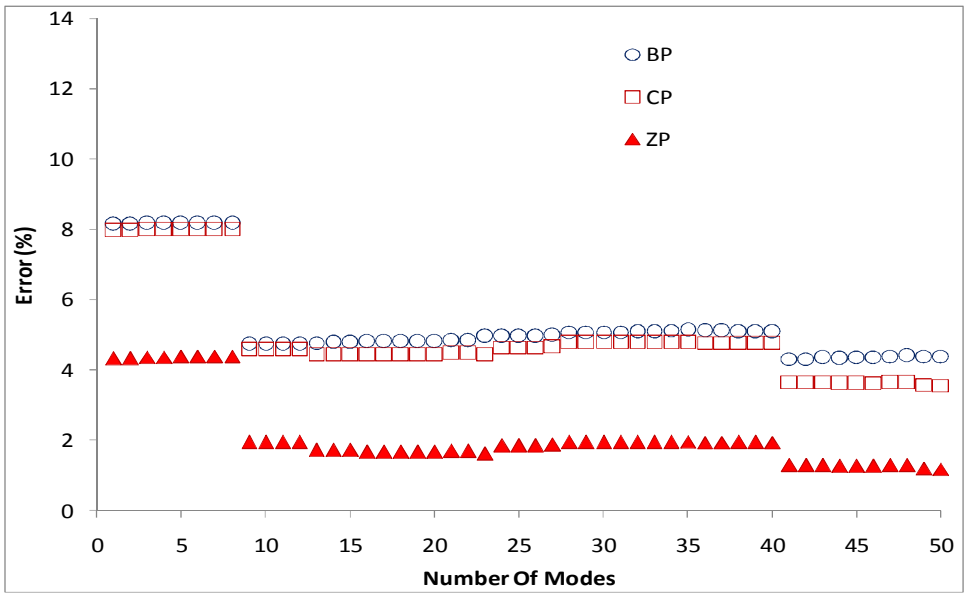

Fig. 8.4. RMS error in BP, CP and ZP by MFS method against number of K-modes

8.6. Numerical Results

In this section, the fluxes estimated by each of the four methods are used to compute BP, CP and ZP values. They will be compared with the "true" values obtained by the fine mesh calculation. The RMS error in BP, CP and ZP is computed for all the ten test cases for various methods. The typical computational times taken by FS, IBC, CLSQ and MFS are about 1 sec, 2-3 minute, 6-7 minute, and 10 sec respectively on 2.6 GHz Pentium 4 machine. The results are given in Table 8.3. The main observations are as follows.

The last row in Table 8.3 gives average of the ten test cases. It is seen that the CLSQ method has much smaller errors than the FS method and IBC method. The MFS method with 23 K-modes has slightly larger error than CLSQ method. The MFS method with 44 K-modes has slightly less error than CLSQ method.

The values of CP predicted by the four methods (FS, IBC, CLSQ and MFS using 23 K-modes) for test case 1 are shown in Fig.8.6 for the channels in 20^{th} vertical column in Fig.8.1. The actual CP predicted by the fine mesh simulation (or "true" values) is also shown. The labels 5, 6, 7,...., 20 on the X-axis denote channels (S,20), (R,20),……,(E,20) in Fig.8.1. The errors in various methods are generally smaller in the central part of the core where CP values are high.

It may be mentioned that the K-eigenvalue problem was solved for the 10 test cases using 28×28×24 mesh also. The RMS errors in BP, CP and ZP with respect to "true" values (obtained by fine mesh) are

about 8.2%, 7.9% and 4.4% respectively. The RMS errors in all the four methods studied here are smaller than these values.

Table 8.3: Relative error (%) in BP, CP and ZP for 10 test cases

Case	FS method (*I=23, *p=14)			IBC method			CLSQ method			MFS method (I=23)			MFS method (I=44)		
	BP	CP	ZP	BP	CP	ZP	BP	CP	ZP	BP	CP	ZP	BP	CP	ZP
1	7.5	5.6	2.3	7.0	6.7	3.3	4.7	4.2	1.6	4.9	4.5	1.7	4.3	3.7	1.3
2	7.1	5.4	2.0	6.9	6.7	3.3	4.7	4.2	1.6	4.9	4.5	1.7	4.2	3.6	1.3
3	7.3	5.8	2.2	7.0	6.6	3.2	4.7	4.1	1.6	5.0	4.5	1.7	4.4	3.6	1.3
4	7.1	5.6	2.2	7.0	6.7	3.3	4.7	4.2	1.6	4.9	4.5	1.8	4.3	3.6	1.3
5	7.1	5.5	1.9	7.0	6.7	3.3	4.7	4.2	1.6	4.9	4.5	1.7	4.3	3.6	1.3
6	6.9	5.5	2.0	7.0	6.7	3.3	4.7	4.2	1.6	4.9	4.5	1.7	4.3	3.7	1.3
7	7.0	5.8	2.3	7.0	6.7	3.3	4.7	4.2	1.6	5.0	4.5	1.7	4.3	3.7	1.3
8	6.9	5.5	2.0	7.0	6.8	3.3	4.7	4.3	1.6	5.0	4.5	1.7	4.3	3.7	1.4
9	7.3	5.5	1.5	6.9	6.7	3.2	4.7	4.2	1.5	5.0	4.4	1.6	4.4	3.6	1.2
10	6.7	5.4	1.9	7.0	6.8	3.3	4.7	4.2	1.6	5.0	4.4	1.6	4.4	3.6	1.2
Avg	***7.1***	***5.5***	***2.0***	***7.0***	***6.7***	***3.3***	***4.7***	***4.2***	***1.6***	***5.0***	***4.4***	***1.7***	***4.3***	***3.6***	***1.3***

*I: number of K-modes; *p: number of perturbed shapes

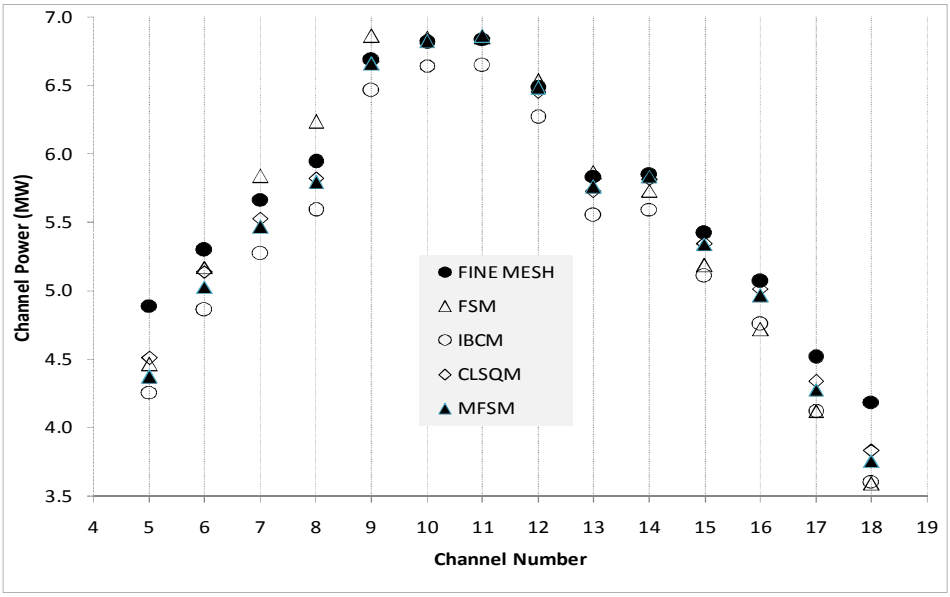

Fig. 8.5. Channel power distribution for channels in 20th vertical column (of Fig. 8.1)

8.7. Studies on detector failures

The proposed MFS method is further examined for the cases of failures of the flux measuring self power neutron detectors (SPNDs). Sometimes the thermal neutron flux read by these detectors may be lower than the flux value at that location. The reason is that the insulation resistance (IR) of SPNDs

decreases because of moisture. The SPNDs having lower IR read a lower value than the actual flux. To estimate the effect of this, a parametric study was carried out for the test case 1. It is assumed that a certain number of SPNDs are reading fluxes which are lower by 25%, 50% and 75% than the true fluxes. The number of such defective detectors is varied. In each case, the RMS error in CP computed by MFS method with 23 K-modes was found out. The variation of RMS error with number of failed detectors is shown in Fig. 8.7. It is clear that if such failed detectors are considered in flux mapping the error is unacceptable. Hence, it may be better to neglect such failed detectors. Fig. 8.8 illustrates the error in BP, CP and ZP estimated by MFS method using 23 K-modes for total detector number ranging from 102 to 25. Fig. 8.9 illustrates the error in BP, CP and ZP estimated by MFS method using 44 K-modes for total detector number ranging from 102 to 45. It can be seen that the result are sufficiently accurate by using only about 50 detectors. Hence, it should be preferable to discard the faulty detectors from the analysis. The faulty detectors can be easily identified by comparing the detector reading with fluxes obtained by solving K-eigenvalue problem for fundamental mode.

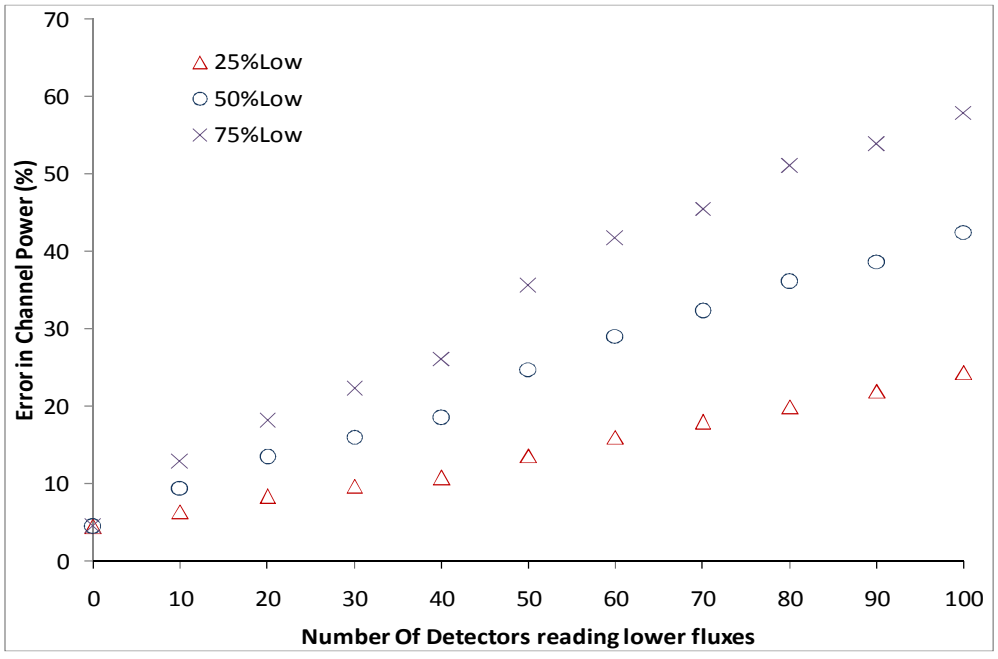

Fig. 8.6. RMS error in channel power versus number of detectors reading 25%, 50% and 75% lower thermal fluxes

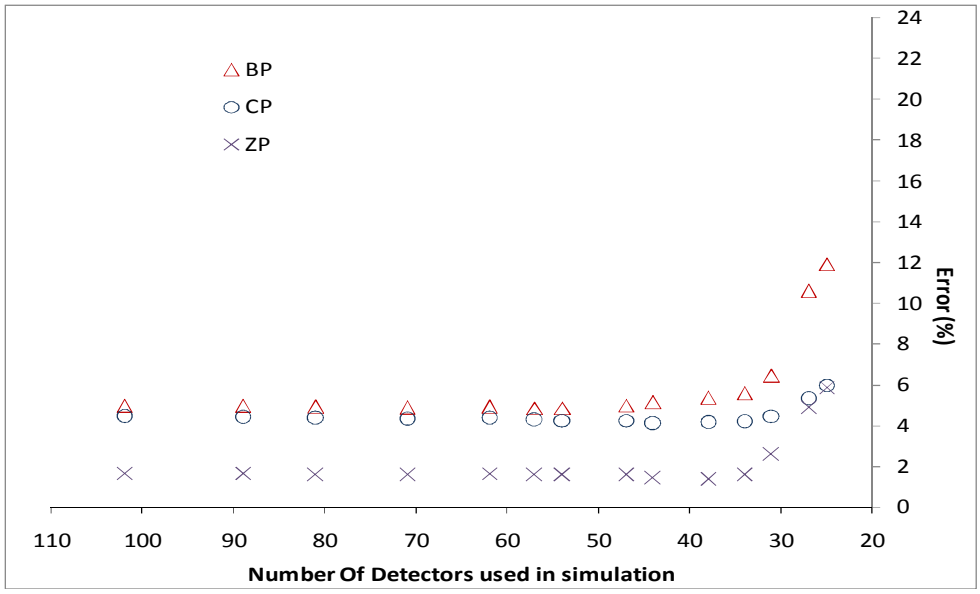

Fig. 8.7. RMS error in BP, CP and ZP using 23 modes versus number of detectors used in simulation

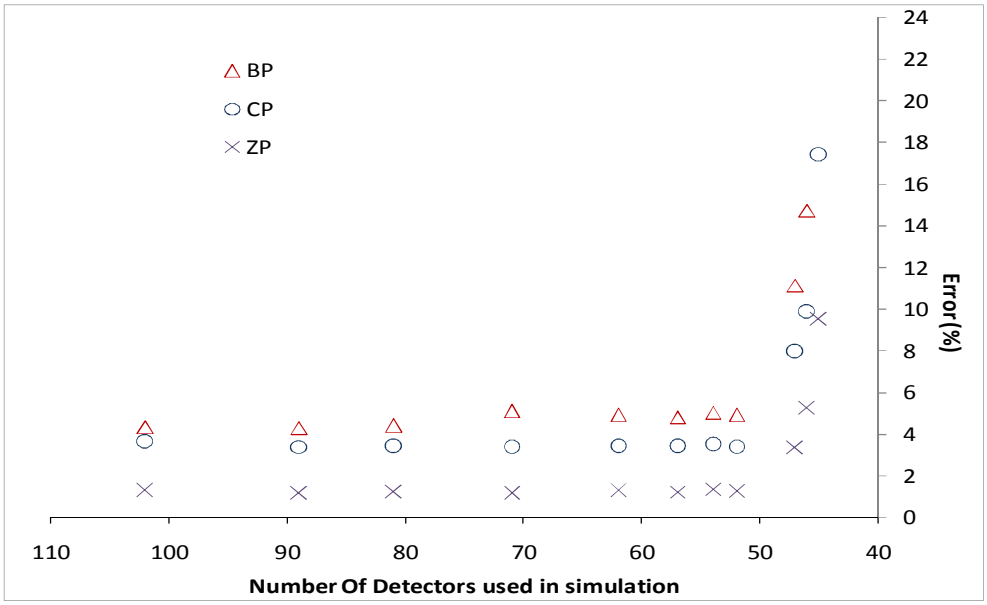

Fig. 8.8. RMS error in BP, CP and ZP using 44 modes versus number of detectors used in simulation

In conclusion, MFS method has been identified as an optimum method for flux map generation in on-line flux mapping system. It gives reasonably accurate results with moderate computational effort and works well even with some failed detectors.

CHAPTER 9

SUMMARY AND FUTURE WORK

This thesis presents optimization studies on some of the physics problems related to the Indian Pressurized Heavy Water Reactors (PHWRs). Chapters 1 to 4 provide background information on PHWRs, optimization methods and neutronics computational methods. The problems discussed in chapters 5 and 6 are related to initial fuelling schemes. The problems discussed in chapter 7 and 8 are related to the performance of Regulating System.

The initial state is unique in the lifetime of a PHWR. In this state, in contrast with any subsequent state, there is no fuel with burn-up. This leads to relatively higher power peaking which prohibits operation at full power. The situation can be improved by adding some depleted Uranium or Thorium bundles to reduce power peaking and yet preserve all other safety criteria. This is a very large-sized combinatorial optimization problem. It has been solved for various kinds of requirements in both 220 MWe and 700 MWe Indian PHWRs. Modern stochastic optimization techniques namely Genetic Algorithm (GA) and Estimation of Distribution Algorithm (EDA) were used. These algorithms are also suitable for parallel processing. Thus, a working methodology has been developed to optimize initial loading in a PHWR. A loading pattern obtained by this method has been actually loaded in the KAPS-1 plant in December 2010. Another loading pattern obtained by present method has been accepted for future loading in 700 MWe PHWR. It may be noted that use of stochastic optimization techniques is not at all new to the nuclear industry. They have been abundantly used for the fuelling optimization in Light Water Reactors. However, the use of these techniques in PHWR presented in this thesis is a new development.

There is scope for further studies on the fuelling optimization. There are many other stochastic optimization tools such as Particle Swarm Optimization, Ant colony optimization etc and the field is continuously evolving. It is possible to try these methods. In the present thesis, the problem was always reduced to a single objective form by using penalty method. However, it may be worth trying the full-fledged multi-objective approach. So far, the use of stochastic optimization has not been found effective

for day-to-day fuelling optimization in PHWRs. However, with the use of new and emerging techniques, this remains an open problem.

The reactor core is equipped with regulation and protection system. The regulation and protection system operates on the basis of signals derived from various monitoring systems. Thermal Power Monitoring System (TPMS) is used to estimate total reactor power and power produced by different zones of the reactor. Flux Mapping System (FMS) is used to estimate power produced from each zone, each channel and each bundle of the core. The accuracy of the output obtained from TPMS and FMS depends on various quantities and this is the area where one needs optimization.

The problem of selecting the best possible fuel channels for TPMS is a large-sized combinatorial optimization problem. It was earlier solved by manual trials. It is solved in present thesis using the EDA method which had worked well for the fuelling optimization discussed in chapters 5 and 6. Chapter 7 describes the TPMS optimization by EDA. It brings down the error in predicted zone powers and bulk reactor power as compared to the manual optimization.

FMS uses flux readings measured by detectors placed inside the reactor core and produces a detailed flux map with the help of basis functions which include some higher K- modes. There are various methods of computing the flux map. There is scope for optimizing the choice of computational method and the number of K-modes to be used. These studies are covered in Chapter 8. This problem is not very large-sized and stochastic optimization techniques are not needed. There are only a few computational methods and up to about 50 K-modes from which a best choice is to be made. This problem was solved by judicious trials. There is some scope for further studies which include effect of uncertainties arising from various sources on the accuracy of flux map. It would be interesting to extend this work to other type of reactors like PWR and fast reactors.

REFERENCES

[1] S. A. Bhardwaj; "The Future 700 MWe Presurrized Heavy Water Reactor". Nuclear Engineering and Design, 236, 861, 2006.

[2] Samuel Glasstone and Alexander Sesonske; Nuclear Reactor Engineering. CBS publishers & destributors, 1998.

[3] Lewis E. E. and Miller W. F. Jr.; Computational Methods of Neutron Transport, John Wiley & Sons, New York, 1984.

[4] W. M. Stacey, Nuclear Reactor Physics, John Wiley and Sons Inc, New York, 2001.

[5] R. J. Stammler and M. J. Abbate, Methods of Steady State Reactor Physics in Nuclear Design, Academic Press, London, 1983.

[6] J. J. Duderstadt and L. J. Hamilton, Nuclear Reactor Analysis, Wiley, New York, 1976.

[7] R. A. Bonalumi, CRC Handbook of Nuclear Reactors Calculations, Vol. II, Y. Ronen, Ed., CRC Press, 1986.

[8] Suetomi E., Sekimoto H.; Conjugate Gradient Like Methods and Their Application to Eigenvalue Problems for Neutron Diffusion Equations, Annals Nuclear Energy, 18(4), 205-227, 1991.

[9a] Krishnani P. D.; CLUB- A Multi-group Integral Transport Code for Lattice Calculations of PHWR cells. Report BARC/1992/E/017, 1992.

[9b] Krishnani P. D., Srinivasan K. R.; A Method for Solving Integral Transport Equation for Pressurized Heavy Water Reactor Cluster Geometry, Nuclear Science & Engineering, 78, 97-103, 1981.

[9c] Krishnani P. D.; CLUB- A Multigroup Integral Transport Theory Code for Analysis of Cluster Lattices, Annals of Nuclear Energy, 9, 255-260, 1982.

[9d] Krishnani P. D.; Interface Current Method for PHWR Cluster Geometry with Anisotropy in the Angular Flux at Interfaces, Annals of Nuclear Energy, 9, 287-296, 1982.

[10] Degwekar, S. B.; "BOXER-3 A Three Dimensional Integral Transport Theory Code for PHWR Supercell". BARC-1295, 1987.

[11] S. C. Chapra and R. P. Canale, Numerical Methods for Engineers, Mc Graw Hill, New York, 2006.

[12] D. Nagesh Kumar, Department of civil engineering, Indian Institute of Sciences, Banglore, Course Material on Optimization Method. Weblink: http://nptel.iitm.ac.in/.

[13] Kropaczek D. J., Turinsky P. J.; In-core Fuel Management Optimization for PWRs Utilizing Simulated Annealing. Nuclear Technology, 95, p.9-31, 1991.

[14] D. Bertsimas and J. Tsitsiklis, "Simulated Annealing," Statistical Science, 8, 10-15, 1993.

[15] Goldberg, D. E.; Genetic Algorithms in Search, Optimization and Machine Learning. Addison-Wesley, Reading, New York, 1989.

[16] M. E. H. Pedersen and A. J. Chipperfield, "Simplifying Particle Swarm Optimization," Applied Soft Computing, 10, 618-628, 2010.

[17] Marco Dorigo and Thomas Statzle; Ant Colony Optimization, MIT Press, 2004.

[18] Jiang, S., Ziver, A.K., Carter, J. N., Pain, C. C., Goddard, A.J.H., Franklin, S., Phillips, H.J.; Estimation of Distribution Algorithms for Nuclear Reactor Fuel Management Optimization. Annals of Nuclear Energy 33, 1039-1057, 2006.

[19] Pereira, C.M.N.A., Schirru, R., Martinez, A.S.; Basic Investigations Related to Genetic Algorithm in Core Designs. Annals of Nuclear Energy 26, 173–193, 1999.

[20] Pereira, C.M.N.A., Sacco, W.F.; A Parallel Genetic Algorithm with Niching Technique Applied to a Nuclear Reactor Core Design Optimization Problem. Progress in Nuclear Energy 50, 740–746, 2008.

[21] Montes, J.L., Ortiz, J.J., Requena, I., Perusquia, R.; Searching for Full Power Control Rod Patterns in a Boiling Water Reactor Using Genetic Algorithm. Annals of Nuclear Energy 31 (16), 1939, 2004.

[22] Turinsky, P.J. et al.; Evolution of Nuclear Fuel Management and Reactor Operational Aid Tools. Nuclear Engineering and Technology 37 (1), 79–90, 2005.

[23] Balakrishnan, K., Kakodkar, A.; Optimization of the Initial Fuel Loading of the Indian PHWR with Thorium Bundles for Achieving Full Power. Annals of Nuclear Energy 21, 1-9, 1994.

[24] Surendra Mishra, R. S. Modak and S. Ganesan, Optimization of Thorium Loading in Fresh Core of Indian PHWR by Evolutionary Algorithms, Annals of Nuclear Energy 36, 948-955, 2009.

[25] Michalewicz, Z.; Genetic Algorithms + Data Structures = Evolution Programs. Springer, 1995.

[26] Carter J. N.; Genetic Algorithm for Incore Fuel Management and Other Recent Developments in Optimization. Advances in Nuclear Science and Technology 25, 113-149, 1997.

[27] Pacheco, P.S.; Parallel Programming with MPI. Morgan Kaufmann publishers Inc., San Francisco, California, 1997.

[28] Apte, A.G. et al.; The Evolution of ANUPAM Supercomputers. BARC Newsletter (291), 2008. <www.barc.gov.in/publications/nl/2008/20080401.pdf>.

[29] Surendra Mishra, R. S. Modak and S. Ganesan, Optimization of Depleted Uranium Bundle Loading in Fresh Core of Indian PHWR by Evolutionary Algorithm, Annals of Nuclear Energy 37, 208-217, 2010.

[30] Surendra Mishra, R. S. Modak and S. Ganesan, Optimization of Depleted Uranium Loading in Fresh Core of Large Sized Indian PHWR by Evolutionary Algorithm, Annals of Nuclear Energy 38, 905-909, 2011.

[31] Lima D. et al; A Nuclear Reactor Core Fuel Reload Optimisation Using Artificial Ant Colony Connective Networks. Annals of Nuclear Energy 35, 1606-1612, 2008.

[32] Meneses A. A. M. et al; Particle Swarm Optimisation Applied to Nuclear Reload Problem of a PWR. Progress in Nuclear Energy 51, 319-326, 2009.

[33] A. A. Pasanen, "Fundamental of CANDU Reactor Nuclear Design: A Lecture series," Atomic Energy of Canada Limited, 1980.

[34] M. E. Pomerantz, C. R. Calabrese and C. Grant, "Nuclear Reactor Power and Flux Distribution Fitting from a Diffusion Theory Model and Experimental Data," Annals of Nuclear Energy, 29, 1073, 2002.

[35] G. M. Frescura, "CANDU-PHW Fuel Management: Course on Operational Physics of Power Reactors," Atomic Energy of Canada Limited, 1980.

[36] N. Roy, S. D. Arguner, A. U. Rehman, and A. L. Wight, "Improved Method for Calculation of Harmonic Modes for CANDU Reactors," Third Int. Conf. Simulation Methods in Nuclear Engineering, Montreal, Quebec, April 18–20, 1990.

[37] R. S. Modak and A. Gupta, "New Applications of Orthomin(1) Algorithm for K-Eigenvalue Problem in Reactor Physics," Annals of Nuclear Energy, 33, 538, 2006.

[38] S. Mishra, R. S. Modak, S. Ray, and A. N. Kumar, "Solution of K-Eigenvalue Problem by Nodal Diffusion Method Using Orthomin(1) Algorithm," Int. Conf. Physics of Reactors (PHYSOR '08), September 14–19, 2008.

[39] R. S. Modak and V. K. Jain, "Sub-Space Iteration Scheme for the Evaluation of λ-Modes of Finite-Differenced Multi-Group Neutron Diffusion Equations," Annals of Nuclear Energy, 23, 229, 1996.

[40] S. Hong, C. H. Kim, and H. C. Suk, "Advanced Online Flux Mapping of CANDU PHWR by Least-Square Method," Nuclear Science and Engineering, 150, 299, 2005.

[41] B. G. Kim, I. S. Kim, and Y. S. Kim, "Core Simulation Using Actual Detector Reading for CANDU Reactors," Nuclear Technology, 93, 138, 1991.

[42] K. Lee and C. H. Kim, "The Least Square Method for Three-Dimensional Core Power Distribution Monitoring in Pressurized Water Reactors," Nuclear Science and Engineering, 143, 268, 2003.

[43] Y. Saad, Iterative Methods for Sparse Linear Systems, PWS Publishing Company, St. Paul, Minnesota, 1996.

[44] Surendra Mishra, R. S. Modak and S. Ganesan, Computational Schemes for On-line Flux Mapping System in a Large Sized Pressurized Heavy Water Reactor, Nuclear Science Engineering, 170, 280-289, 2012.

[45] Surendra Mishra, R. S. Modak and S. Ganesan, Selection of Fuel Channels for Thermal Power Measurement in 700 MWe Indian PHWR by Evolutionary Algorithm, Nuclear Engineering and Design, 247, 116-122, 2012.

[46] Surendra Mishra, R. S. Modak, S. Ray, A.N. Kumar and S. Ganesan, On the Optimization of Thorium Bundle Distribution in the initial core loading for a PHWR, International Conference on Peaceful Uses of Atomic Energy-2009, Sep.29-Oct. 1, 2009, New Delhi, India.